Experiments and Computational Modeling of Pulverized-Coal Ignition

SEMI-ANNUAL

Reporting Period Start Date: 04/01/1998 End Date: 09/30/1998

Authors:
John C. Chen
Samuel Owusu-Ofori"

Report Issue Date: 10/31/1998

DE-FG22-96PC96221--05

North Carolina A&T State University
Department of Mechanical Engineering
1601 East Market Street
Greensboro, NC 27411

Disclaimer

Abstract

Under typical conditions of pulverized-coal combustion, which is characterized by fine particles heated at very high rates, there is currently a lack of certainty regarding the ignition mechanism of bituminous and lower rank coals. It is unclear whether ignition occurs first at the particle-oxygen interface (heterogeneous ignition) or if it occurs in the gas phase due to ignition of the devolatilization products (homogeneous ignition). Furthermore, there have been no previous studies aimed at determining the dependence of the ignition mechanism on variations in experimental conditions, such as particle size, oxygen concentration, and heating rate. Finally, there is a need to improve current mathematical models of ignition to realistically and accurately depict the particle-to-particle variations that exist within a coal sample. Such a model is needed to extract useful reaction parameters from ignition studies, and to interpret ignition data in a more meaningful way.

We propose to examine fundamental aspects of coal ignition through (1) experiments to determine the ignition mechanism of various coals by direct observation, and (2) modeling of the ignition process to derive rate constants and to provide a more insightful interpretation of data from ignition experiments.

We propose to use a novel laser-based ignition experiment to achieve our objectives. The heating source will be a pulsed, carbon-dioxide (CO_2) laser in which both the pulse energy and pulse duration are independently variable, allowing for a wide range of heating rates and particle temperatures — both of which are decoupled from each other and from the particle size. This level of control over the experimental conditions is truly novel in ignition and combustion experiments. Laser-ignition experiments also offer the distinct advantage of easy optical access to the particles because of the absence of a furnace or radiating walls, and thus permit direct observation and particle temperature measurement. The ignition mechanism of different coals under various experimental conditions can therefore be easily determined by direct observation with high-speed photography. The ignition rate-constants, when the ignition occurs heterogeneously, and the particle heating rates will both be determined from analyses based on direct, particle-temperature measurements using two-color pyrometry.

For the modeling portion of this study we will complete the development of the Distributed Activation Energy Model of Ignition (DAEMI), which simulates the conventional drop-tube furnace ignition experiment. The DAEMI accounts for particle-to-particle variations in reactivity

by having a single preexponential factor and a Gaussian distribution of activation energies among the particles. Previous results show that the model captures the key experimental observations, and that adjustments to the model parameters permit a good fit to experimental data. We will complete the model by (1) examining the effects of other variations in physical parameters on the model, (2) applying the model to published results in order to extract reaction parameters, and (3) extending the model for application to laser-based ignition studies, such as our own.

Table of Contents

Executive Summary

During the past reporting period, modifications to the DAEMI were completed. The changes were implemented to examine two aspects of ignition modeling: (1) the effect of varying the number of particles chosen to interact with the laser, and (2) the size distribution for particle sizes.

We have also completed making initial measurements of the ignition temperatures of a suite of coals at three oxygen concentrations, and for three particle size ranges. The reduction of this data from raw signals to temperatures has begun, and we expect it to be completed during the next reporting period.

Introduction

The ignition of pulverized coal has been the subject of research for nearly 150 years, with the initial motivation being the avoidance of coal-dust explosions in mines. In more recent times, due to the world's increased reliance on coal for power generation and the need to maximize energy-conversion efficiency, research has shifted to understanding the fundamental mechanism of coal ignition and measuring its kinetic rates. The importance of ignition to coal-flame stability is obvious — the more easily a particular coal ignites after injection into a boiler furnace, the better its flame-stability characteristics. A less obvious ramification of the ignition process is its role in establishing extended, fuel-rich zones in coal flames which are responsible for the destruction of NOx and its conversion to benign N_2. Certainly, the ignition process is inextricably linked to the formation of this NOx-reduction zone, and the ignition behavior of coals and coal blends will strongly affect the ease and extent of formation of this zone. This connection is deserving of further study and its understanding is the goal toward which we hope to apply the results of this proposed study. Specifically, we propose to examine fundamental aspects of coal ignition through (1) experiments to elucidate the ignition behavior of coals, and (2) modeling of the process to derive accurate and useful rate constants, and to provide a more insightful interpretation of data from ignition experiments.

Objectives

Our objectives for this project are to:

1. develop a novel experimental facility with extensive optical-diagnostic capabilities to study coal ignition;
2. determine the ignition mechanism of coals under simulated combustion conditions by direct observation with high-speed photography;
3. examine the effects of various experimental conditions, including coal rank, particle size, oxygen concentration and heating rate, on the ignition mechanism; and
4. measure the ignition rate constants of various coals.
5. modify our existing ignition model to examine the effect of particle-size distribution on the ignition behavior;
6. incorporate, if necessary, a size distribution into the model;
7. apply the model to extract ignition rate constants from previously published data from conventional experiments;

8. modify the model and apply it to our laser-based ignition studies for determination of ignition rate constants.

Results from This Reporting Period and Discussion

During the past reporting period, we have made excellent progress on model development for this project. We are nearing completion of two manuscripts for submission and possible publication. The first, "The Ignition Behavior of Pulverized Coals," concerns mainly the experimental measurements that we have obtained, and interprets these measurements in terms of the model in its current form. The second manuscript, "Modeling the Ignition of Pulverized Coals," will focus on the current modifications to the Distributed Activation Energy Model of Ignition (DAEMI) which we are in the process of implementing, along with some supporting experimental measurements.

Personnel

The MS-candidate student working on the experiment portion of this project, Ms. Vida Agyeman, has taken maternity leave as of late September. She has recovered and is back to attend classes. We expect that she will return to full time work on this project by the end of this calendar year.

The MS-candidate working on the modeling portion of this project, Ms. Jianping Zheng, has completed her thesis and will be defending it on November 13, 1998. A portion of her draft thesis, completed on October 22, 1998, is included as an appendix to this report, and forms the bulk of the work completed during the past reporting period.

Finally, Professor John Chen, the Project Director for this project, has resigned his position at North Carolina A&T State University, and is currently an Associate Professor of Mechanical Engineering at Rowan University, effective August 1998. Professor Chen will continue to consult on this project, which has been transferred to Dr. Samuel Owusu-Ofori, Professor of Mechanical Engineering at North Carolina A&T State University.

Computational Model

A portion of Ms. Jianping Zheng's MS thesis, titled "Modeling the Ignition Behavior of Pulverized Coals," is included as Appendix A of this report. The two sections included are Model Analysis and Results, and Discussion.

Experiment

During the past reporting period we have completed the measurement of ignition temperatures for a suite of four coals (Pittsburgh #8 high-volatile bituminous, Pocahontas low-volatile bituminous, Wyodak subbituminous, and Pust lignite) at three oxygen concentrations, and for two or three particle size ranges. The data reduction is currently underway to convert the raw signal measurements to temperatures. We expect this to be completed during the next reporting period. The complete set of data will be used as inputs to the modified Distributed Activation Energy Model of Ignition (DAEMI).

Meetings and Conferences

A paper describing the results contained in this report was prepared and submitted to the 1999 Combustion Institute Joint US National Meeting, to be held in March 1999 in Washington, DC.

At the Spring 1998 American Chemical Society National Meeting, we presented a paper describing our research. This paper, co-authored by John Chen, Maurice Richardson, and Jianping Zheng, won the Richard A. Glenn Award, the Fuel Chemistry Division's Best Paper Award.

Goals for Next Quarter

During the next reporting period, we will complete the data reduction for the temperature measurements made during this summer. The data will form the basis for further model development using the DAEMI.

Appendix A

MODEL ANALYSIS AND RESULTS

3.1 Introduction Experiment

3.1.1 Laser Ignition Experiment

The experimental setup consists of a wind tunnel, gas flow system, coal feeder, detector, laser gate, pulse generators laser and Optical system.

Figure 3.1 shows a schematic of the laser ignition experiment. Sieve-sized coal particles are dropped batch-wise into a laminar upward-flow wind tunnel with quartz test section (5cm square cross-section). The gas is not preheated, The gas flow rate was set so that the particles emerged from the feeder tube, fell approximately 5 cm, then turned and traveled upward out of the tunnel. This ensured that the particles were moving slowly downward at the ignition point, chosen to be 2 cm below the feeder-tube exit.

A single pulse from a Nd:YAG laser was focused through the rest section, then defocused after exiting the test section, and two sides in this manner achieved more spatial uniformity and allowed for higher energy input than a single laser pass. For nearly every case, one to three particles were particles were contained in the volume formed by the two intersecting beams, as determined by previous observation with high-speed video.

The laser operated at 10 Hz and emitted a nearly collimated beam (6 mm diameter) in the near-infrared (1.06 μm wavelength). The laser pulse duration was 100 μs and the pulse energy was fixed at 830 mJ per pulse, with pulse-to-pulse energy fluctuations of less than 3%. The laser pulse energy delivered to the test section was varied by a polarizer placed outside of the laser head, variation from 150 to 750 mJ was achieved by rotating

the polarizer. Increases in the laser pulse energy result in heating of the coal particles to higher temperatures. At the ignition point the beam diameter normal to its propagation direction was 3 mm on each pass of the beam. An air-piston-driven laser gate (see Fig. 3.1) permitted the passage of a single pulse to the test section. The system allowed for control of the delay time between the firing of feeder and he passage of the laser pulse. Finally, ignition or non-ignition was determined by examining the signal generated by a high-speed silicon photodiode connected to a digital oscilloscope. Figure 3.2 presents typical signal traces from the photodetector for both ignition and non-ignition events. Features of the trace for the ignition case is similar to that described previously.

Particle temperature was measured by two-wavelength pyrometry. A simple lens coupled to an optical fiber bundle collected light emitted by the igniting particles. The output from the fiber bundle is collimated and separated into two beams via a dichroic filter. Light of wavelengths below 0.75 μm (the dichroic filter's cut-off wavelength) was passed through a bandpass interference filtered centered at 0.7 μm with a optical bandwidth of 40 nm. The remaining light was passed through an interference filter centered at 0.9 μm with an optical bandwidth of 10 nm. Separate high-speed silicon photodiodes detected each beam following the optical filters. The pyrometer was calibrated using a 2-mm diameter blackbody source at 990^{o}C.

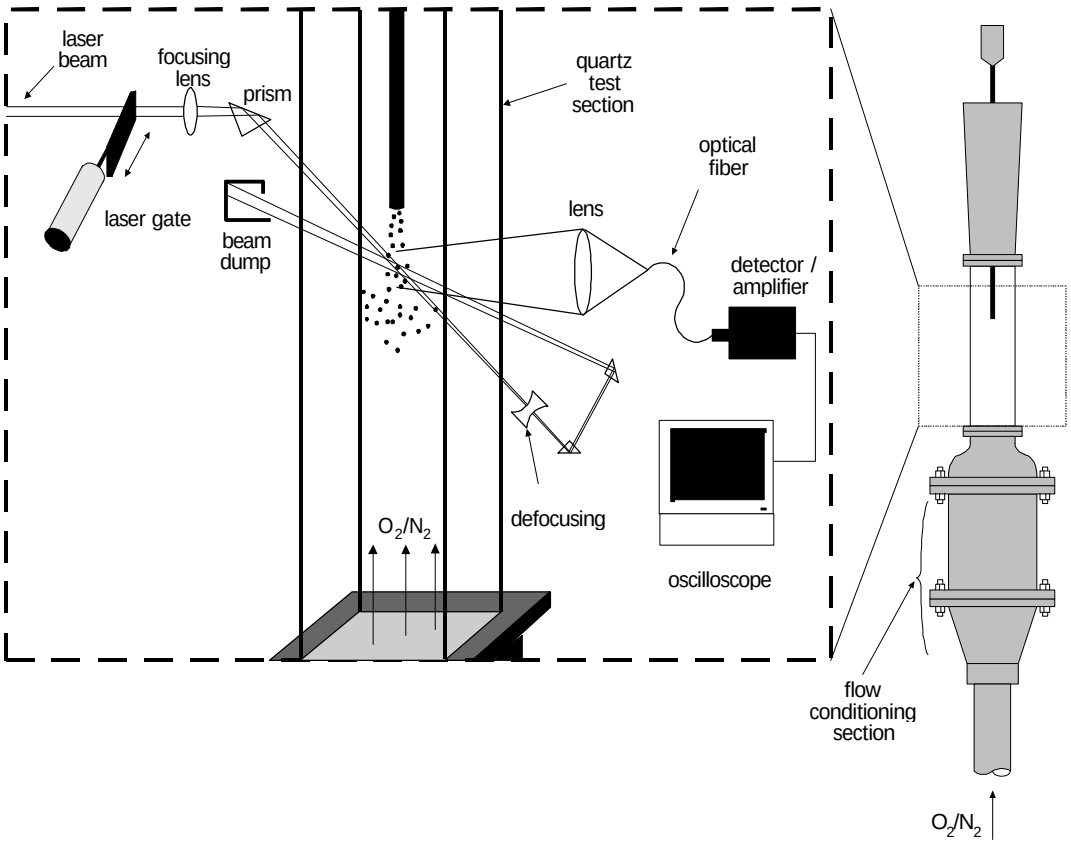

Figure 3.1 Schematic of the laser ignition experiment

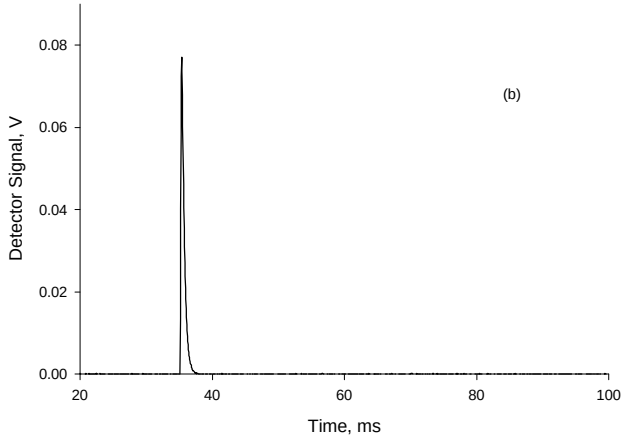

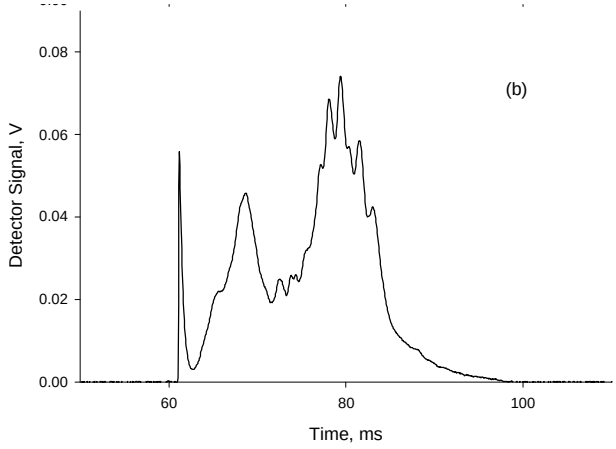

Figure 3.2 Signal traces from photodetectors showing (a) non-ignition and (b) ignition events for the Pittsburgh #8 bituminous coal. Particle size was 125-158 μm, and oxygen concentration was 100%. The short-lived spike in both traces result from laser heating of the coal surface and subsequent cooling. Ignition and combustion of the coals causes the long-lived emission of (b).

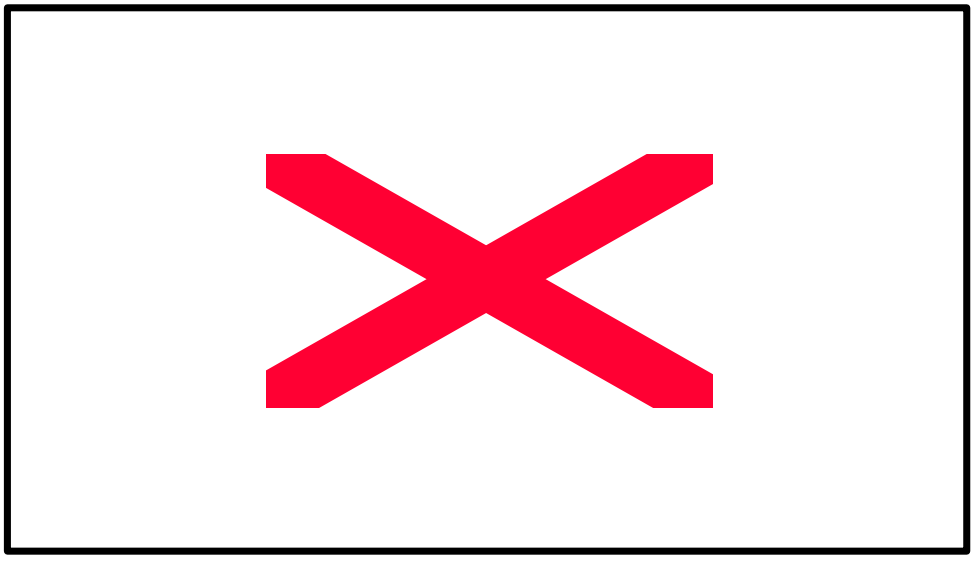

Figure 3.3 Typical data from a conventional ignition experiment showing the relation between ignition frequency (or probability) and gas temperature for a bituminous coal. Data extracted from Ref.4.

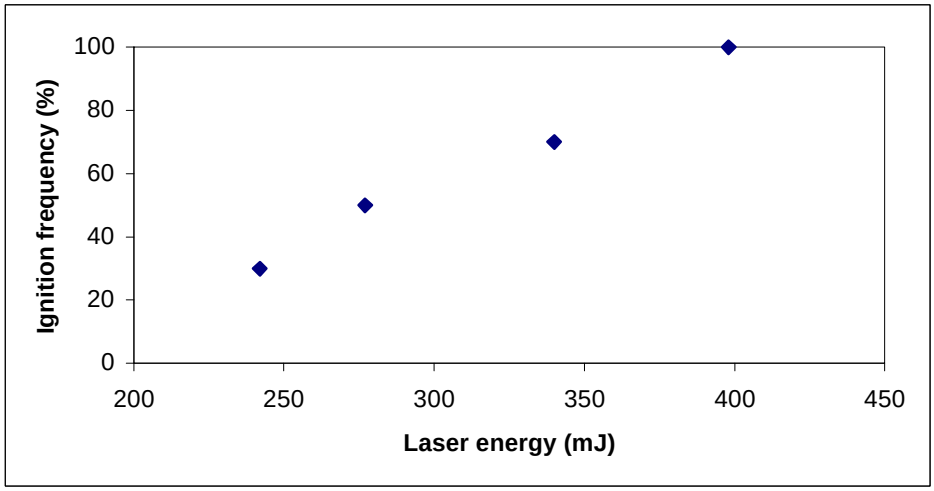

Figure 3.4 Typical data from our laser ignition experiment showing the relation between ignition frequency and laser energy for bituminous coal.

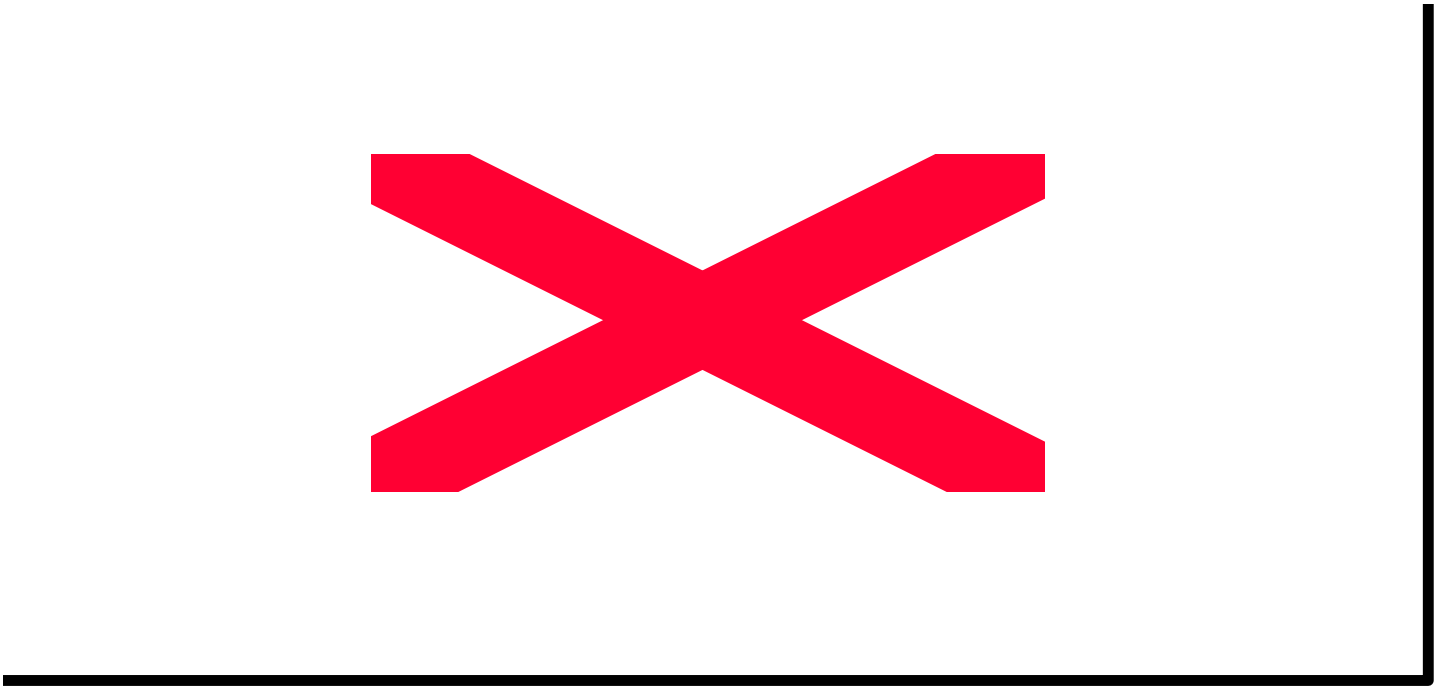

Figure 3.5 Distribution of Activation Energy as a Gaussian Distribution

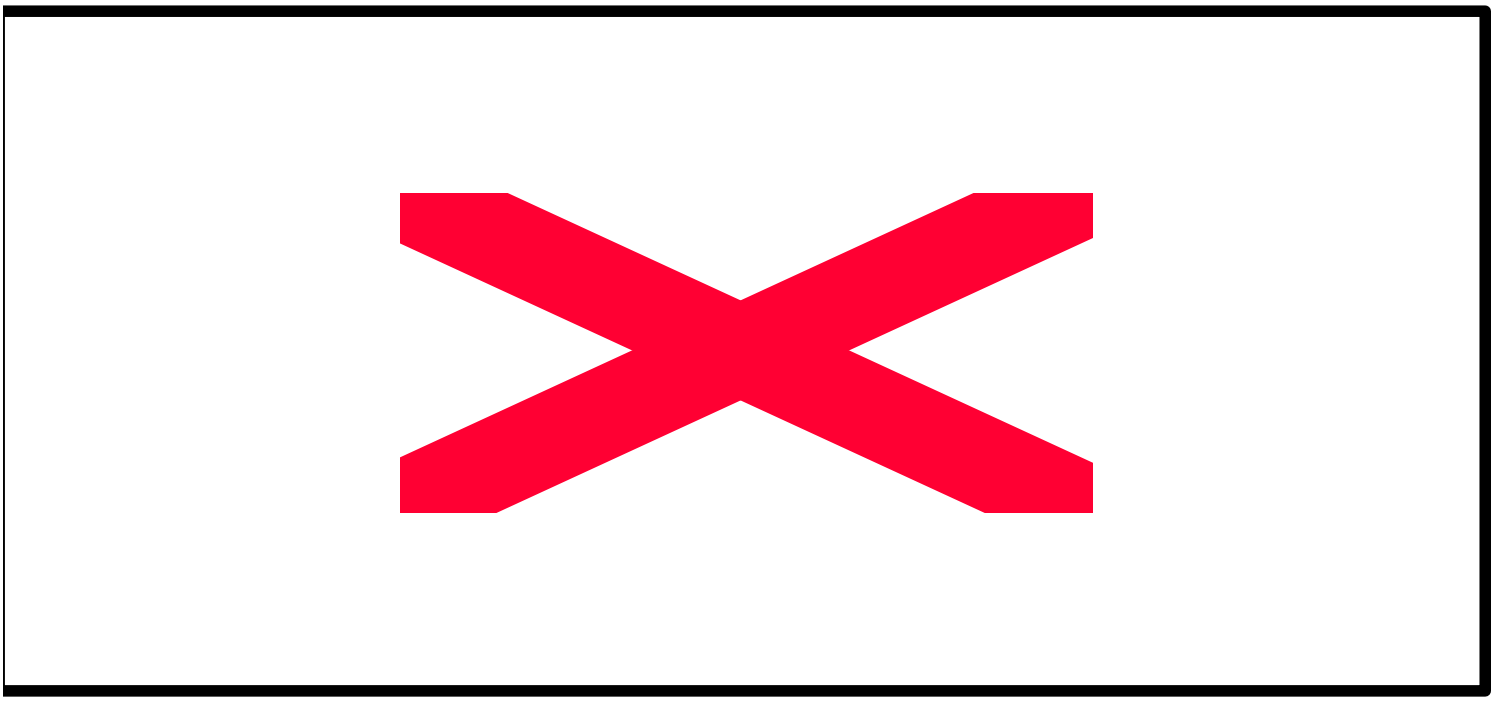

Figure 3.6 Distribution of coal particle size as a Top-Hat Distribution

3.1.2 Drop-Tube Experiment by T. F. Wall's Group [4]

The ignition experiments were carried out using a pulse ignition technique. Metered flows of O_2 and N_2 were passed through an electrically heated tubular furnace at a rate of 500ml/min (s.t.p.). A small quantity of sample was contained in a glass funnel with a capillary stem. By gently tapping the funnel with an electric vibrator, a pulse of fuel (0.2-0.5mg or 1170 particle for 75-90μm size coal) was dropped into the furnace through a water-cooled probe. A photomultiplier was used to detect the occurrence of ignition, which was indicated by the visual flash of an igniting particle. The furnace was maintained at a fixed temperature. Ten to twenty pulses of fuel were injected, and the number of pulses for which ignition responses were detected was noted on a chart recorder. Figure 3.3 give typical results of ignition response versus furnace gas temperature and indicate a temperature range over which the percentage of pulses resulting in observed ignition flashes increases from 0 to 100.

3.2 Model Formulation

Figure 3.4 show typical data obtained from our ignition experiment conducted by varying the laser energy while holding oxygen concentration, particle size and type of coal. Fig. 3.4 and Fig. 3.3 show that ignition frequency increases approximately linearly with plus laser energy or gas temperature, and these are inconsistent with the heterogeneous ignition theory previously described. If all particles of a coal sample used in an experiment have the same reactivity, that is if they are described by a common Arrhenius rate constant as in Eq. (2.7), then the data would show an ignition frequency of 0% until the critical laser energy corresponding to that at the critical ignition condition is reached. At any laser energy or gas temperature above critical ignition condition, the ignition frequency would be 100.

One of the reasons why ignition frequency increases gradually with increasing laser energy or gas temperature is obvious: Within any coal sample, there exists a distribution of reactivity among the particles. Thus, in the laser ignition experiment, in which a batch of perhaps 4×10^5 particles of a sample is dropped into the furnace, there is the probability (or frequency) that at least one particle has a reactivity that meets or exceeds the critical ignition condition set forth in equations (2.1) and (2.2) as the laser energy is increased. This is the ideal of DAEMI [10]. Of course, there exist other variations among the particles within a sample, such as particle size and specific heat. Variation in size alone could account for the observed increase in ignition frequency with the laser energy pulse (or gas temperature) [1,4,5,8]. It cannot account for other experimental observation, namely, the variation in the slope of the ignition frequency with oxygen concentration. A distribution in specific heat would only affect the rate at which a particle attains its equilibrium temperature, but would not change the value or the reactivity. Perhaps other variations could cause the observed behavior of ignition frequency. It is our premise that the distribution in reactivity and particle size dominates all other variations. We propose to add the distribution of particle size into the DAEMI.

3.3 Simulation Procedure

Fig.3.5 shows the distribution of activation energy versus frequency for a sample for which E_0=58 kJ mol^{-1} and σ=5.5 kJ mol^{-1}. The intervals of activated energy is 1kJ mol^{-1} (ΔE=1kJ mol^{-1}).

The Distributed Activated Energy Model of Ignition (DAEMI) simulates our laser ignite and drop-tube experiment by allowing for the particles within the coal sample to have a distribution of reactivity (Chapter 2.3). We first calculate the probability of particles for being in each of the intervals.

The distributed of particle size model of ignition assumes that in a small range of particle size, the distribution of particle size is Top-Hat distribution (Fig 3.6). The interval of particle size is 1μm ($\Delta Dp=1.0\times10^{-6}$m). Particle sizes are grouped into three. These are 106.0 to 125.0μm, 125 to 150μm, 150.0 to 180.0μm respectively.

3.3.1 Base Case

Now, the heat generated by a spherical carbon particle undergoing oxidation on its external surface is given by the kinetic expression:

$$\frac{Q_{gen}}{S} = H_c x_{o_2}^n A_0 \exp\left(\frac{-E}{RT_p}\right) \tag{3.1}$$

Similarly, the heat loss from the surface of a particle at temperature T_p is the sum of losses due to convection and radiation. Thus, heat loss from the surface is given as:

$$\frac{Q_{loss}}{S} = hS(T_p - T_g) + es_b S\left(T_p^4 - T_g^4\right) \tag{3.2}$$

For the convection-loss term, we assume that the Nusselt number equals 2, as is appropriate for very small particles, which leads to $h = 2k_g / d_p$.

$$\frac{Q_{loss}}{S} = \frac{2k_g}{d_p} S(T_p - T_g) + es_b S\left(T_p^4 - T_g^4\right) \tag{3.3}$$

At the critical ignition condition, $Q_{gen} = Q_{loss}$, we obtain

$$E = -RT_p \ln\left(\frac{\left(\frac{2k_g}{d_p}\right)\left(T_p - T_g\right) + es_b\left(T_p^4 - T_g^4\right)}{H_c x_{o_2}^n A_0}\right) \tag{3.4}$$

where the required parameters for this equation were calculated as follows:

For base case of the model, we assumed that T_p was obtained from the equilibrated temperature calculations by use of a linear regression to regress Tp as a function of laser energy (see appendix 1). For example, for 70μm.116μm and 165μm coal particle the temperature are given as functions of laser energy as [19]

$$T_{p\,(116mm)} = 0.7266E_{laser} + 385.22 \tag{3.5}$$

$$T_{p(70mm)} = 1.0707E_{laser} + 427.08 \tag{3.6}$$

$$T_{p(165mm)} = 0.5505E_{laser} + 367.57 \tag{3.7}$$

For variable particle size, we use interpalation mathematics method define:

$$T_p = \frac{\left(T_{p(70mm)} - T_{p(116mm)}\right)\left(d_p - 116e-6\right)}{(70-116)\times 1\times e-6} + T_{p(116mm)} \qquad d_p<116\mu m \tag{3.8}$$

$$T_p = \frac{\left(T_{p(165mm)} - T_{p(116mm)}\right)\left(d_p - 116e-6\right)}{(165-116)\times 1\times e-6} + T_{p(116mm)} \qquad d_p>116\mu m \tag{3.9}$$

k_g the gas thermal conductivity in the boundary layer around a heated particle was given by a linear fit to the conductivity of air [11].

$$k_g = 7.0\times 10^{-5}\left(\frac{T_p + T_g}{2}\right) \tag{3.10}$$

H_c is defined by the equation [16]

$$H_c = \frac{y}{y+1}H'_{C,CO} + \frac{1}{y+1}H'_{C,CO_2} \tag{3.11}$$

It is well known that the product of carbon oxidation is both CO and CO_2, $H'_{C,CO}$ and H'_{C,CO_2} are the heats of combustion corresponding to the following oxidation reaction [11].

$$C + \frac{1}{2}O_2 \rightarrow CO; H'_{C,CO} = 9{,}210\frac{kJ}{kgC}$$
$$C + O_2 \rightarrow CO_2; H'_{C,CO_2} = 32{,}790\frac{kJ}{kgC} \quad (3.12)$$

Where

$$y = \frac{molCO}{molCO_2} = 59.95\exp\left(\frac{-3214}{T_p}\right) \quad (3.13)$$

ε, the emissivity of coal particles was taken as 0.8.

n, the reaction order was taken as 1.

χ_{o2} was chosen to be 1.0 corresponding to a 100% oxygen concentration.

For each laser energy, twenty runs were made to obtain ignition-frequency distributions.

3.3.2 laser Ignition Experiment

When we were using this version of DAEMI to fit the laser ignition experiment. The experiment data of Tp was reading directly from data files (see appendix 3). Then to calculate average temperature (T_{avg}) and standard deviation (T_σ), base on Normal Distribution,

$$T_{avg} = \frac{\sum T_p}{N} \qquad \text{(N is the number of } T_p\text{)} \quad (3.14)$$

$$T_s = \sqrt{\frac{\sum (T_p - T_{avg})^2}{N-1}} \quad (3.15)$$

to obtain the range of temperature, namely, $T_{avg}-2T_\sigma < T_p < T_{avg}+2T_\sigma$, by randomly choosing particle temperature from the range to obtain critical energy at each condition.

In this experiment, in which a batch with several hundred particles are dropped in to the test section, and only a few are heated by the laser pulse. There is an increasing probability (or frequency) as the laser energy is increased that at least one of the heated particles is reactive

enough to ignition under the given conditions. For nearly every case, one to three particles are hit in the test section by two intersecting laser beams. This is determined by observations with high-speed video. For simulation, thirteen hundred particles are then selected randomly as they feed into the test section and two particles are further selected randomly from these 1300 to be hit by the laser pulse, keeping in mind that no particle can be selected twice.

For randomly selected two particles with particle size and activation energy. Substituting preexponential factor (A_0), mean of Gaussian distribution of activation energy (E_0), standard deviation of Gaussian distribution (σ) and reaction order (n) in Eq. (3.4), E can be calculated as the critical (or threshold) activation energy that a particle may have and still ignite under the given conditions. The result (E) is compared with the activation energy. If the result (E) is greater than the activation energy among the particles that were hit, then the particle is considered ignited.

At each set of operating conditions (coal type and size, oxygen concentration, and laser energy), 20 attempts at ignition are made in order to get the ignition frequency, or probability, which is the parameter sought from these studies. We compare this simulated ignition frequency with the experimental results over a range of laser pulse energy.

3.2.3 Drop-Tube Experiment

In simulating the drop-tube ignition experiment, we assumed that 10^6 particle are in the initial batch. A batch of 1170 particles of a sample is dropped into the furnace in each simulation of an experimental run. No particle can be selected more than once. Whether or not ignition occurs for a run is determined by the particle in the batch of 1170 with the lowest activation energy.

Now, using Eq. (3.1) and Eq. (3.3) we can obtain the heat generated Q_{gen} and Q_{loss}. In order to determine the critical ignition temperature of the particle, Tp, and critical activation

energy, E, the critical ignition condition, Q_{gen} = $Q_{loss,}$ and $\frac{dQ_{gen}}{dT_p} = \frac{dQ_{loss}}{dT_p}$ are solved simultaneously. Q_{gen} and Q_{loss} are given in Eqs. (3.1) and (3.3), and lead to the following derivatives with respect to temperature:

$$\frac{dQ_{gen}}{dT_p} = SH_c x_{o_2}^n A_0 \exp\left[\frac{-E}{RT_p}\right]\left(\frac{E}{RT_p^2}\right) \tag{3.16}$$

$$\frac{dQ_{loss}}{dT_p} = \frac{2k_g}{d_p} S + 4es_b ST_p^3 \tag{3.17}$$

Note that the neglection of the T_p dependence in k_g introduces a small error in Eq. (3.15).

Following $\frac{dQ_{gen}}{dT_p} = \frac{dQ_{loss}}{dT_p}$, we set Eq. (3.14) equal to Eq. (3.15) and solve for the quantity E/RT_p:

$$\frac{E}{RT_p} = \frac{\frac{2k_g}{d_p} T_p + 4es_b T_p^4}{H_c x_{o_2}^n A_0 \exp\left[\frac{-E}{RT_p}\right]} \tag{3.18}$$

The denominator is recognized to be Q_{gen}/S Eq. (3.1), which by Q_{gen} = Q_{loss} is also Q_{loss}/S Eq. (3.2). Thus Eq. (3.16) can be rewritten as:

$$\frac{E}{RT_p} = \frac{\frac{2k_g}{d_p} T_p + 4es_b T_p^4}{\frac{2k_g}{d_p}(T_p - T_g) + es_b (T_p^4 - T_g^4)} \tag{3.19}$$

This relation for E/RT_p is substituted into the expression Q_{gen} -Q_{loss} = 0 to obtain a function, F, which is a function of T_p only:

$$F(T_p) = Q_{gen} - Q_{loss}$$

$$= H_c x_{o_2}^n A_0 \exp\left[\frac{\frac{2k_g}{d_p}T_p - 4es_b T_p^4}{\frac{2k_g}{d_p}(T_p - T_g) + es_b(T_p^4 - T_g^4)}\right] - \frac{2k_g}{d_p}(T_p - T_g) - es_b(T_p^4 - T_g^4) = 0 \quad (3.20)$$

The reasonable root of F (T_p) corresponds to the critical ignition temperature of the particle, and substitution of this value into Eq. (3.19) produces the critical activation energy at the critical ignition condition.

k_g, the gas thermal conductivity in the boundary layer around a heated particle was given by Eq. (3.10).

χ_{o2} was chosen to be 0.5 corresponding to a 50% oxygen concentration.

ε, the emissivity of coal particle was taken as 0.8.

H_c was defined by the equation from (3.11) to (3.13).

Substituting all the required values in Eq. (3.4), E obtain the result as the critical (or maximum) activation energy that a particle may have and still ignite under the given conditions. By randomly choosing each particle with activation energy for a run, then get the particle in the batch of 1170 with the lowest activation energy. we compared the result (E) with the lowest activation energy. If the result (E) is greater than the lowest activation energy among the particle that was heated in a run, The particle was ignited.

3.3 Modeling Results

3.3.1 Results of the Base Case of the Model

Figure 3.7 and Fig. 3.8 shows the effect of oxygen concentration and number of particle (M) on ignition frequency for particle size range of 106-125μm and 150-180μm, respectively. It can be seen that at each oxygen concentration, ignition frequency increases monotonically over the range of laser pulse energy. Below this range, the ignition frequency is zero, and above this range the result is 100% ignition frequency. As the number of particle (M) is increased from 1 to 300, the frequency distribution shifts to lower laser energy values. This behavior is due to the fact that, within any coal sample, there exists a distribution of reactivity among the particles.

As the oxygen concentration is decreased from 100% to 67%, the frequency distribution shifts to higher laser energies or equivalently, higher particle temperatures, as expected. This is consistent with the ignition theory since at decreased oxygen concentration, higher temperatures are necessary for heat generation by the particles (due to chemical reactions) to exceed heat loss from the particles and lead to ignition. The shift in distribution can be viewed in two ways: for a fixed laser pulse energy, a decrease in oxygen concentration leads to a decrease in the ignition frequency, all else being equal; Second, a decrease in oxygen concentration implies that a higher laser pulse energy is needed, in order to achieve the same ignition frequency.

Figure 3.9 and Fig. 3.10 show the same effect of Distribution Particle Size in 150-180μm and average particle size (165μm) on ignition frequency for oxygen concentration of 100% and 67%. Fig.3.11 and Fig.3.12 also show that the same effect of distribution particle size in 106-125μm and average particle size (115μm) on ignition frequency for 100% and 67% of O_2.

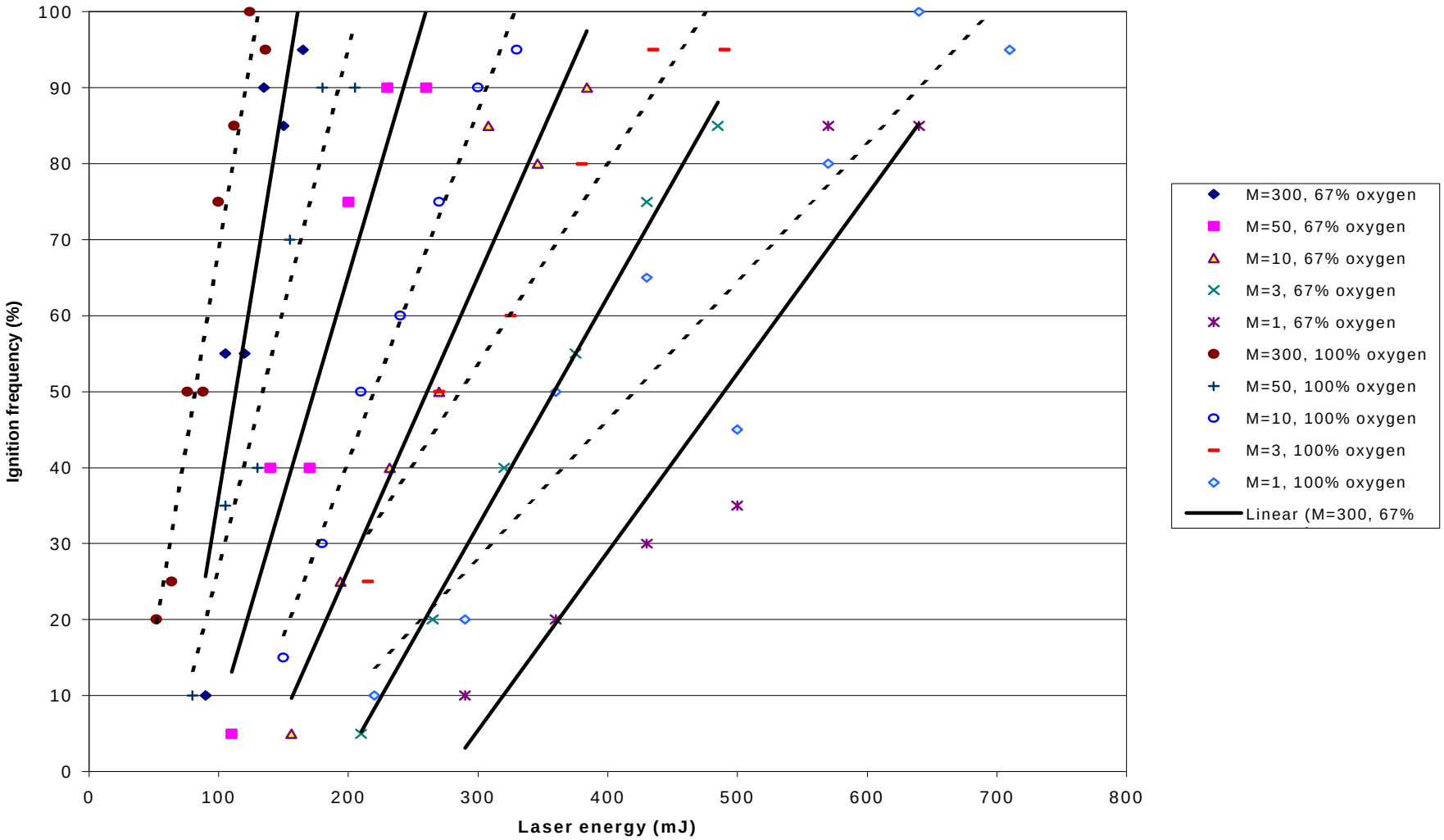

Figure 3.7 Modeling results showing the effect of M (numbers of particles were ignited at one drop time) and oxygen concentration on ignition frequency. (a) Solid-line express 67% oxygen concentration (x_{o2} =67%); (b) Dash-line express 100% oxygen concentration (x_{o2} =100%). Particle size is 106-125 μm, and all other parameters are as listed in Table 3.1.

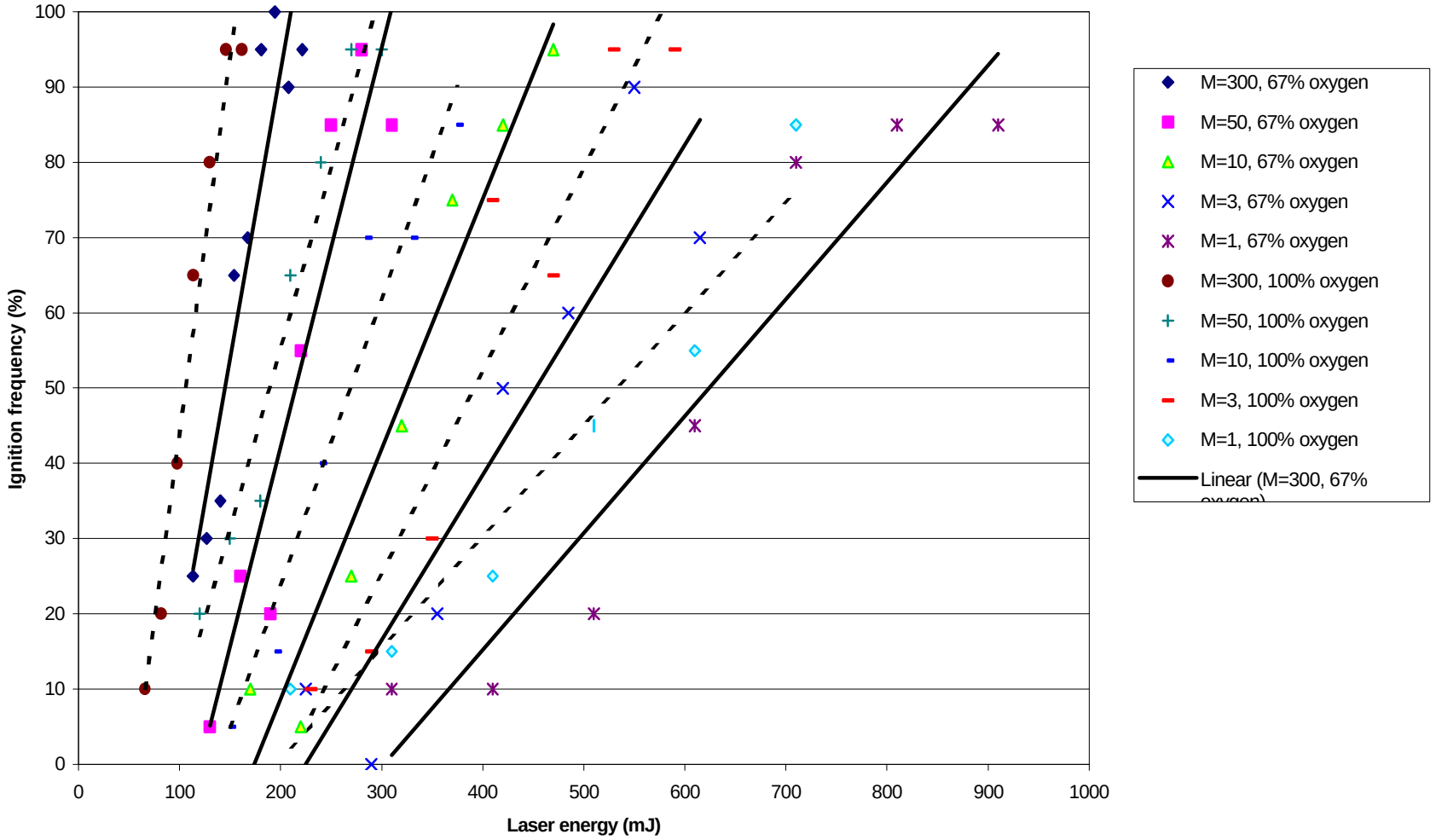

Figure 3.8 Modeling results showing the effect of M (numbers of particles were ignited at one drop time) on ignition frequency. (a) Solid-line express 67% oxygen concentration (x_{o2} =67%); (b) Dash-line express 100% oxygen concentration (x_{o2} =100%). Particle size is 150-180 μm, and all other parameters are as listed in Table 3.1.

Table 3.1 Parameters Used in the Base Case of the Model of Laser Ignition Experiment

Variable	Value
E_0	58 kJ/mol
A_0	250 kg/m^2s
σ	5.5 KJ/mol
n	1.0
ε	0.8

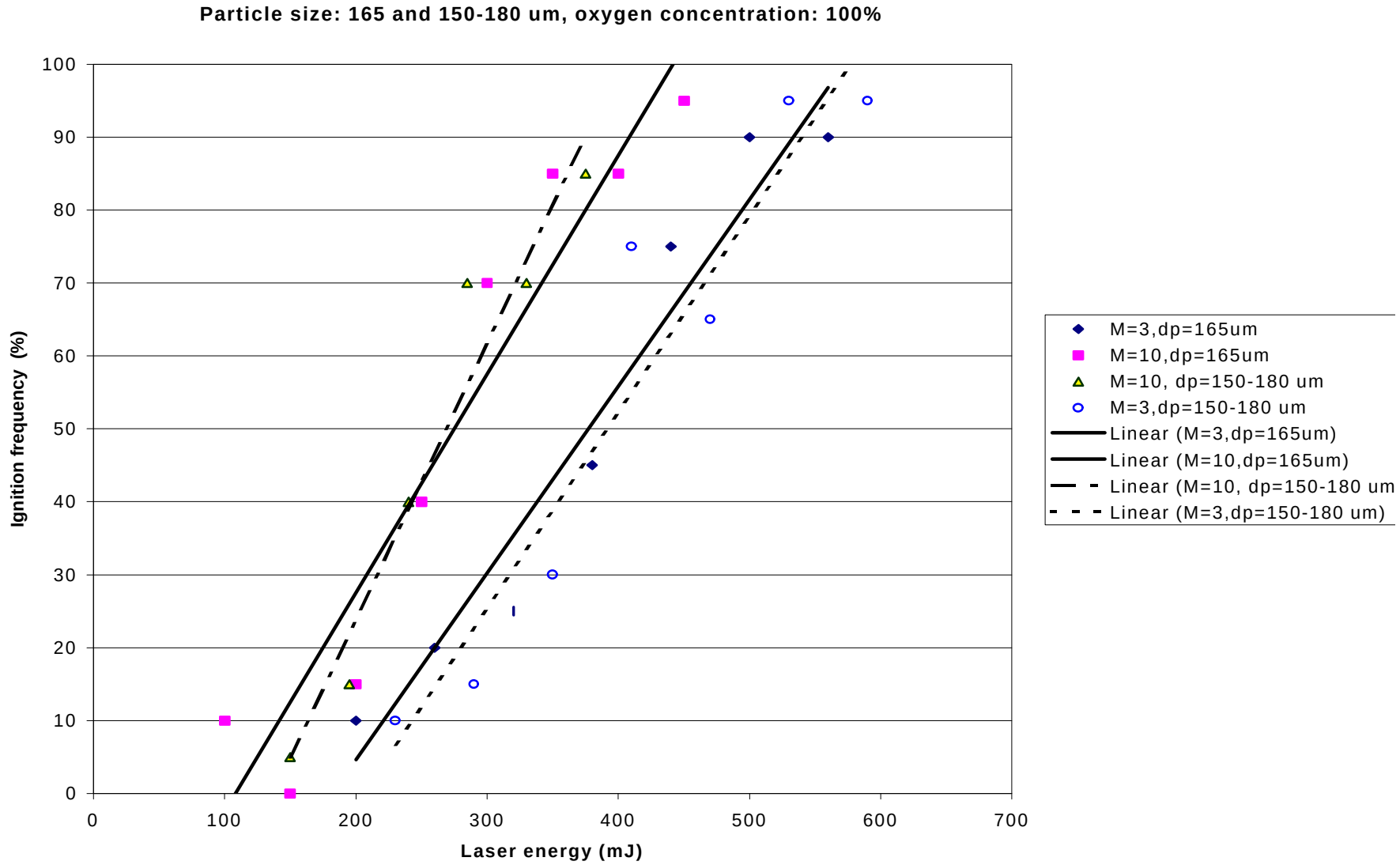

Figure 3.9 Modeling results showing the effect of average particle size 165μm and the range of particle size 150-180μm in ignition frequency. Oxygen concentration is 100%. All other parameters are as listed in Table 3.1. (a) Solid-line express particle size d_p=165μm; (b) Dash-line express distribution particle size D_p in 150-180μm.

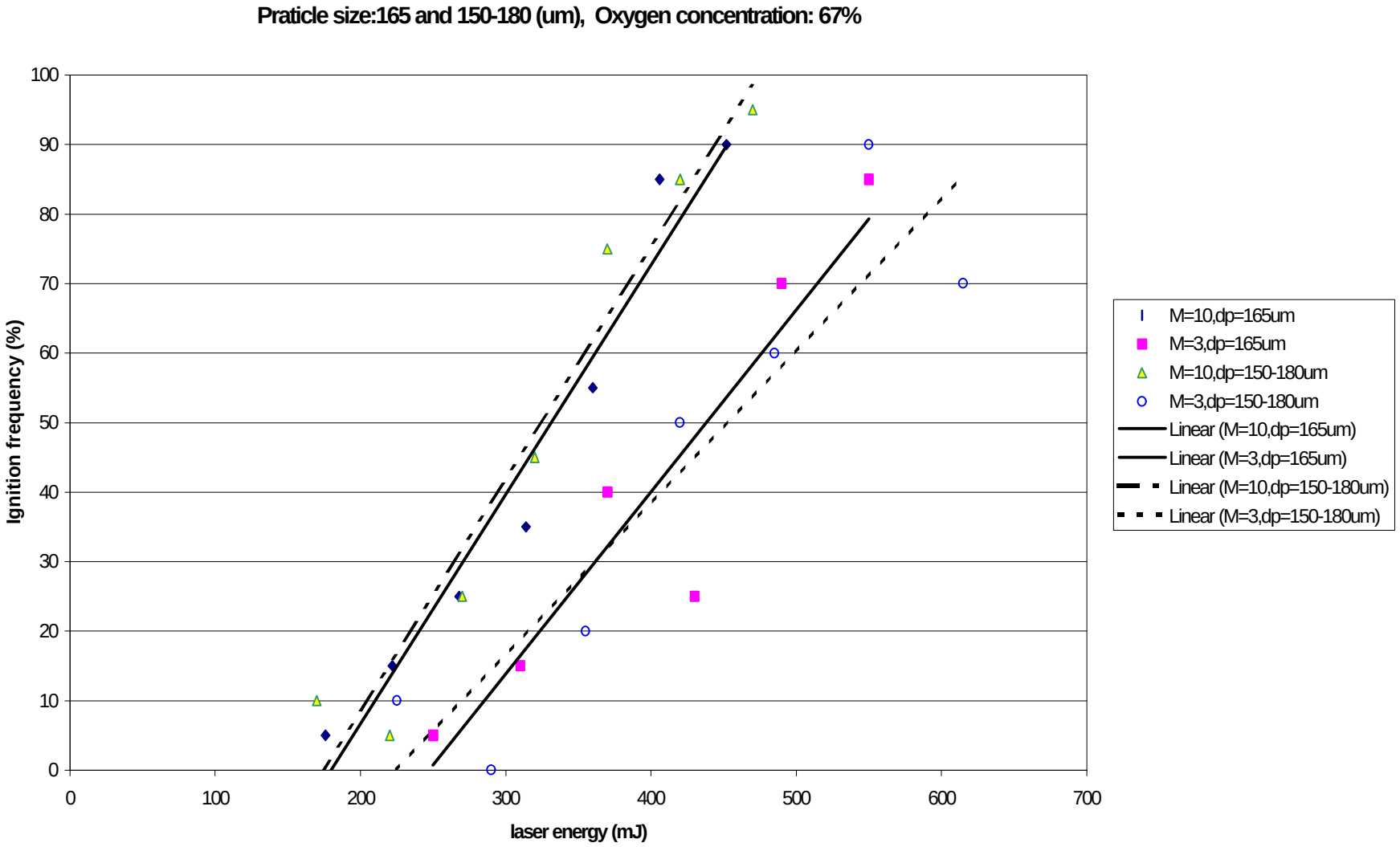

Figure 3.10 Modeling results showing the effect of the average particle size 165μm and the range of particle size150-180 μm on ignition frequency. Oxygen concentration is 67%. All other parameters are as listed in Table 3.1. (a) Solid-line express particle size d_p=165μm; (b) Dash-line express distribution particle size d_p in 150-180μm.

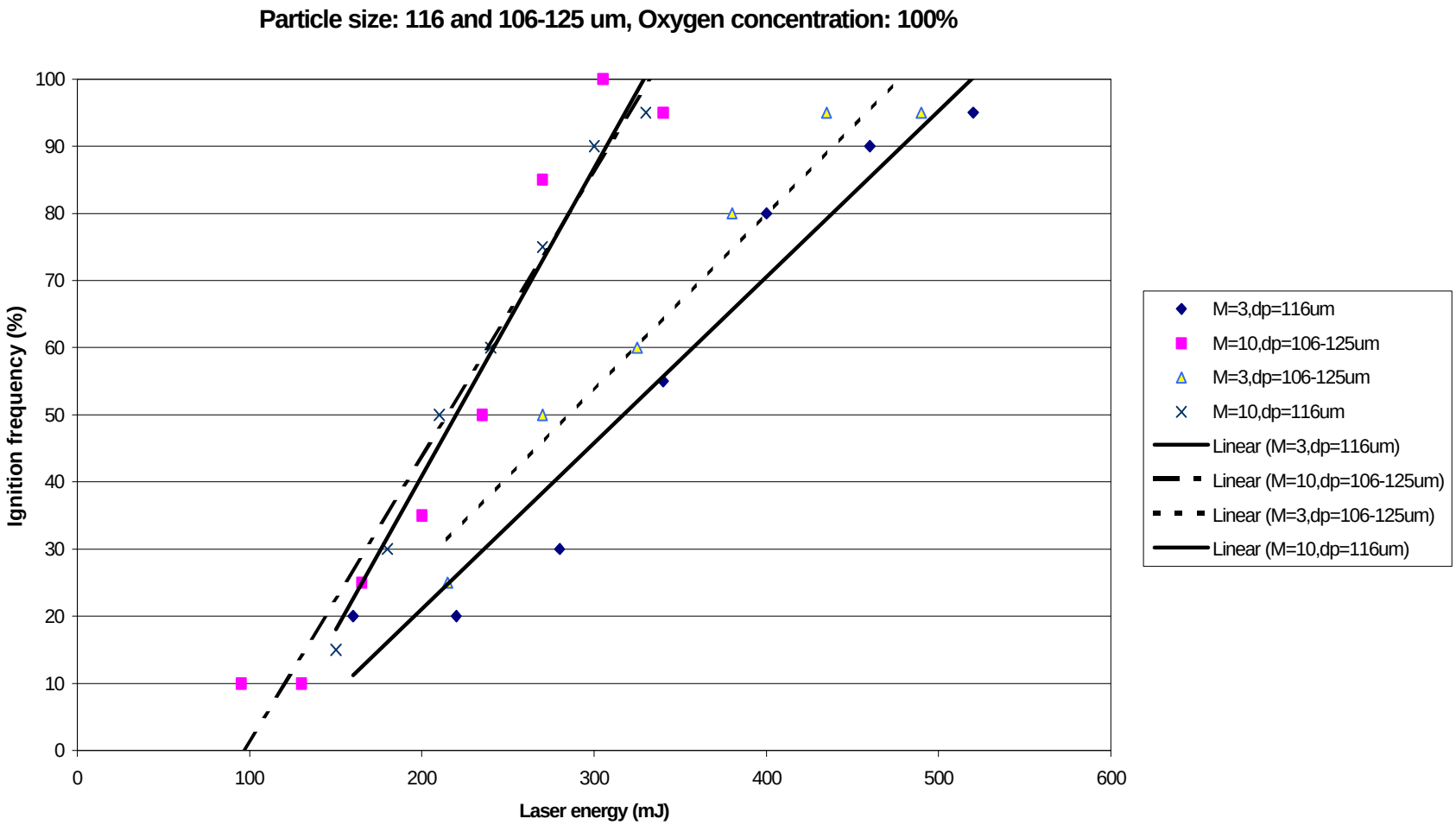
Particle size: 116 and 106-125 um, Oxygen concentration: 100%
Ignition frequency (%)
Laser energy (mJ)
0
10
20
30
40
50
60
70
80
90
100
0
100
200
300
400
500
600
M=3,dp=116um
M=10,dp=106-125um
M=3,dp=106-125um
M=10,dp=116um
Linear (M=3,dp=116um)
Linear (M=10,dp=106-125um)
Linear (M=3,dp=106-125um)
Linear (M=10,dp=116um)

Figure 3.11 Modeling results showing the effect of average particle size 116 μm and the range of particle size 106-125μm in ignition frequency. Oxygen concentration is 100%. All other parameters are as listed in Table 3.1. (a) Solid-line express particle size d_p=116μm; (b) Dash-line express the distribution of particle size d_p in 106-125μm.

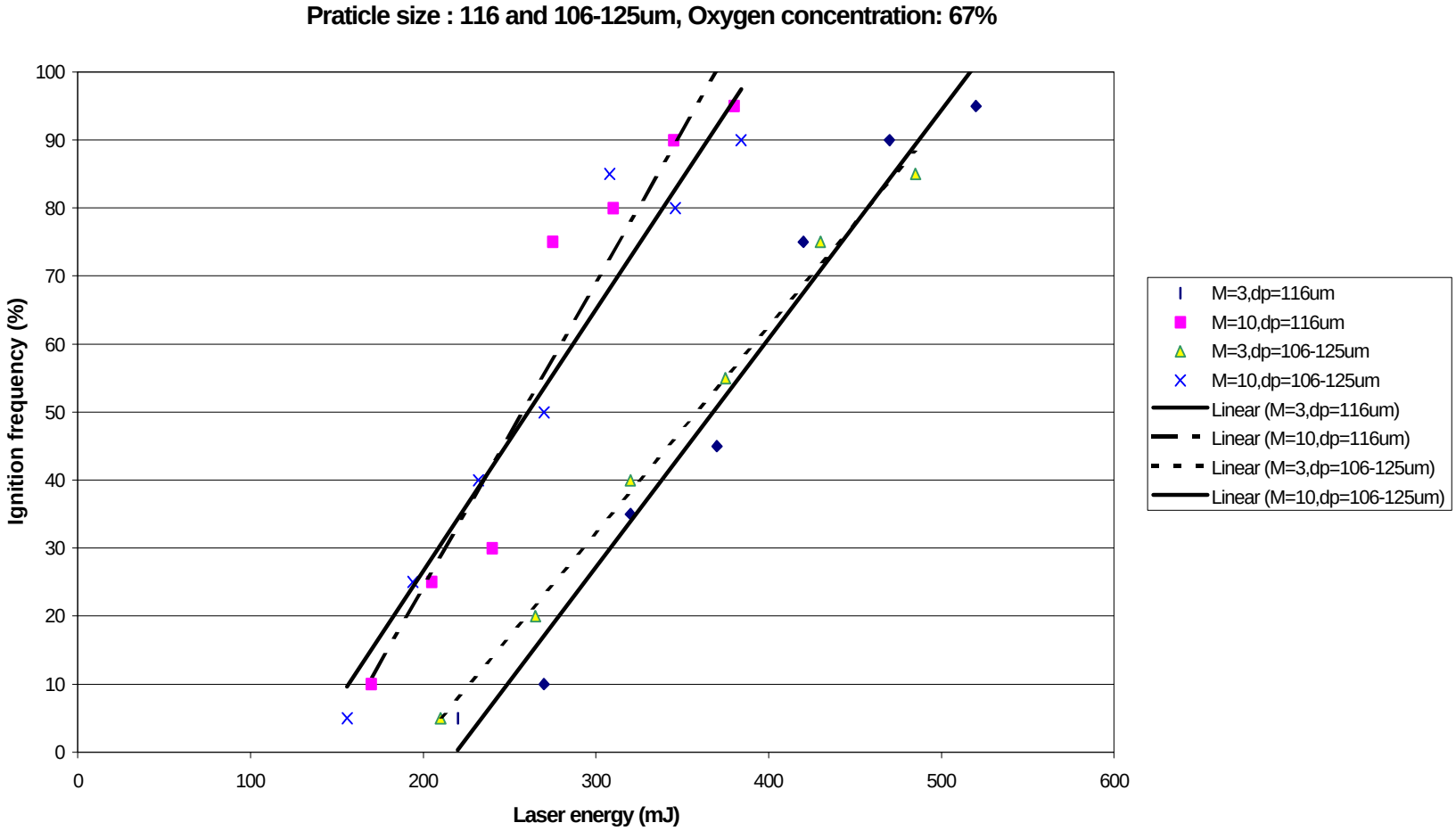

Figure 3.12 Modeling results showing the effect of the average particle size 116 μm and the range of particle size106-125 μm on ignition frequency. Oxygen concentration is 67%. All other parameters are as listed in Table 3.1. (a) Solid-line express particle size d_p=116μm; (b) Dash-line express distribution particle size d_p in 106-125μm.

3.3.2 Results of Simulation Laser Ignition Experiment

The simulations for the experiments were performed via a FORTRAN code (Appendix 3). The code was designed to produce frequency distribution data for a given particle size (diameter, dp) range, oxygen concentration and, temperature of particle and laser pulse energy. As discussed earlier, for each run two particles are selected randomly from 1300 particles. The particle size and activation energy are determined whether or not ignition occurred for the run. For each type coal, the parameters required as input are the average activation energy (E_0), standard deviation for the Gaussian distribution (σ), and pre-exponential factor (A_0).

Figure 3.13-3.15 show the experiment data for the Pittsburgh #8 coal with modeling results using anther method, that calculate average temperature and standard deviation to obtain the range of particle temperature at each condition. Figure 3.16-3.17 show the experiment data for the Pust coal with the modeling results using the range of particle temperature. Figure 3.18 shows the experiment data for the Wyodak coal with the modeling results using the range of particle temperature. The behavior of the model with respect to changes in each of the parameters was first observed. The parameters are then modified to obtain a final set of values to improve the model. The final parameters that fit our laser ignition experimental data of each type coal are given the following table.

Table 3.2 shows all Pittsburgh#8 coal's parameters of Figure 3.13-3.15. There are all Pust coal's parameters of Figure 3.16-3.17 in Table 3.3. There are all Wyodak coal's parameters of Figure 3.18 in Table 3.4.

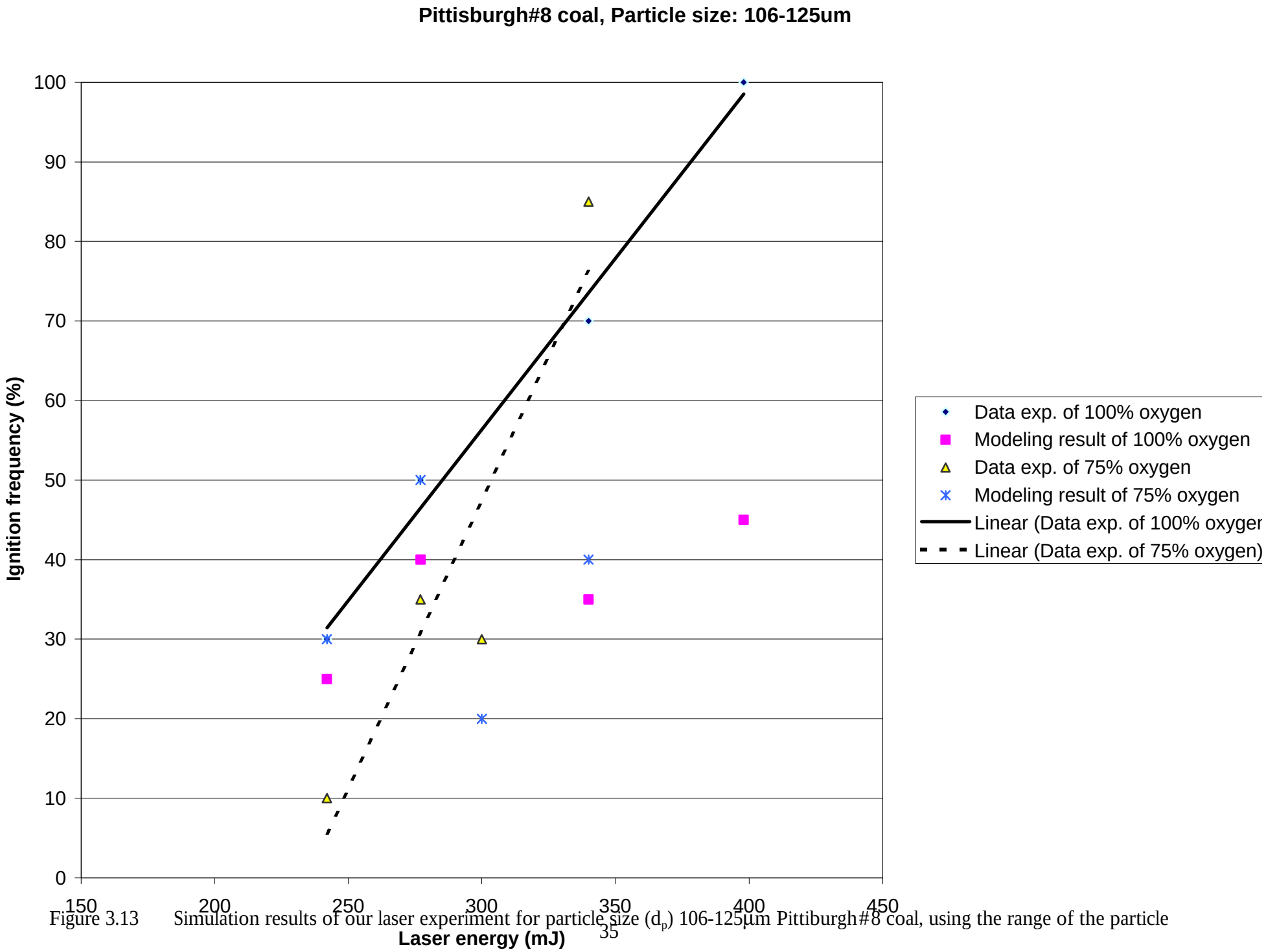

Figure 3.13 Simulation results of our laser experiment for particle size (d_p) 106-125μm Pittiburgh#8 coal, using the range of the particle

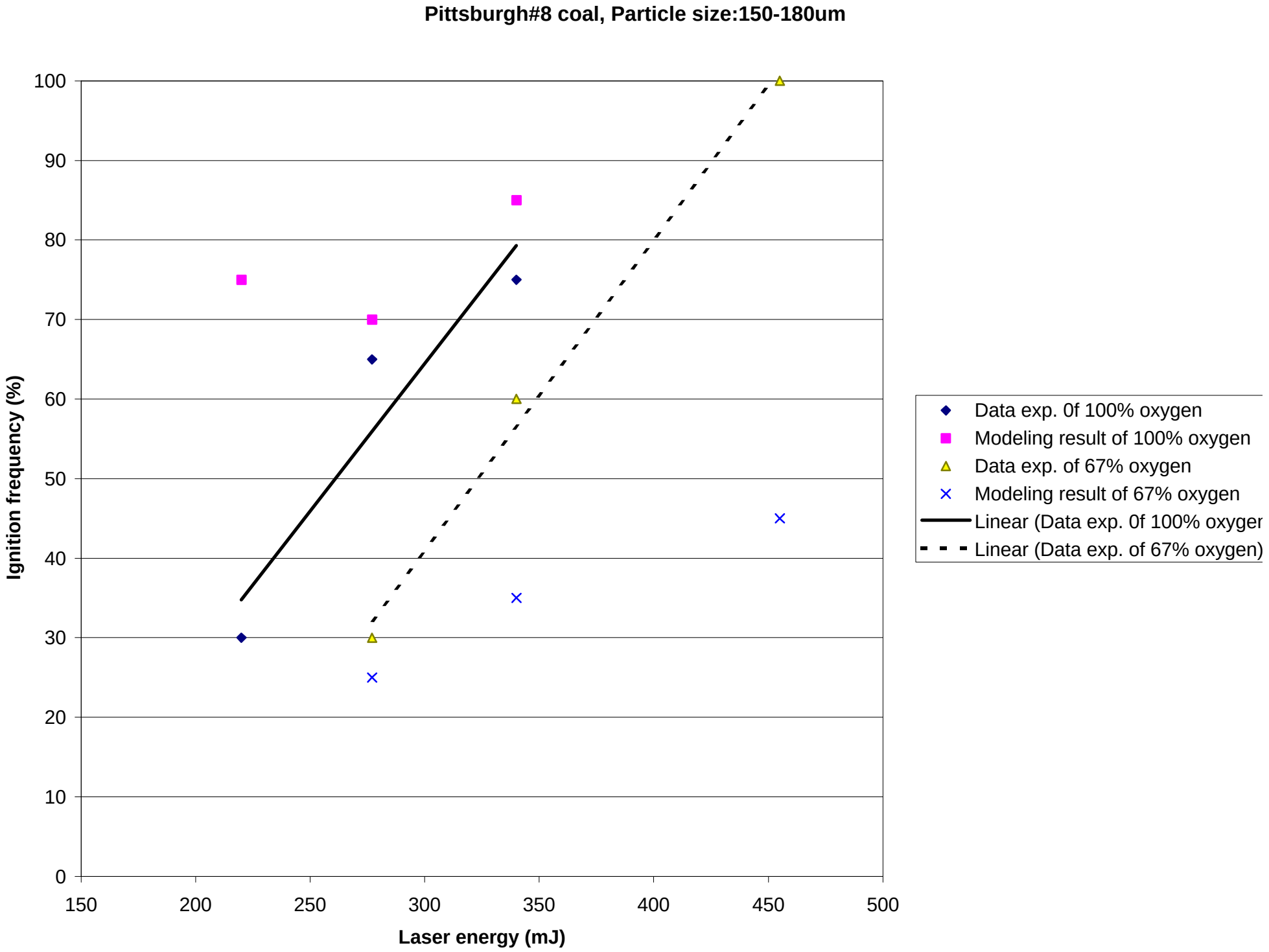
Pittsburgh#8 coal, Particle size:150-180um
Ignition frequency (%)
Laser energy (mJ)
0
10
20
30
40
50
60
70
80
90
100
150
200
250
300
350
400
450
500
Data exp. 0f 100% oxygen
Modeling result of 100% oxygen
Data exp. of 67% oxygen
Modeling result of 67% oxygen
Linear (Data exp. 0f 100% oxyger
Linear (Data exp. of 67% oxygen)

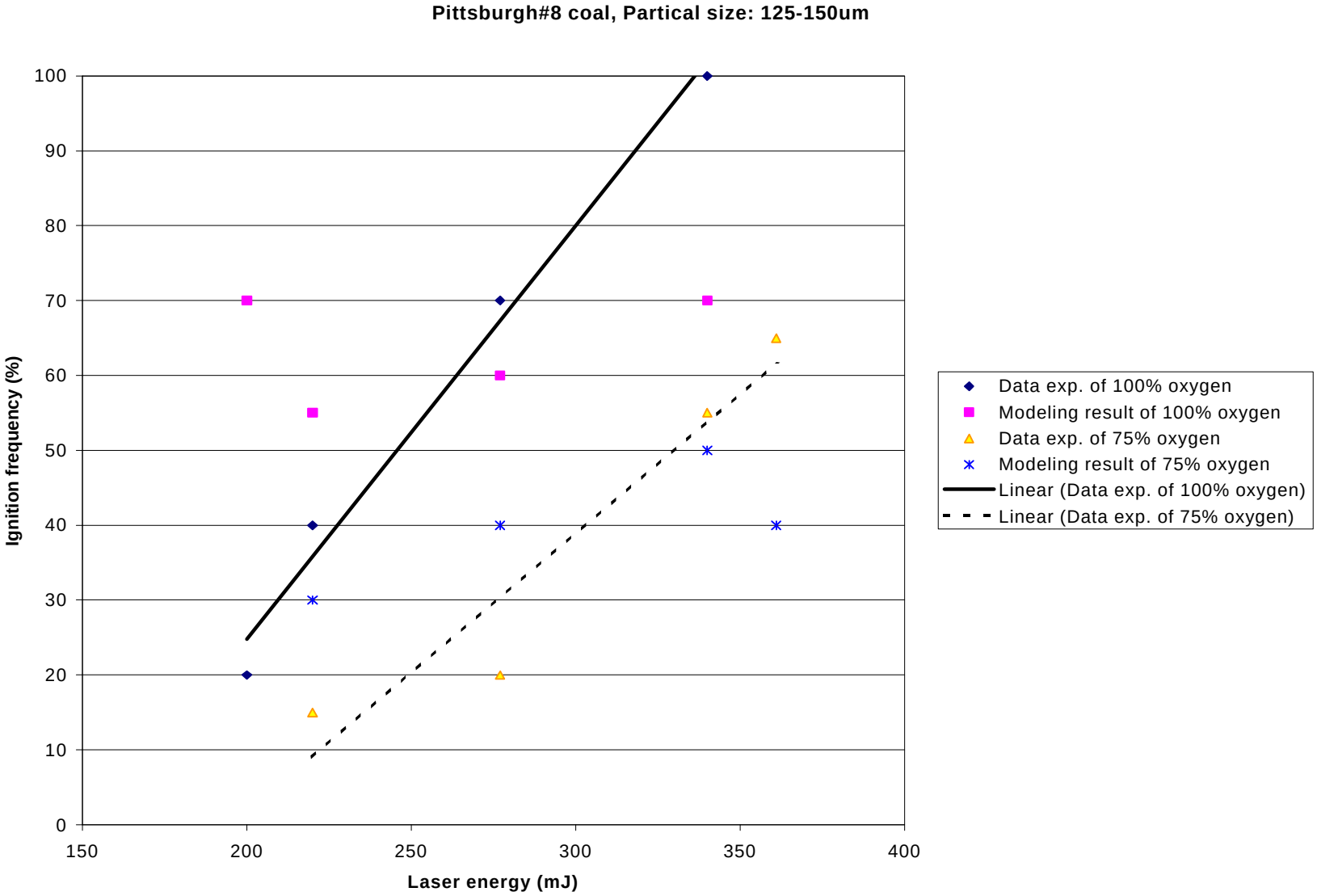

Figure 3.15 Simulation results of our laser experiment for particle size (d_p) 125-150μm Pittiburgh#8 coal, using the range of the particle temperatures. All other parameters are as listed in Table 3.2

Table 3.2 Parameters Simulate Pittsburgh#8 Coal in Laser Ignition Experiment using the range of measured particle temperature

Variable	Value
E_0	135 kJ/mol
A_0	250 kg/m^2s
σ	12 KJ/mol
n	1
ε	0.8

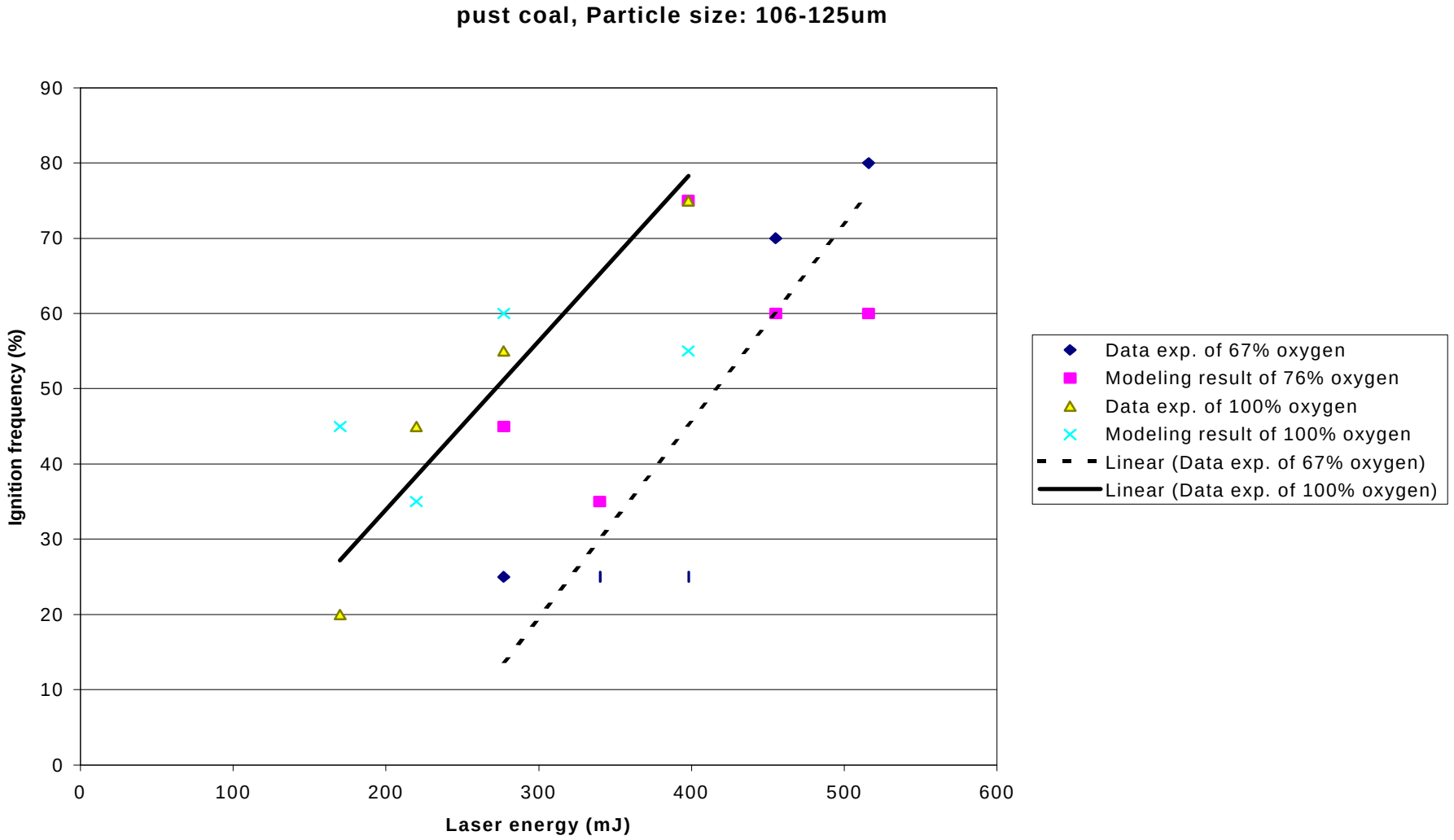

Figure 3.16 Simulation results of the laser Experiment for particle size (d_p) 106-125 μm Pust coal, using the range of the particle temperatures. All other parameters are as listed in table 3.3.

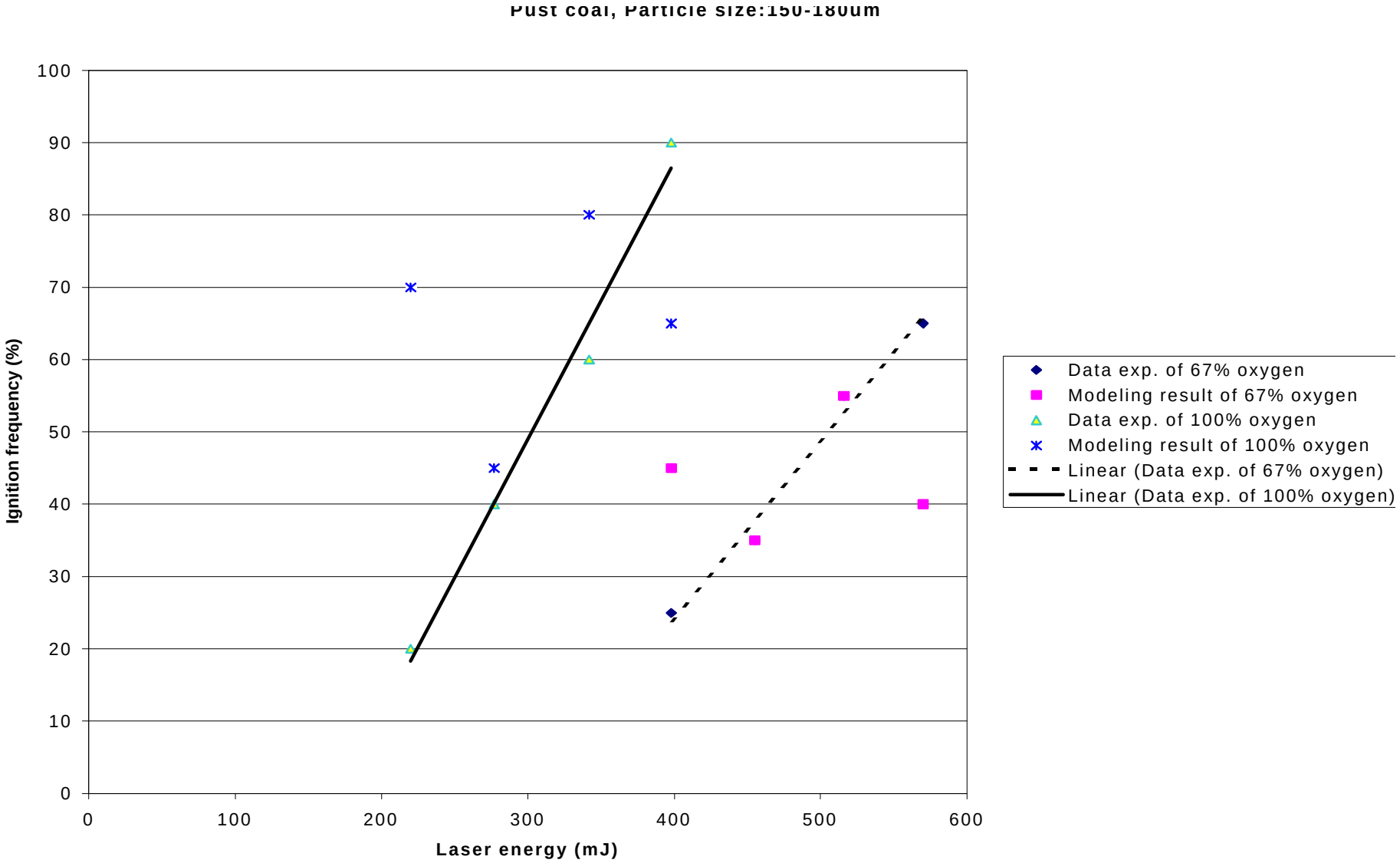

Figure 3.17 Simulation results of the laser Experiment for particle size (d_p) 150-180 μm Pust coal, using the range of particle temperatures. All other parameters are as listed in table 3.3.

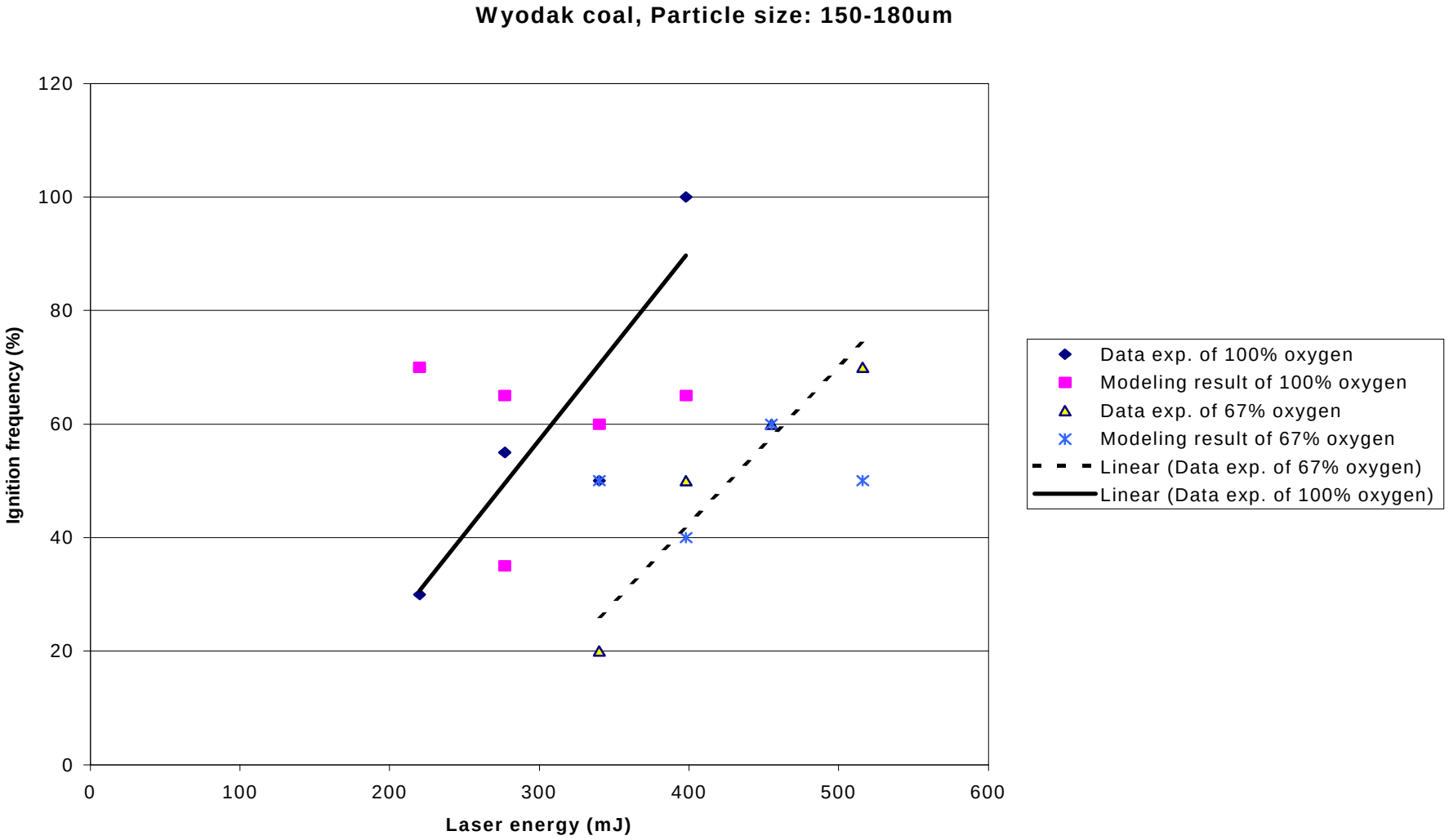

Figure3.18 Simulation results of the laser experiment for particle size 150-180μm Wyodak coal, using the range of particle temperatures. All other parameters are as listed in table 3.4.

Table 3.3 Parameters Simulate Pust Coal in Laser Ignition Experiment

Variable	Value
E_0	120 (kJ/mol)
A_0	200 (kg/m^2s)
σ	40 (KJ/mol)
n	1
ε	0.8

Table 3.4 Parameters Simulate Wyodak Coal in Laser Ignition Experiment

Variable	Value
E_0	115 (kJ/mol)
A_0	100 (kg/m^2s)
σ	40 (KJ/mol)
n	1
ε	0.8

3.3.3 Drop-Tube Experiment

The required simulations for drop-tube experiments have performed by a FORTRAN code (Appendix 2). The code was designed to produce frequency distribution data for a given average particle size (diameter dp) or the maximum diameter (dpmax) and minimum diameter (dpmin) of particle size range, oxygen concentration and, temperature of gas. The particle with the lowest activation energy determines whether or not ignition occurred for a run. The parameters required to be input were average activation energy (E_0), standard deviation for the Gaussian distribution (σ), preexponential factor (A_0) and reaction order (n).

Respectively, Figure 3.19-3.20 show the experiment data for coal#1 and coal#2 with the modeling results using distribution of particle size. There are all parameters of coal#1 and coal#2 for Figure 3.19-3.20 in Table 3.5 and Table 3.6. Figure 3.21-3.22 show the experiment data for coal#1 and coal#2 with the modeling results by average particle size. These parameters of coal#1 and coal#2 for Figure 3.21-3.22 are listed in Table 3.7 and Table 3.8.

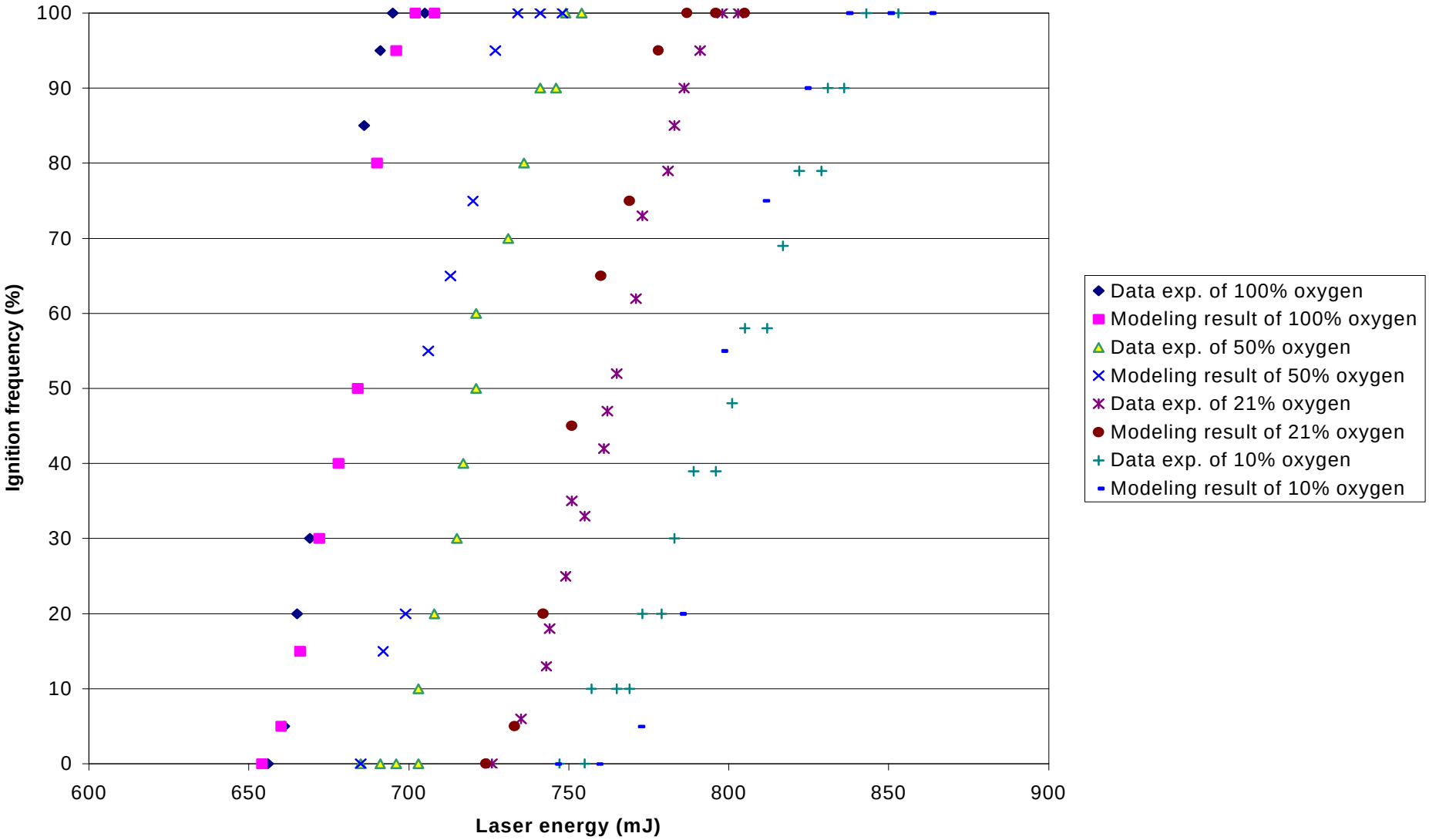

Figure3.19 Simulate result of drop-tube experiment [4] for particle size 75-90μm coal #1, using distribution particle size is incorporated into the DAEMI. All other parameters are as listed in Table 3.5.

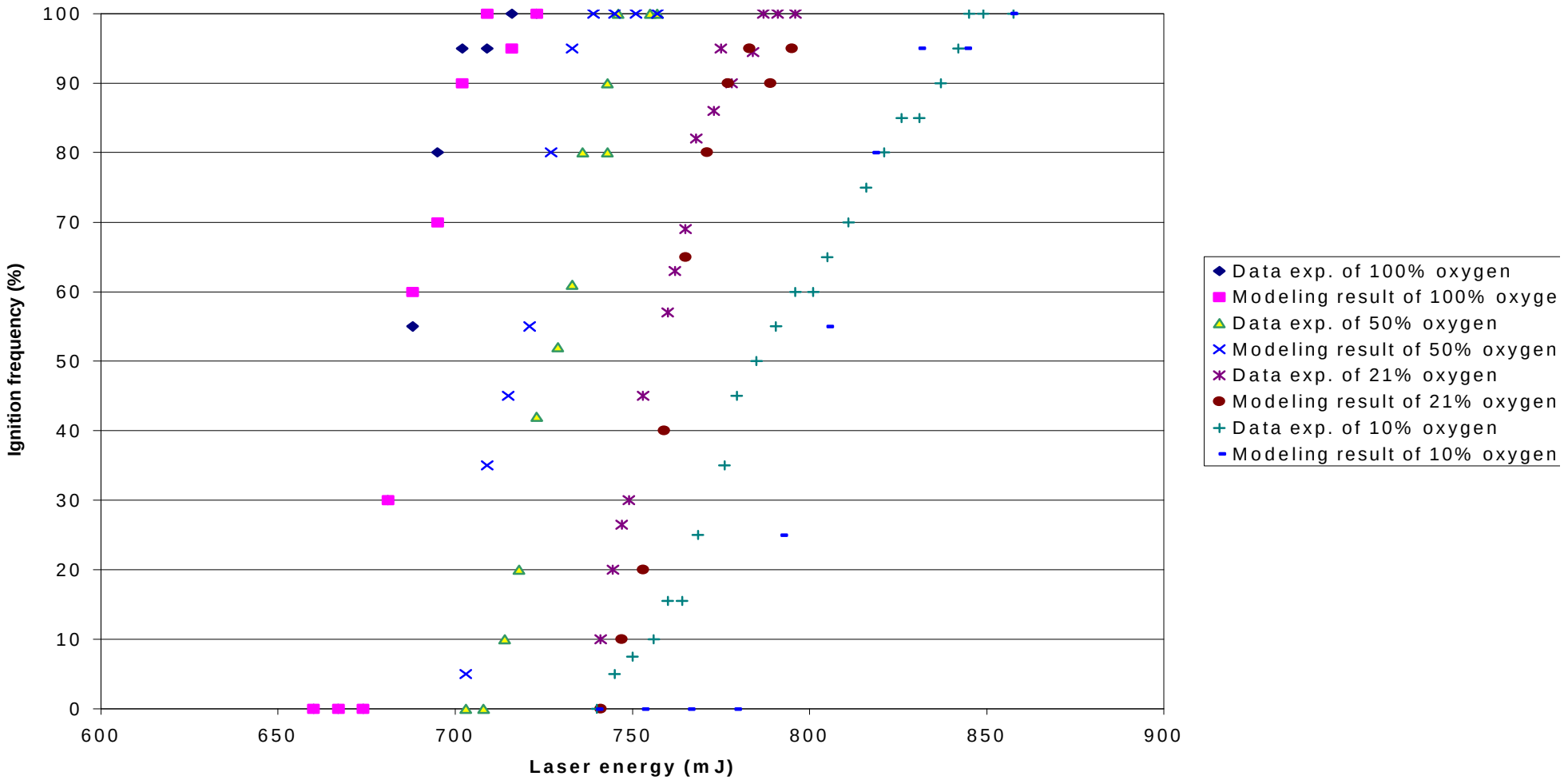

Figure 3.20 Simulation results of drop-tube experiment [1] for particle size 75-90 μm coal#2, using distribution particle size is incorporated into the DAEMI. All other parameters are as listed in Table 3.6.

Table 3.5 Parameters Simulate cola#1 in Drop-Tube Experiment [4] (Using distribution of particle size in DAEMI)

Variable	Value
E_0	70.0 (kJ/mol)
A_0	300.0 (kg/m^2s)
σ	1.0 (KJ/mol)
n	0.5
ε	0.8

Table 3.6 Parameters Simulate cola#2 in Drop-Tube Experiment [4] (Using distribution of particle size in DAEMI)

Variable	Value
E_0	71.0 (kJ/mol)
A_0	320.0 (kg/m^2s)
σ	1.0 (KJ/mol)
n	0.5
ε	0.8

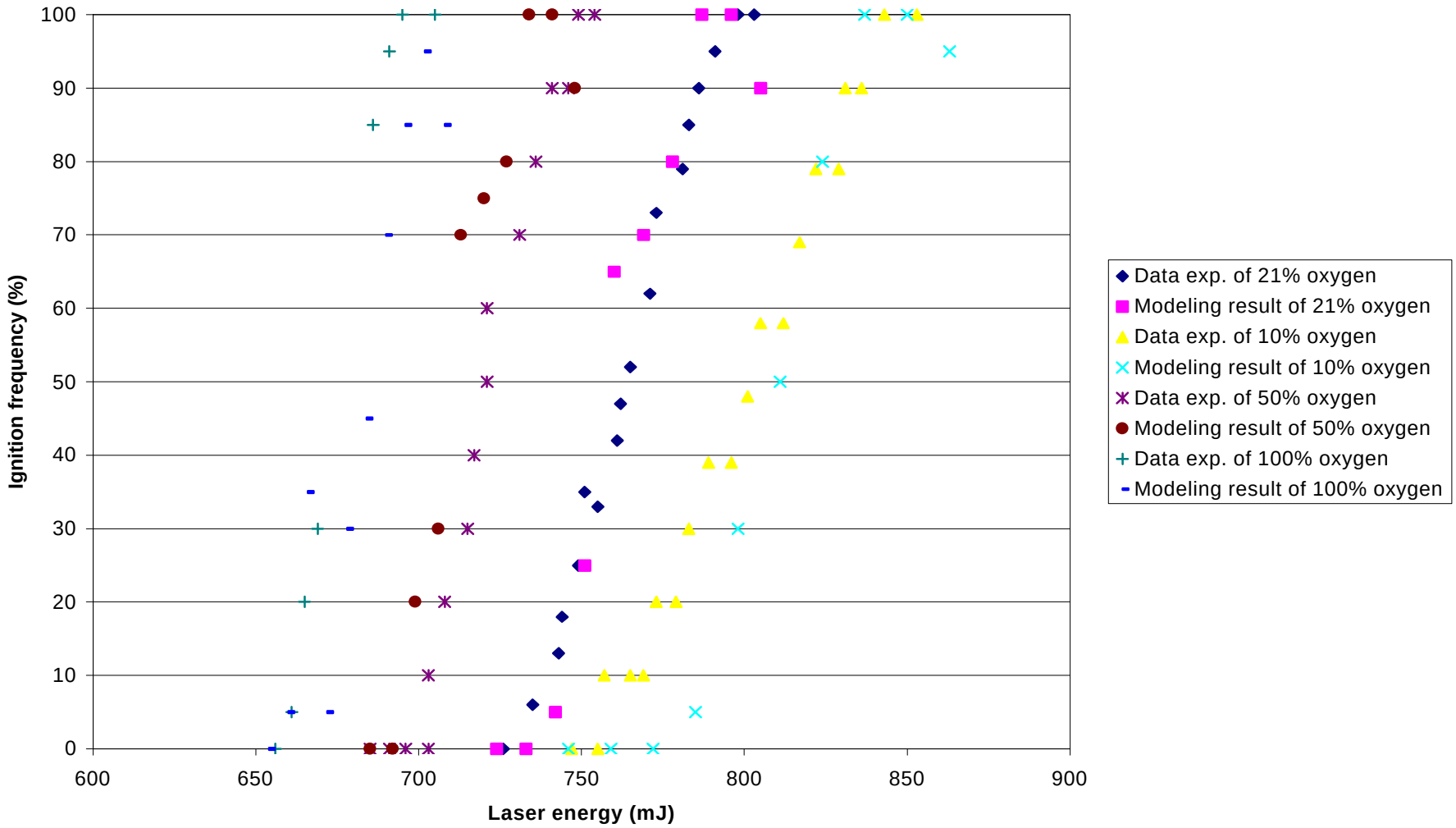

Figure 3.21 Simulation results of drop-tube experiment [4] for particle size 83 μm coal #1. All other parameters are as listed in Table 3.7.

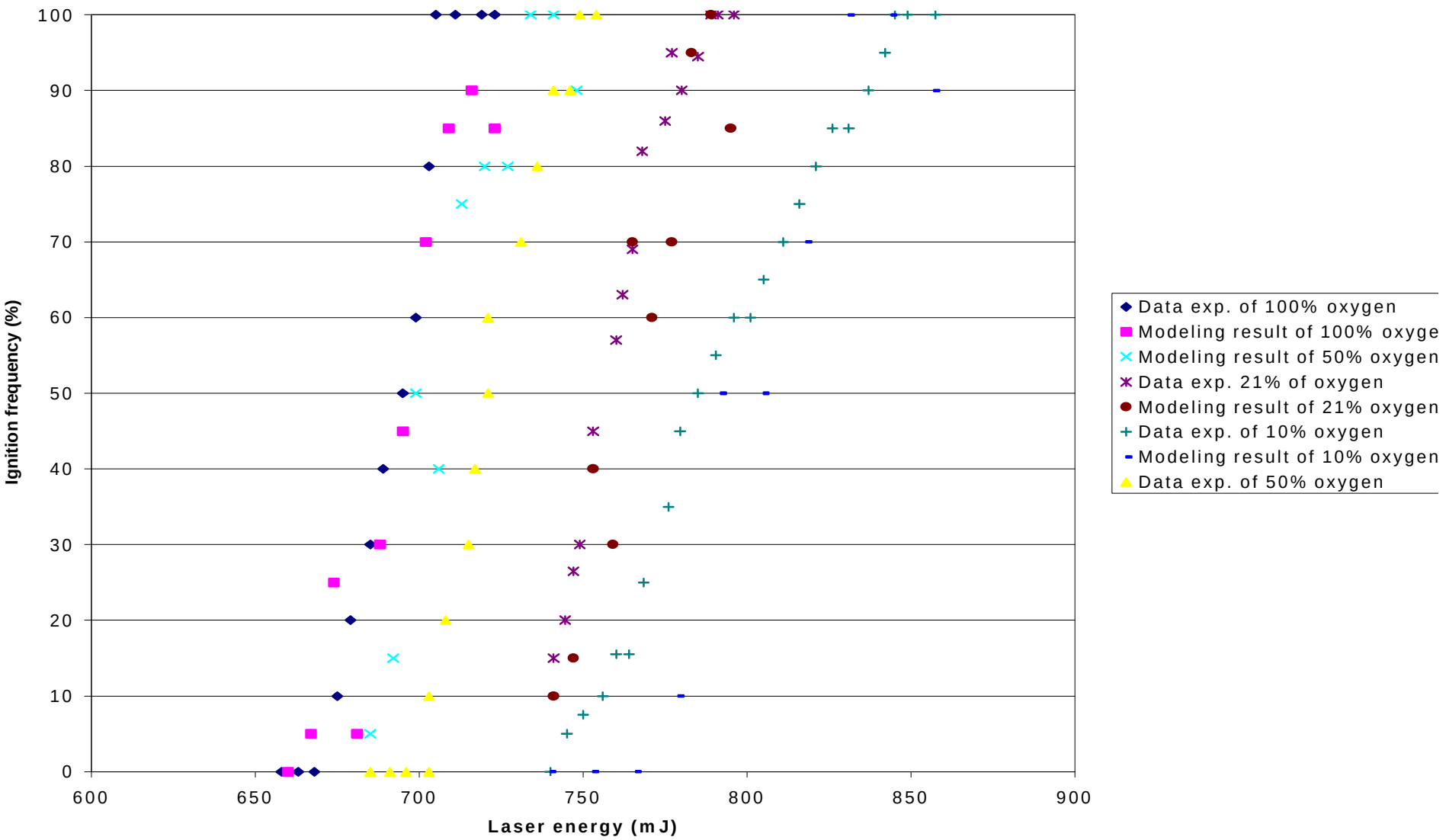

Figure 3.22 Simulation results of drop-tube experiment [4] for particle size 83 μm coal #2. All other parameters are as listed in Table 3.8

Table 3.7 Parameters Simulate cola#1 in Drop-Tube Experiment [4], using the average particle size.

Variable	Value
E_0	92 (kJ/mol)
A_0	110 (kg/m^2s)
σ	10 (KJ/mol)
n	0.44
ε	0.8

Table 3.8 Parameters Simulate cola#2 in Drop-Tube Experiment [4], using average particle size.

Variable	Value
E_0	98.6 (kJ/mol)
A_0	111 (kg/m^2s)
σ	12 (KJ/mol)
n	0.37
ε	0.8

DISCUSSION OF RESULTS

4.1 Comparison with Drop-Tube Experiment

Either the range of particle size (75-90μm) or the average particle size (83μm) can be used in the current version of DAEMI. The DAEMI can be fitted to the experimental data [4] shown in Figures 3.19-3.22. Figures 3.19-22 also shown the almost same effect of Distribution Particle Size in 75-90 μm and average particle size 83 μm on ignition frequency for oxygen concentration from 10% to 100%. The small standard deviation, σ (1.0 kJ/mol) is used to obtain the results from the current version of DAEMI using the distribution of particle size and the average particle size. The narrow distribution (small standard deviation) leads to a small energy range since most particles have similar activation energies. This behavior is due to the fact that a distribution of reactivity exists among the particles. The particle diameters are randomly selected from the range of particle size to calculate the critical activation energy. Different particle diameters correspond to the different critical activation energies. When the different critical activation energy is larger than the activation energy that a particle has, that particle is considered ignition.

The larger σ (10.0-12.0 kJ/mol) is used to obtain the modeling results from the old version of DAEMI using the average particle size. Since the subsidiary simulation condition is that the particle own the lowest activation energy in the batch could be ignited. According to the experiment phenomenon, it is not always true that only the particle own the lowest activation energy can be ignited. In Tables 3.7-3.8, these parameters that were obtain by consider the particle in the batch of 1170 particles could has the lowest activation

energy was ignited, are different with E_0=84.0 kJ/ml, σ=4.0 kJ/mol and n=0.4 that Dr. Chen got from the batch of 100 particles before. So the different simulation process and experiment value obtain the different simulation parameter.

Figures 3.19-3.22 show the effect of oxygen concentration for both the modeling results and experiment data: As oxygen level is decreased from 100% to 10%, the frequency distribution shifts to higher laser energies or, equivalently, higher particle temperatures. This is consistent with ignition theory since at decreased oxygen levels, higher temperatures are necessary for heat generations (due to chemical reactions) that exceed the heat loss from the particles and leads to ignition.

As shown in Tables3.5-3.6, whether we used the distribution of particle size or the average particle size, the modeling result that is obtained by one set of parameters only fits the experiment data of one type of coal. The results show clearly that ignition reactivity is strongly dependent on the coal type. Particle-to-particle variation in physical and/or chemical property of the fuel can be accounted for in order to model the ignition data correctly, and to accurately describe the ignition reactivity. In the future research, statistical test should be used to calculate the confidence intervals, according to a specified significance level to decide on the best set of ignition reactivity parameters.

According to the experimental data, for same coal type, oxygen concentration and particle size, ignition frequency increases with increasing gas temperature. This case is similar to the base case, namely, ignition frequency increases with particle or gas temperature. So the modeling results fit the Drop-Tube experiment data [4] of one particle size. The simulation gave the best results for the 75-90 μm coal#1 particle using E_0=70.0

kJ/mol, σ=1.0 kJ/mol, A_0=300 kg/m^2s, n=0.5. The model also was found to give the best fit to the 75-90 μm coal#2 particle for E_0=71.0 kJ/mol, σ=1.0 kJ/mol, A_0=320 kg/m^2s, n=0.5. It is also found that using n=1.0 difficult to fit to the experiment data [4].

4.2 Comparison with Laser Experiment

For the laser experiment, the DAEMI incorporated the distribution of particle size. The modeling results and the experimental data are shown in Figures 3.13-3.18. These figures all show the effect of oxygen concentration for both the modeling results and experimental data at the same particle size. As the oxygen level is decreased from 100% to 67%, the frequency distribution shifts to higher laser energies, this phenomenon is same as the Drop-Tube experiment. Using those different experimental techniques, we could improve the ignition theory.

Figures 3.13-18 and Tables 3.2-3.4 indicate that the model could account for particle-to-particle variations in reactivity by having a single pre-exponential factor and a Gaussian distribution of activation energies among the particles within a type coal (a sample). The simulation gives final result for the Pust coal all over the laser energies considered, the oxygen concentration and particle size using E_0=120.0 kJ/mol, σ=40.0 kJ/mol, A_0=200 kg/m^2s, n=1.0. The modeling results fit the Wyodak coal all over the laser energies, the oxygen concentration and the particle size using E_0=115.0 kJ/mol, σ=40.0 kJ/mol, A_0=100 kg/m^2s, n=1.0. The modeling results also fit the Pittsburgh#8 all over the laser energy, the oxygen concentration and the particle size using E_0=135.0 kJ/mol, σ=12.0 kJ/mol, A_0=250 kg/m^2s, n=1.0.

The measured particle temperatures of Pust and Wyodak coal are lower than the Pittsburgh#8. The simulation result of Pust and Wyodak are better than that of the Pittsburgh#8. The heat generated by a spherical carbon particle undergoing oxidation on its external surface, it is determined by the kinetic expression and the oxidant diffusion expression. At the lower range of particle temperature, the heat is mainly generated by the kinetic expression; at the higher range of particle temperature, the heat is mainly generated by the oxidant diffusion expression. In the current version of DAEMI, the generated heat is considered to be by the kinetic expression. So the simulation result of coal at the lower particle temperature is better than that at the higher particle temperature.

Figure 4.1 shows the measured particle temperature of the laser experiment. According to the DAEMI, the ignition frequency increases with increasing laser energy. The reason could be effect of the distribution of activation energies among the particles within a sample. When the higher laser energy is used, the ignition could happen between the higher and lower activation energy levels, so the ignition frequency at higher laser energy is higher than that at the lower laser energy. For each activation energy, we can calculate the particle temperature by the ignition theory, the higher range of particle temperature is obtained by the higher laser energy. But the measured particle temperatures of the laser experiment are not like this shown in Figure 4.1.

For the base case, Figures 3.9-3.12 also show the same effect of Distribution Particle Size in 106-125 μm, 150-180 μm and average particle size 116 μm, 165 μm on ignition frequency for oxygen concentration 67% and 100%.

For the heterogeneous coal ignition, it is well known that the product of carbon oxidation is both CO and CO_2, and the reaction order n is depended on the carbon

oxidation. The proportion of the product CO and CO_2 could assume is different using the different ignition experimental mechanism. Since the different particle temperature was obtained by the different ignition experimental mechanism [3]. So the reaction order n=0.5 obtained from simulating the Drop-Tube experiment, n=1.0 obtained from simulating the laser ignition experiment.

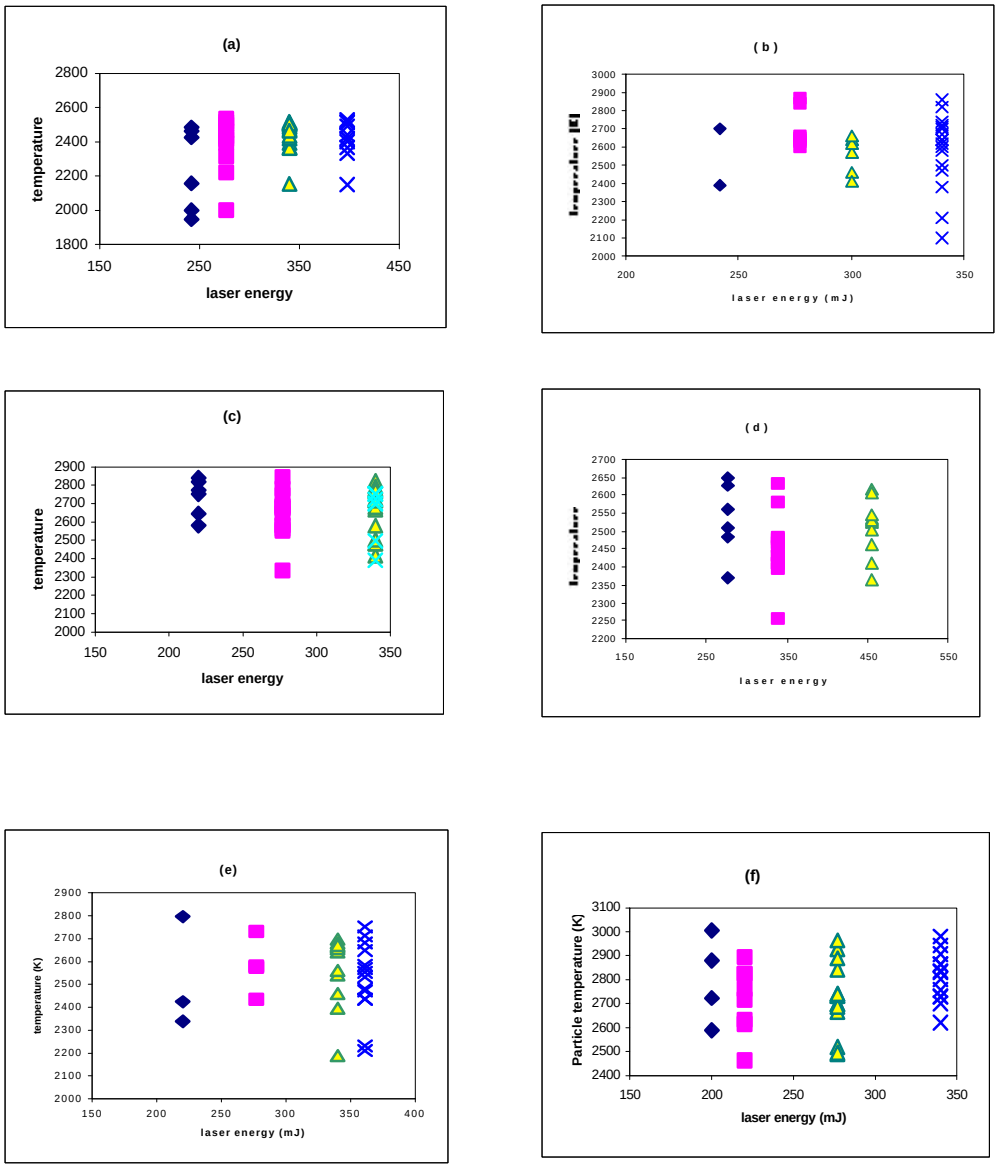

Figure 4.1 Temperature distribution versus laser energy for Pittsburgh#8 coal. (a) Particle size: 106-125μm, O_2: 100%; (b) Particle size: 106-125μm, O_2: 75%; (c) Particle size: 150-180μm, O_2: 100%; (d) Particle size: 150-180μm, O_2: 67%; (e) Particle size: 125-150μm, O_2: 75%; (f) Particle size: 125-150μm, O_2: 100%.

Disclaimer

Abstract

Under typical conditions of pulverized-coal combustion, which is characterized by fine particles heated at very high rates, there is currently a lack of certainty regarding the ignition mechanism of bituminous and lower rank coals. It is unclear whether ignition occurs first at the particle-oxygen interface (heterogeneous ignition) or if it occurs in the gas phase due to ignition of the devolatilization products (homogeneous ignition). Furthermore, there have been no previous studies aimed at determining the dependence of the ignition mechanism on variations in experimental conditions, such as particle size, oxygen concentration, and heating rate. Finally, there is a need to improve current mathematical models of ignition to realistically and accurately depict the particle-to-particle variations that exist within a coal sample. Such a model is needed to extract useful reaction parameters from ignition studies, and to interpret ignition data in a more meaningful way.

We propose to examine fundamental aspects of coal ignition through (1) experiments to determine the ignition mechanism of various coals by direct observation, and (2) modeling of the ignition process to derive rate constants and to provide a more insightful interpretation of data from ignition experiments.

We propose to use a novel laser-based ignition experiment to achieve our objectives. The heating source will be a pulsed, carbon-dioxide (CO_2) laser in which both the pulse energy and pulse duration are independently variable, allowing for a wide range of heating rates and particle temperatures — both of which are decoupled from each other and from the particle size. This level of control over the experimental conditions is truly novel in ignition and combustion experiments. Laser-ignition experiments also offer the distinct advantage of easy optical access to the particles because of the absence of a furnace or radiating walls, and thus permit direct observation and particle temperature measurement. The ignition mechanism of different coals under various experimental conditions can therefore be easily determined by direct observation with high-speed photography. The ignition rate-constants, when the ignition occurs heterogeneously, and the particle heating rates will both be determined from analyses based on direct, particle-temperature measurements using two-color pyrometry.

For the modeling portion of this study we will complete the development of the Distributed Activation Energy Model of Ignition (DAEMI), which simulates the conventional drop-tube furnace ignition experiment. The DAEMI accounts for particle-to-particle variations in reactivity

by having a single preexponential factor and a Gaussian distribution of activation energies among the particles. Previous results show that the model captures the key experimental observations, and that adjustments to the model parameters permit a good fit to experimental data. We will complete the model by (1) examining the effects of other variations in physical parameters on the model, (2) applying the model to published results in order to extract reaction parameters, and (3) extending the model for application to laser-based ignition studies, such as our own.

Table of Contents

Executive Summary

During the past reporting period, modifications to the DAEMI were completed. The changes were implemented to examine two aspects of ignition modeling: (1) the effect of varying the number of particles chosen to interact with the laser, and (2) the size distribution for particle sizes.

We have also completed making initial measurements of the ignition temperatures of a suite of coals at three oxygen concentrations, and for three particle size ranges. The reduction of this data from raw signals to temperatures has begun, and we expect it to be completed during the next reporting period.

Introduction

The ignition of pulverized coal has been the subject of research for nearly 150 years, with the initial motivation being the avoidance of coal-dust explosions in mines. In more recent times, due to the world's increased reliance on coal for power generation and the need to maximize energy-conversion efficiency, research has shifted to understanding the fundamental mechanism of coal ignition and measuring its kinetic rates. The importance of ignition to coal-flame stability is obvious — the more easily a particular coal ignites after injection into a boiler furnace, the better its flame-stability characteristics. A less obvious ramification of the ignition process is its role in establishing extended, fuel-rich zones in coal flames which are responsible for the destruction of NOx and its conversion to benign N_2. Certainly, the ignition process is inextricably linked to the formation of this NOx-reduction zone, and the ignition behavior of coals and coal blends will strongly affect the ease and extent of formation of this zone. This connection is deserving of further study and its understanding is the goal toward which we hope to apply the results of this proposed study. Specifically, we propose to examine fundamental aspects of coal ignition through (1) experiments to elucidate the ignition behavior of coals, and (2) modeling of the process to derive accurate and useful rate constants, and to provide a more insightful interpretation of data from ignition experiments.

Objectives

Our objectives for this project are to:

1. develop a novel experimental facility with extensive optical-diagnostic capabilities to study coal ignition;
2. determine the ignition mechanism of coals under simulated combustion conditions by direct observation with high-speed photography;
3. examine the effects of various experimental conditions, including coal rank, particle size, oxygen concentration and heating rate, on the ignition mechanism; and
4. measure the ignition rate constants of various coals.
5. modify our existing ignition model to examine the effect of particle-size distribution on the ignition behavior;
6. incorporate, if necessary, a size distribution into the model;
7. apply the model to extract ignition rate constants from previously published data from conventional experiments;

8. modify the model and apply it to our laser-based ignition studies for determination of ignition rate constants.

Results from This Reporting Period and Discussion

During the past reporting period, we have made excellent progress on model development for this project. We are nearing completion of two manuscripts for submission and possible publication. The first, "The Ignition Behavior of Pulverized Coals," concerns mainly the experimental measurements that we have obtained, and interprets these measurements in terms of the model in its current form. The second manuscript, "Modeling the Ignition of Pulverized Coals," will focus on the current modifications to the Distributed Activation Energy Model of Ignition (DAEMI) which we are in the process of implementing, along with some supporting experimental measurements.

Personnel

The MS-candidate student working on the experiment portion of this project, Ms. Vida Agyeman, has taken maternity leave as of late September. She has recovered and is back to attend classes. We expect that she will return to full time work on this project by the end of this calendar year.

The MS-candidate working on the modeling portion of this project, Ms. Jianping Zheng, has completed her thesis and will be defending it on November 13, 1998. A portion of her draft thesis, completed on October 22, 1998, is included as an appendix to this report, and forms the bulk of the work completed during the past reporting period.

Finally, Professor John Chen, the Project Director for this project, has resigned his position at North Carolina A&T State University, and is currently an Associate Professor of Mechanical Engineering at Rowan University, effective August 1998. Professor Chen will continue to consult on this project, which has been transferred to Dr. Samuel Owusu-Ofori, Professor of Mechanical Engineering at North Carolina A&T State University.

Computational Model

A portion of Ms. Jianping Zheng's MS thesis, titled "Modeling the Ignition Behavior of Pulverized Coals," is included as Appendix A of this report. The two sections included are Model Analysis and Results, and Discussion.

Experiment

During the past reporting period we have completed the measurement of ignition temperatures for a suite of four coals (Pittsburgh #8 high-volatile bituminous, Pocahontas low-volatile bituminous, Wyodak subbituminous, and Pust lignite) at three oxygen concentrations, and for two or three particle size ranges. The data reduction is currently underway to convert the raw signal measurements to temperatures. We expect this to be completed during the next reporting period. The complete set of data will be used as inputs to the modified Distributed Activation Energy Model of Ignition (DAEMI).

Meetings and Conferences

A paper describing the results contained in this report was prepared and submitted to the 1999 Combustion Institute Joint US National Meeting, to be held in March 1999 in Washington, DC.

At the Spring 1998 American Chemical Society National Meeting, we presented a paper describing our research. This paper, co-authored by John Chen, Maurice Richardson, and Jianping Zheng, won the Richard A. Glenn Award, the Fuel Chemistry Division's Best Paper Award.

Goals for Next Quarter

During the next reporting period, we will complete the data reduction for the temperature measurements made during this summer. The data will form the basis for further model development using the DAEMI.

Appendix A

MODEL ANALYSIS AND RESULTS

3.1 Introduction Experiment

3.1.1 Laser Ignition Experiment

The experimental setup consists of a wind tunnel, gas flow system, coal feeder, detector, laser gate, pulse generators laser and Optical system.

Figure 3.1 shows a schematic of the laser ignition experiment. Sieve-sized coal particles are dropped batch-wise into a laminar upward-flow wind tunnel with quartz test section (5cm square cross-section). The gas is not preheated, The gas flow rate was set so that the particles emerged from the feeder tube, fell approximately 5 cm, then turned and traveled upward out of the tunnel. This ensured that the particles were moving slowly downward at the ignition point, chosen to be 2 cm below the feeder-tube exit.

A single pulse from a Nd:YAG laser was focused through the rest section, then defocused after exiting the test section, and two sides in this manner achieved more spatial uniformity and allowed for higher energy input than a single laser pass. For nearly every case, one to three particles were particles were contained in the volume formed by the two intersecting beams, as determined by previous observation with high-speed video.

The laser operated at 10 Hz and emitted a nearly collimated beam (6 mm diameter) in the near-infrared (1.06 μm wavelength). The laser pulse duration was 100 μs and the pulse energy was fixed at 830 mJ per pulse, with pulse-to-pulse energy fluctuations of less than 3%. The laser pulse energy delivered to the test section was varied by a polarizer placed outside of the laser head, variation from 150 to 750 mJ was achieved by rotating

the polarizer. Increases in the laser pulse energy result in heating of the coal particles to higher temperatures. At the ignition point the beam diameter normal to its propagation direction was 3 mm on each pass of the beam. An air-piston-driven laser gate (see Fig. 3.1) permitted the passage of a single pulse to the test section. The system allowed for control of the delay time between the firing of feeder and he passage of the laser pulse. Finally, ignition or non-ignition was determined by examining the signal generated by a high-speed silicon photodiode connected to a digital oscilloscope. Figure 3.2 presents typical signal traces from the photodetector for both ignition and non-ignition events. Features of the trace for the ignition case is similar to that described previously.

Particle temperature was measured by two-wavelength pyrometry. A simple lens coupled to an optical fiber bundle collected light emitted by the igniting particles. The output from the fiber bundle is collimated and separated into two beams via a dichroic filter. Light of wavelengths below 0.75 μm (the dichroic filter's cut-off wavelength) was passed through a bandpass interference filtered centered at 0.7 μm with a optical bandwidth of 40 nm. The remaining light was passed through an interference filter centered at 0.9 μm with an optical bandwidth of 10 nm. Separate high-speed silicon photodiodes detected each beam following the optical filters. The pyrometer was calibrated using a 2-mm diameter blackbody source at 990^{o}C.

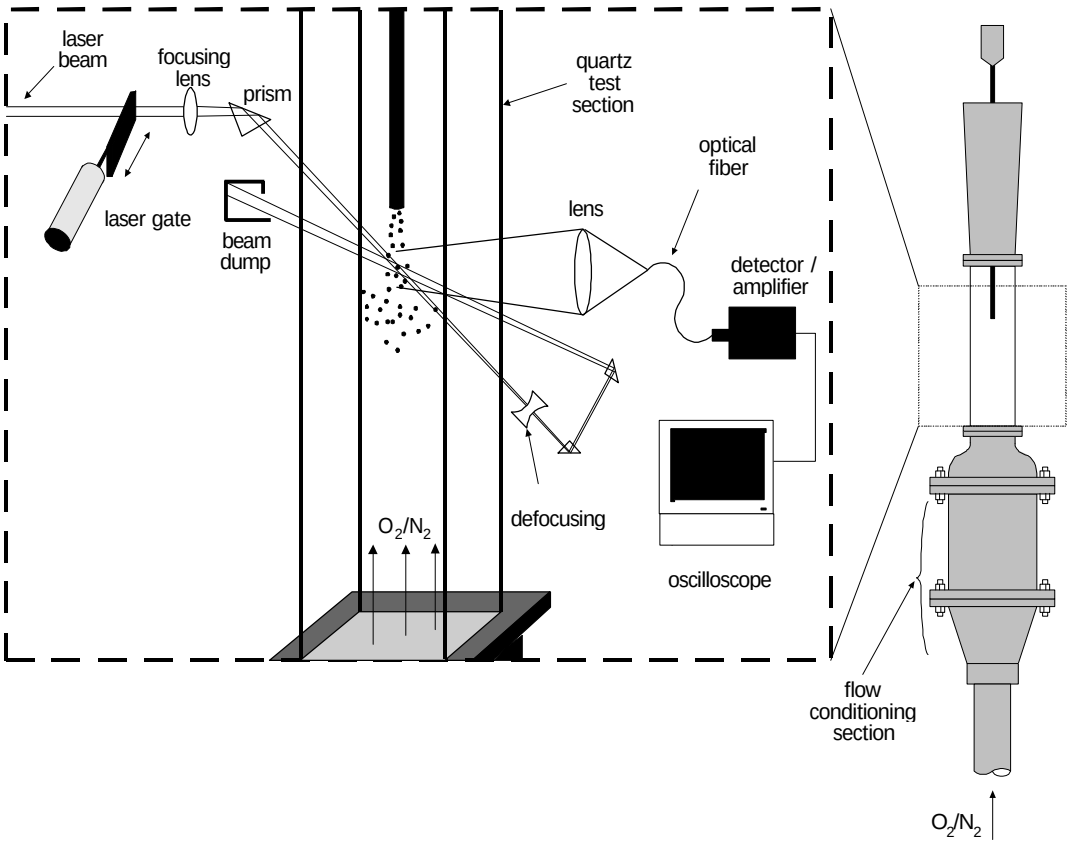

Figure 3.1 Schematic of the laser ignition experiment

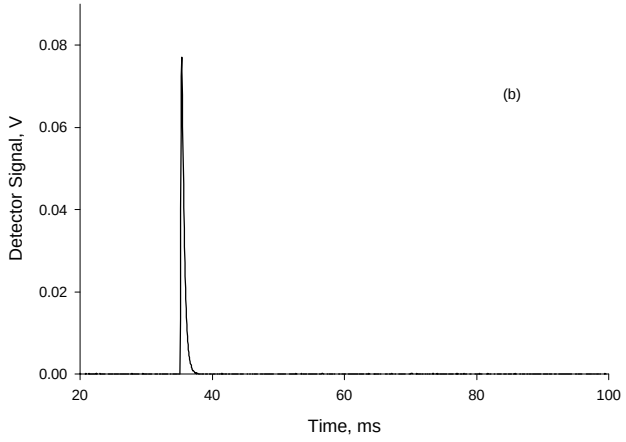

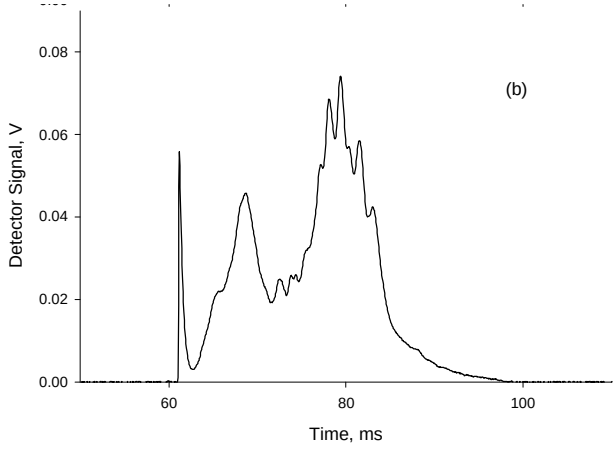

Figure 3.2 Signal traces from photodetectors showing (a) non-ignition and (b) ignition events for the Pittsburgh #8 bituminous coal. Particle size was 125-158 μm, and oxygen concentration was 100%. The short-lived spike in both traces result from laser heating of the coal surface and subsequent cooling. Ignition and combustion of the coals causes the long-lived emission of (b).

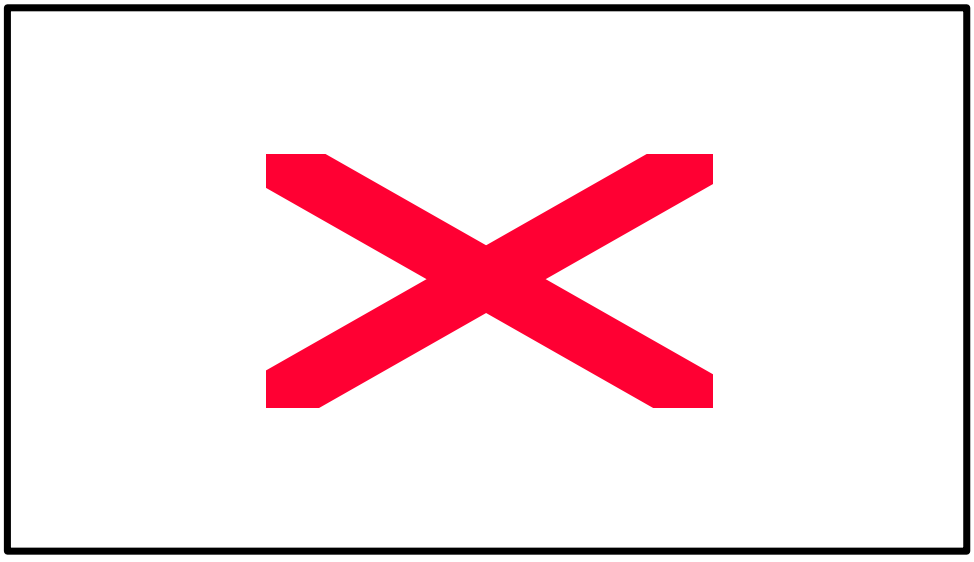

Figure 3.3 Typical data from a conventional ignition experiment showing the relation between ignition frequency (or probability) and gas temperature for a bituminous coal. Data extracted from Ref.4.

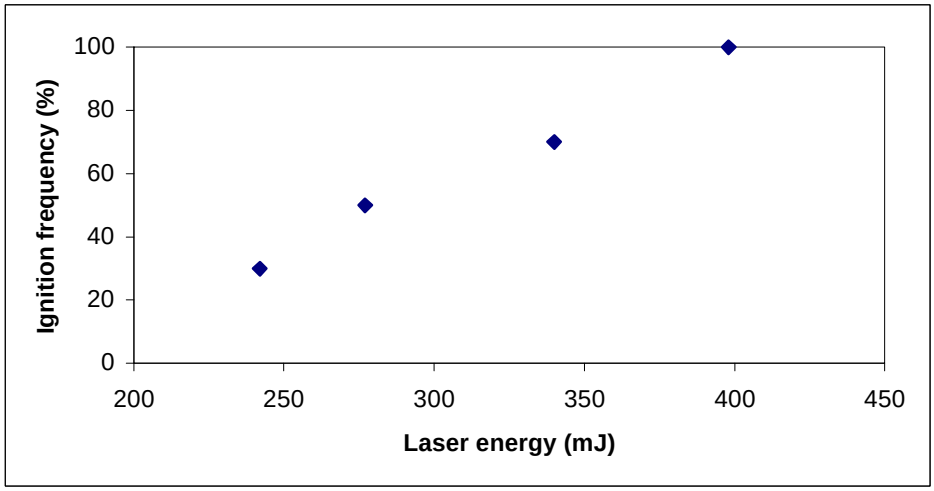

Figure 3.4 Typical data from our laser ignition experiment showing the relation between ignition frequency and laser energy for bituminous coal.

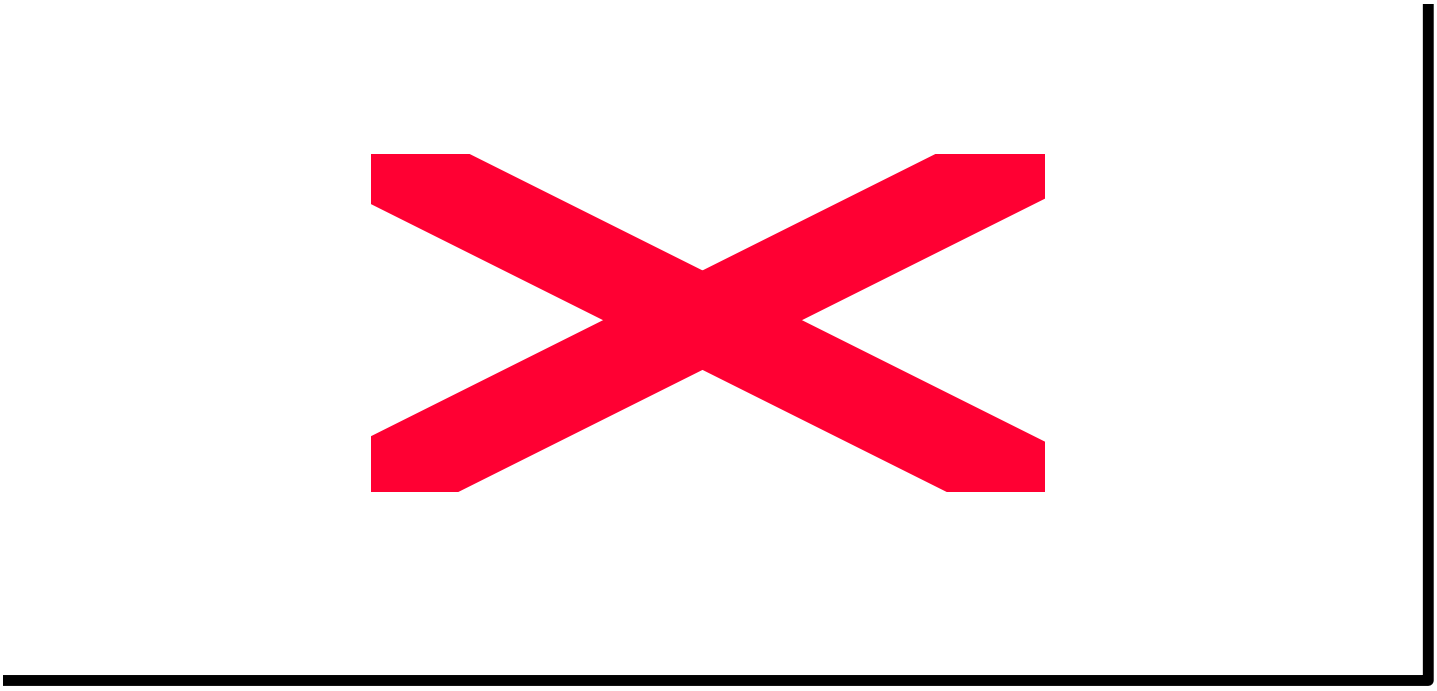

Figure 3.5 Distribution of Activation Energy as a Gaussian Distribution

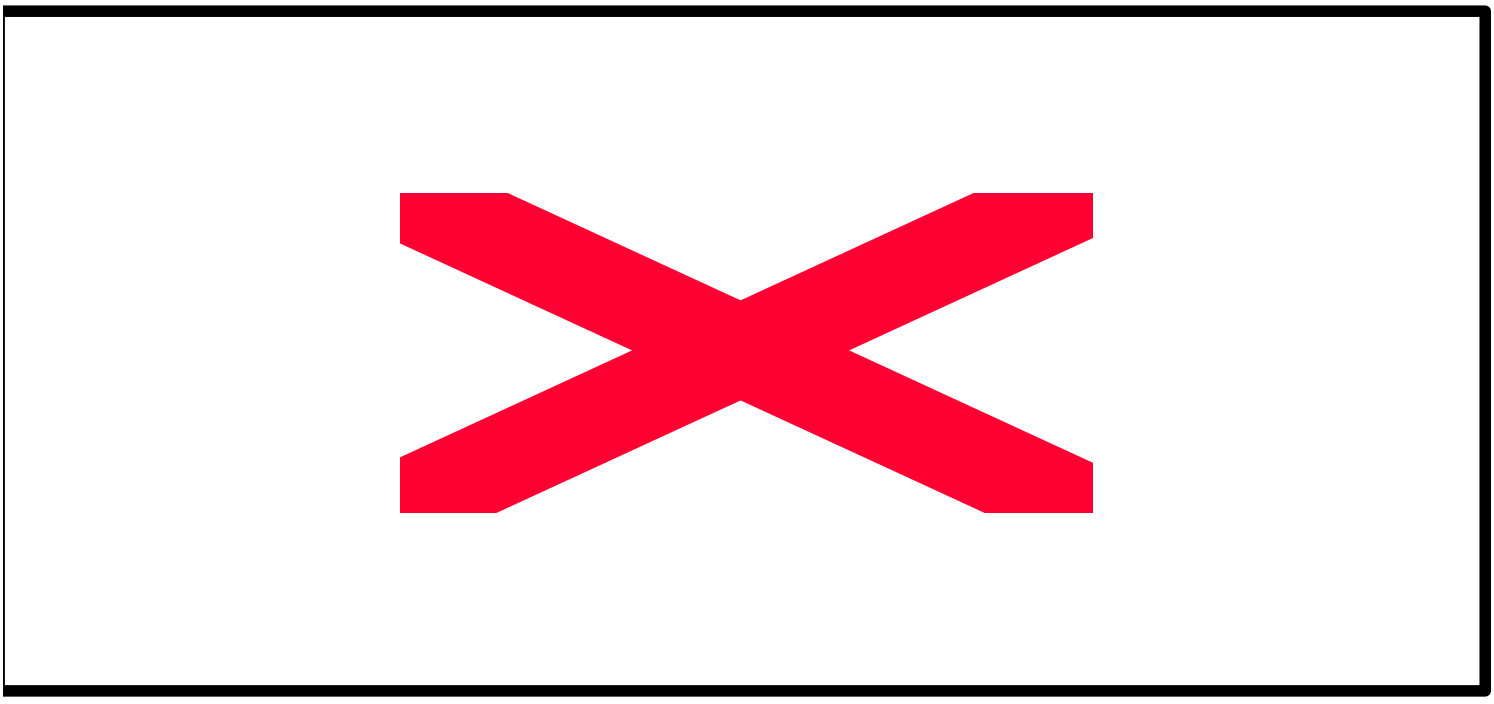

Figure 3.6 Distribution of coal particle size as a Top-Hat Distribution

3.1.2 Drop-Tube Experiment by T. F. Wall's Group [4]

The ignition experiments were carried out using a pulse ignition technique. Metered flows of O_2 and N_2 were passed through an electrically heated tubular furnace at a rate of 500ml/min (s.t.p.). A small quantity of sample was contained in a glass funnel with a capillary stem. By gently tapping the funnel with an electric vibrator, a pulse of fuel (0.2-0.5mg or 1170 particle for 75-90μm size coal) was dropped into the furnace through a water-cooled probe. A photomultiplier was used to detect the occurrence of ignition, which was indicated by the visual flash of an igniting particle. The furnace was maintained at a fixed temperature. Ten to twenty pulses of fuel were injected, and the number of pulses for which ignition responses were detected was noted on a chart recorder. Figure 3.3 give typical results of ignition response versus furnace gas temperature and indicate a temperature range over which the percentage of pulses resulting in observed ignition flashes increases from 0 to 100.

3.2 Model Formulation

Figure 3.4 show typical data obtained from our ignition experiment conducted by varying the laser energy while holding oxygen concentration, particle size and type of coal. Fig. 3.4 and Fig. 3.3 show that ignition frequency increases approximately linearly with plus laser energy or gas temperature, and these are inconsistent with the heterogeneous ignition theory previously described. If all particles of a coal sample used in an experiment have the same reactivity, that is if they are described by a common Arrhenius rate constant as in Eq. (2.7), then the data would show an ignition frequency of 0% until the critical laser energy corresponding to that at the critical ignition condition is reached. At any laser energy or gas temperature above critical ignition condition, the ignition frequency would be 100.

One of the reasons why ignition frequency increases gradually with increasing laser energy or gas temperature is obvious: Within any coal sample, there exists a distribution of reactivity among the particles. Thus, in the laser ignition experiment, in which a batch of perhaps 4×10^5 particles of a sample is dropped into the furnace, there is the probability (or frequency) that at least one particle has a reactivity that meets or exceeds the critical ignition condition set forth in equations (2.1) and (2.2) as the laser energy is increased. This is the ideal of DAEMI [10]. Of course, there exist other variations among the particles within a sample, such as particle size and specific heat. Variation in size alone could account for the observed increase in ignition frequency with the laser energy pulse (or gas temperature) [1,4,5,8]. It cannot account for other experimental observation, namely, the variation in the slope of the ignition frequency with oxygen concentration. A distribution in specific heat would only affect the rate at which a particle attains its equilibrium temperature, but would not change the value or the reactivity. Perhaps other variations could cause the observed behavior of ignition frequency. It is our premise that the distribution in reactivity and particle size dominates all other variations. We propose to add the distribution of particle size into the DAEMI.

3.3 Simulation Procedure

Fig.3.5 shows the distribution of activation energy versus frequency for a sample for which E_0=58 kJ mol^{-1} and σ=5.5 kJ mol^{-1}. The intervals of activated energy is 1kJ mol^{-1} (ΔE=1kJ mol^{-1}).

The Distributed Activated Energy Model of Ignition (DAEMI) simulates our laser ignite and drop-tube experiment by allowing for the particles within the coal sample to have a distribution of reactivity (Chapter 2.3). We first calculate the probability of particles for being in each of the intervals.

The distributed of particle size model of ignition assumes that in a small range of particle size, the distribution of particle size is Top-Hat distribution (Fig 3.6). The interval of particle size is 1μm ($\Delta Dp=1.0\times10^{-6}$m). Particle sizes are grouped into three. These are 106.0 to 125.0μm, 125 to 150μm, 150.0 to 180.0μm respectively.

3.3.1 Base Case

Now, the heat generated by a spherical carbon particle undergoing oxidation on its external surface is given by the kinetic expression:

$$\frac{Q_{gen}}{S} = H_c x_{o_2}^n A_0 \exp\left(\frac{-E}{RT_p}\right) \tag{3.1}$$

Similarly, the heat loss from the surface of a particle at temperature T_p is the sum of losses due to convection and radiation. Thus, heat loss from the surface is given as:

$$\frac{Q_{loss}}{S} = hS(T_p - T_g) + es_b S\left(T_p^4 - T_g^4\right) \tag{3.2}$$

For the convection-loss term, we assume that the Nusselt number equals 2, as is appropriate for very small particles, which leads to $h = 2k_g / d_p$.

$$\frac{Q_{loss}}{S} = \frac{2k_g}{d_p} S(T_p - T_g) + es_b S\left(T_p^4 - T_g^4\right) \tag{3.3}$$

At the critical ignition condition, $Q_{gen} = Q_{loss}$, we obtain

$$E = -RT_p \ln\left(\frac{\left(\frac{2k_g}{d_p}\right)\left(T_p - T_g\right) + es_b\left(T_p^4 - T_g^4\right)}{H_c x_{o_2}^n A_0}\right) \tag{3.4}$$

where the required parameters for this equation were calculated as follows:

For base case of the model, we assumed that T_p was obtained from the equilibrated temperature calculations by use of a linear regression to regress Tp as a function of laser energy (see appendix 1). For example, for 70μm.116μm and 165μm coal particle the temperature are given as functions of laser energy as [19]

$$T_{p\,(116mm)} = 0.7266E_{laser} + 385.22 \tag{3.5}$$

$$T_{p(70mm)} = 1.0707E_{laser} + 427.08 \tag{3.6}$$

$$T_{p(165mm)} = 0.5505E_{laser} + 367.57 \tag{3.7}$$

For variable particle size, we use interpalation mathematics method define:

$$T_p = \frac{\left(T_{p(70mm)} - T_{p(116mm)}\right)\left(d_p - 116e-6\right)}{(70-116)\times 1\times e-6} + T_{p(116mm)} \qquad d_p<116\mu m \tag{3.8}$$

$$T_p = \frac{\left(T_{p(165mm)} - T_{p(116mm)}\right)\left(d_p - 116e-6\right)}{(165-116)\times 1\times e-6} + T_{p(116mm)} \qquad d_p>116\mu m \tag{3.9}$$

k_g the gas thermal conductivity in the boundary layer around a heated particle was given by a linear fit to the conductivity of air [11].

$$k_g = 7.0\times 10^{-5}\left(\frac{T_p + T_g}{2}\right) \tag{3.10}$$

H_c is defined by the equation [16]

$$H_c = \frac{y}{y+1}H'_{C,CO} + \frac{1}{y+1}H'_{C,CO_2} \tag{3.11}$$

It is well known that the product of carbon oxidation is both CO and CO_2, $H'_{C,CO}$ and H'_{C,CO_2} are the heats of combustion corresponding to the following oxidation reaction [11].

$$C + \frac{1}{2}O_2 \rightarrow CO; H'_{C,CO} = 9{,}210\frac{kJ}{kgC}$$
$$C + O_2 \rightarrow CO_2; H'_{C,CO_2} = 32{,}790\frac{kJ}{kgC} \quad (3.12)$$

Where

$$y = \frac{molCO}{molCO_2} = 59.95\exp\left(\frac{-3214}{T_p}\right) \quad (3.13)$$

ε, the emissivity of coal particles was taken as 0.8.

n, the reaction order was taken as 1.

χ_{o2} was chosen to be 1.0 corresponding to a 100% oxygen concentration.

For each laser energy, twenty runs were made to obtain ignition-frequency distributions.

3.3.2 laser Ignition Experiment

When we were using this version of DAEMI to fit the laser ignition experiment. The experiment data of Tp was reading directly from data files (see appendix 3). Then to calculate average temperature (T_{avg}) and standard deviation (T_σ), base on Normal Distribution,

$$T_{avg} = \frac{\sum T_p}{N} \qquad \text{(N is the number of } T_p\text{)} \quad (3.14)$$

$$T_s = \sqrt{\frac{\sum (T_p - T_{avg})^2}{N-1}} \quad (3.15)$$

to obtain the range of temperature, namely, $T_{avg}-2T_\sigma < T_p < T_{avg}+2T_\sigma$, by randomly choosing particle temperature from the range to obtain critical energy at each condition.

In this experiment, in which a batch with several hundred particles are dropped in to the test section, and only a few are heated by the laser pulse. There is an increasing probability (or frequency) as the laser energy is increased that at least one of the heated particles is reactive

enough to ignition under the given conditions. For nearly every case, one to three particles are hit in the test section by two intersecting laser beams. This is determined by observations with high-speed video. For simulation, thirteen hundred particles are then selected randomly as they feed into the test section and two particles are further selected randomly from these 1300 to be hit by the laser pulse, keeping in mind that no particle can be selected twice.

For randomly selected two particles with particle size and activation energy. Substituting preexponential factor (A_0), mean of Gaussian distribution of activation energy (E_0), standard deviation of Gaussian distribution (σ) and reaction order (n) in Eq. (3.4), E can be calculated as the critical (or threshold) activation energy that a particle may have and still ignite under the given conditions. The result (E) is compared with the activation energy. If the result (E) is greater than the activation energy among the particles that were hit, then the particle is considered ignited.

At each set of operating conditions (coal type and size, oxygen concentration, and laser energy), 20 attempts at ignition are made in order to get the ignition frequency, or probability, which is the parameter sought from these studies. We compare this simulated ignition frequency with the experimental results over a range of laser pulse energy.

3.2.3 Drop-Tube Experiment

In simulating the drop-tube ignition experiment, we assumed that 10^6 particle are in the initial batch. A batch of 1170 particles of a sample is dropped into the furnace in each simulation of an experimental run. No particle can be selected more than once. Whether or not ignition occurs for a run is determined by the particle in the batch of 1170 with the lowest activation energy.

Now, using Eq. (3.1) and Eq. (3.3) we can obtain the heat generated Q_{gen} and Q_{loss}. In order to determine the critical ignition temperature of the particle, Tp, and critical activation

energy, E, the critical ignition condition, Q_{gen} = $Q_{loss,}$ and $\frac{dQ_{gen}}{dT_p} = \frac{dQ_{loss}}{dT_p}$ are solved simultaneously. Q_{gen} and Q_{loss} are given in Eqs. (3.1) and (3.3), and lead to the following derivatives with respect to temperature:

$$\frac{dQ_{gen}}{dT_p} = SH_c x_{o_2}^n A_0 \exp\left[\frac{-E}{RT_p}\right]\left(\frac{E}{RT_p^2}\right) \tag{3.16}$$

$$\frac{dQ_{loss}}{dT_p} = \frac{2k_g}{d_p} S + 4es_b ST_p^3 \tag{3.17}$$

Note that the neglection of the T_p dependence in k_g introduces a small error in Eq. (3.15).

Following $\frac{dQ_{gen}}{dT_p} = \frac{dQ_{loss}}{dT_p}$, we set Eq. (3.14) equal to Eq. (3.15) and solve for the quantity E/RT_p:

$$\frac{E}{RT_p} = \frac{\frac{2k_g}{d_p} T_p + 4es_b T_p^4}{H_c x_{o_2}^n A_0 \exp\left[\frac{-E}{RT_p}\right]} \tag{3.18}$$

The denominator is recognized to be Q_{gen}/S Eq. (3.1), which by Q_{gen} = Q_{loss} is also Q_{loss}/S Eq. (3.2). Thus Eq. (3.16) can be rewritten as:

$$\frac{E}{RT_p} = \frac{\frac{2k_g}{d_p} T_p + 4es_b T_p^4}{\frac{2k_g}{d_p}(T_p - T_g) + es_b (T_p^4 - T_g^4)} \tag{3.19}$$

This relation for E/RT_p is substituted into the expression Q_{gen} -Q_{loss} = 0 to obtain a function, F, which is a function of T_p only:

$$F(T_p) = Q_{gen} - Q_{loss}$$

$$= H_c x_{o_2}^n A_0 \exp\left[\frac{\frac{2k_g}{d_p}T_p - 4es_b T_p^4}{\frac{2k_g}{d_p}(T_p - T_g) + es_b(T_p^4 - T_g^4)}\right] - \frac{2k_g}{d_p}(T_p - T_g) - es_b(T_p^4 - T_g^4) = 0 \quad (3.20)$$

The reasonable root of F (T_p) corresponds to the critical ignition temperature of the particle, and substitution of this value into Eq. (3.19) produces the critical activation energy at the critical ignition condition.

k_g, the gas thermal conductivity in the boundary layer around a heated particle was given by Eq. (3.10).

χ_{o2} was chosen to be 0.5 corresponding to a 50% oxygen concentration.

ε, the emissivity of coal particle was taken as 0.8.

H_c was defined by the equation from (3.11) to (3.13).

Substituting all the required values in Eq. (3.4), E obtain the result as the critical (or maximum) activation energy that a particle may have and still ignite under the given conditions. By randomly choosing each particle with activation energy for a run, then get the particle in the batch of 1170 with the lowest activation energy. we compared the result (E) with the lowest activation energy. If the result (E) is greater than the lowest activation energy among the particle that was heated in a run, The particle was ignited.

3.3 Modeling Results

3.3.1 Results of the Base Case of the Model

Figure 3.7 and Fig. 3.8 shows the effect of oxygen concentration and number of particle (M) on ignition frequency for particle size range of 106-125μm and 150-180μm, respectively. It can be seen that at each oxygen concentration, ignition frequency increases monotonically over the range of laser pulse energy. Below this range, the ignition frequency is zero, and above this range the result is 100% ignition frequency. As the number of particle (M) is increased from 1 to 300, the frequency distribution shifts to lower laser energy values. This behavior is due to the fact that, within any coal sample, there exists a distribution of reactivity among the particles.

As the oxygen concentration is decreased from 100% to 67%, the frequency distribution shifts to higher laser energies or equivalently, higher particle temperatures, as expected. This is consistent with the ignition theory since at decreased oxygen concentration, higher temperatures are necessary for heat generation by the particles (due to chemical reactions) to exceed heat loss from the particles and lead to ignition. The shift in distribution can be viewed in two ways: for a fixed laser pulse energy, a decrease in oxygen concentration leads to a decrease in the ignition frequency, all else being equal; Second, a decrease in oxygen concentration implies that a higher laser pulse energy is needed, in order to achieve the same ignition frequency.

Figure 3.9 and Fig. 3.10 show the same effect of Distribution Particle Size in 150-180μm and average particle size (165μm) on ignition frequency for oxygen concentration of 100% and 67%. Fig.3.11 and Fig.3.12 also show that the same effect of distribution particle size in 106-125μm and average particle size (115μm) on ignition frequency for 100% and 67% of O_2.

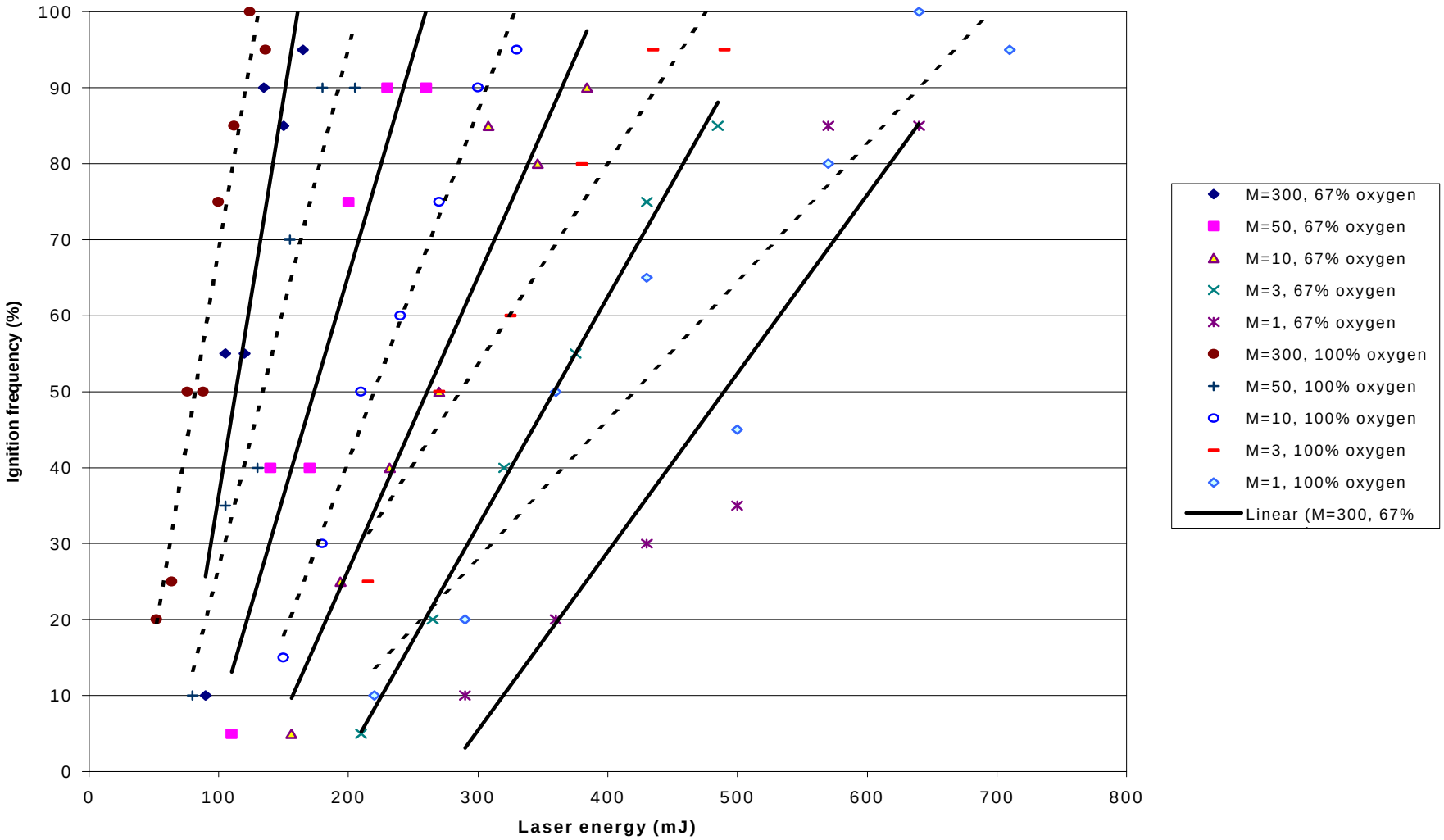

Figure 3.7 Modeling results showing the effect of M (numbers of particles were ignited at one drop time) and oxygen concentration on ignition frequency. (a) Solid-line express 67% oxygen concentration (x_{o2} =67%); (b) Dash-line express 100% oxygen concentration (x_{o2} =100%). Particle size is 106-125 μm, and all other parameters are as listed in Table 3.1.

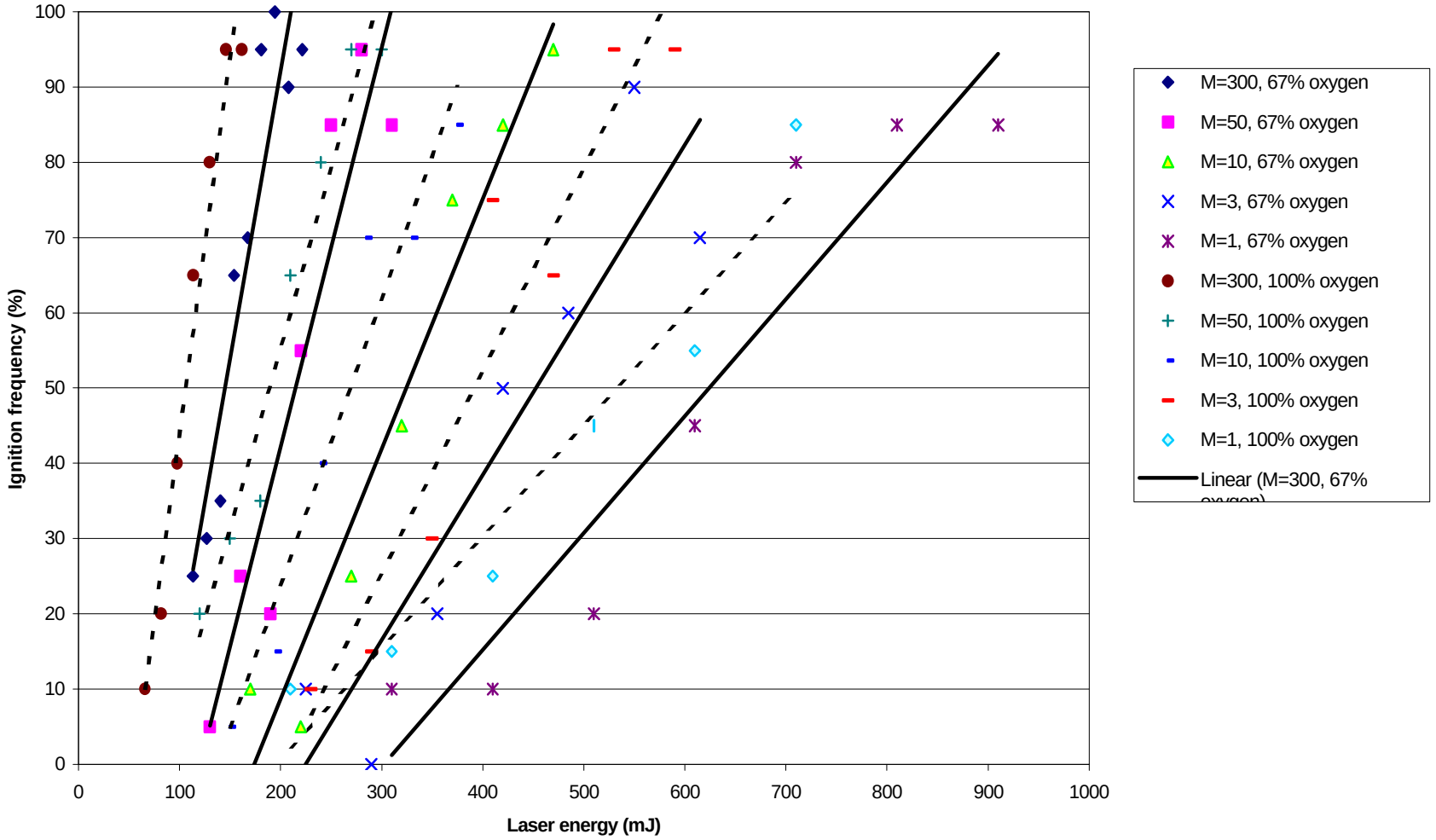

Figure 3.8 Modeling results showing the effect of M (numbers of particles were ignited at one drop time) on ignition frequency. (a) Solid-line express 67% oxygen concentration (x_{o2} =67%); (b) Dash-line express 100% oxygen concentration (x_{o2} =100%). Particle size is 150-180 μm, and all other parameters are as listed in Table 3.1.

Table 3.1 Parameters Used in the Base Case of the Model of Laser Ignition Experiment

Variable	Value
E_0	58 kJ/mol
A_0	250 kg/m^2s
σ	5.5 KJ/mol
n	1.0
ε	0.8

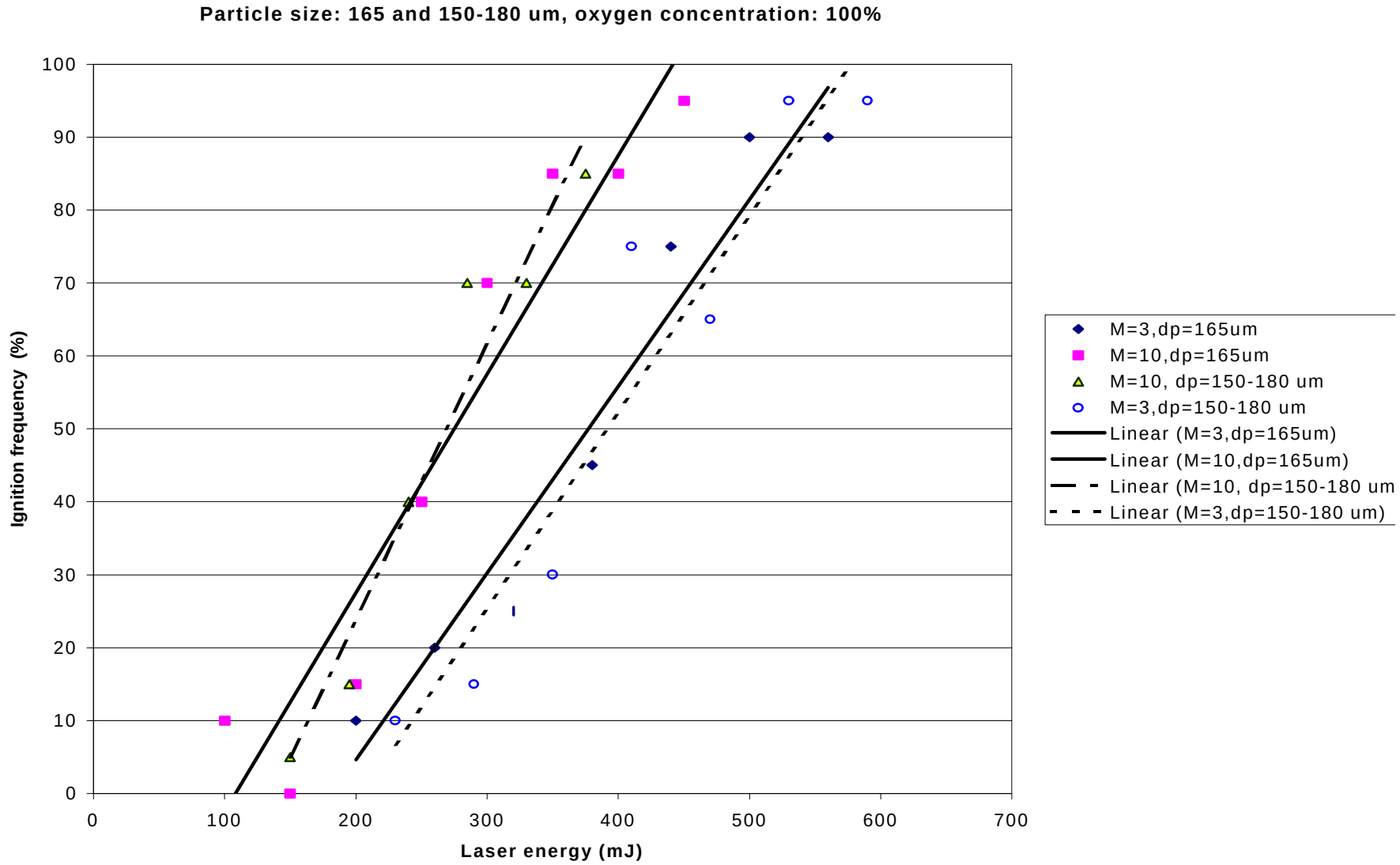

Figure 3.9 Modeling results showing the effect of average particle size 165μm and the range of particle size 150-180μm in ignition frequency. Oxygen concentration is 100%. All other parameters are as listed in Table 3.1. (a) Solid-line express particle size d_p=165μm; (b) Dash-line express distribution particle size D_p in 150-180μm.

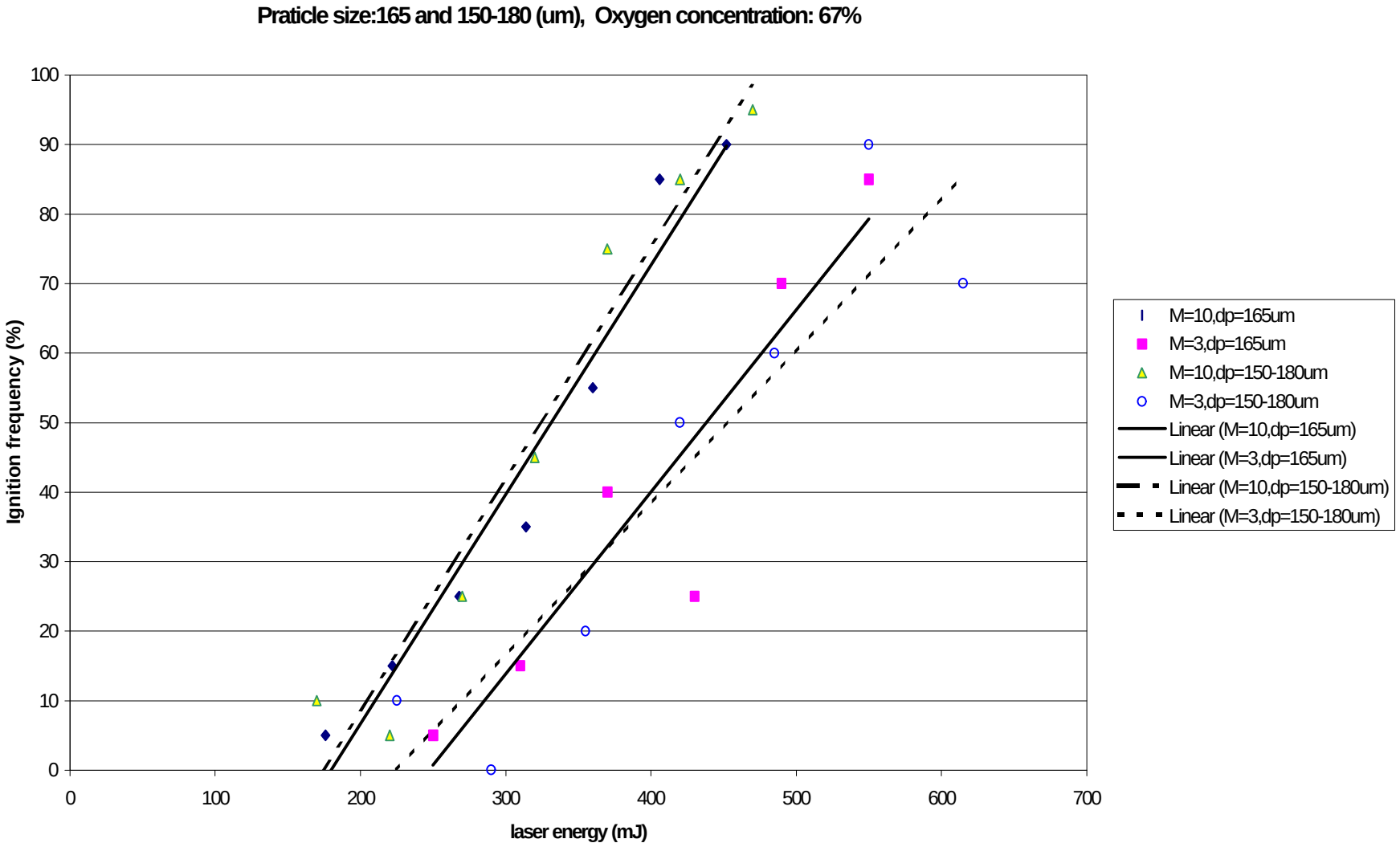

Figure 3.10 Modeling results showing the effect of the average particle size 165μm and the range of particle size150-180 μm on ignition frequency. Oxygen concentration is 67%. All other parameters are as listed in Table 3.1. (a) Solid-line express particle size d_p=165μm; (b) Dash-line express distribution particle size d_p in 150-180μm.

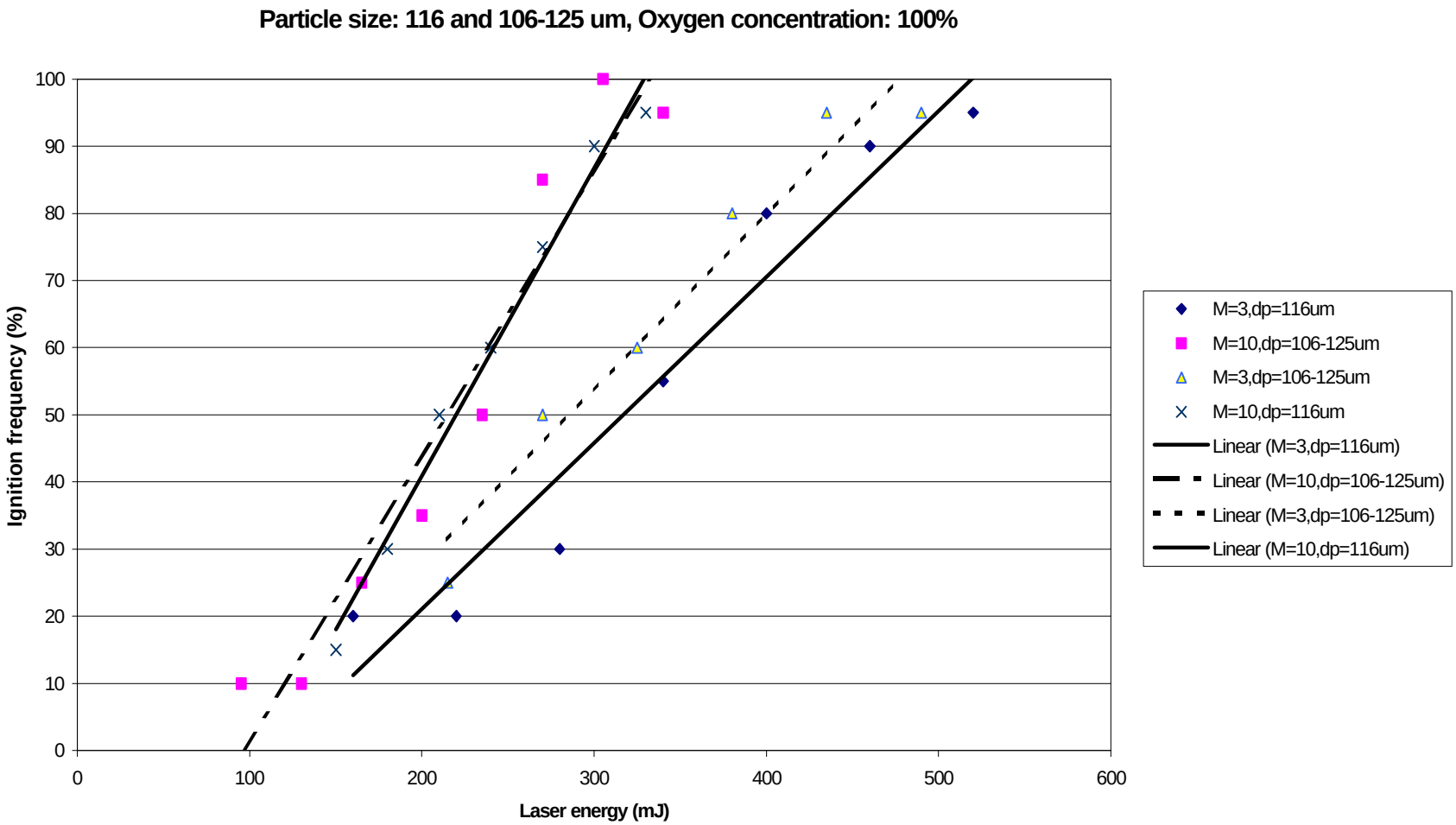
Particle size: 116 and 106-125 um, Oxygen concentration: 100%
Ignition frequency (%)
Laser energy (mJ)
0
10
20
30
40
50
60
70
80
90
100
0
100
200
300
400
500
600
M=3,dp=116um
M=10,dp=106-125um
M=3,dp=106-125um
M=10,dp=116um
Linear (M=3,dp=116um)
Linear (M=10,dp=106-125um)
Linear (M=3,dp=106-125um)
Linear (M=10,dp=116um)

Figure 3.11 Modeling results showing the effect of average particle size 116 μm and the range of particle size 106-125μm in ignition frequency. Oxygen concentration is 100%. All other parameters are as listed in Table 3.1. (a) Solid-line express particle size d_p=116μm; (b) Dash-line express the distribution of particle size d_p in 106-125μm.

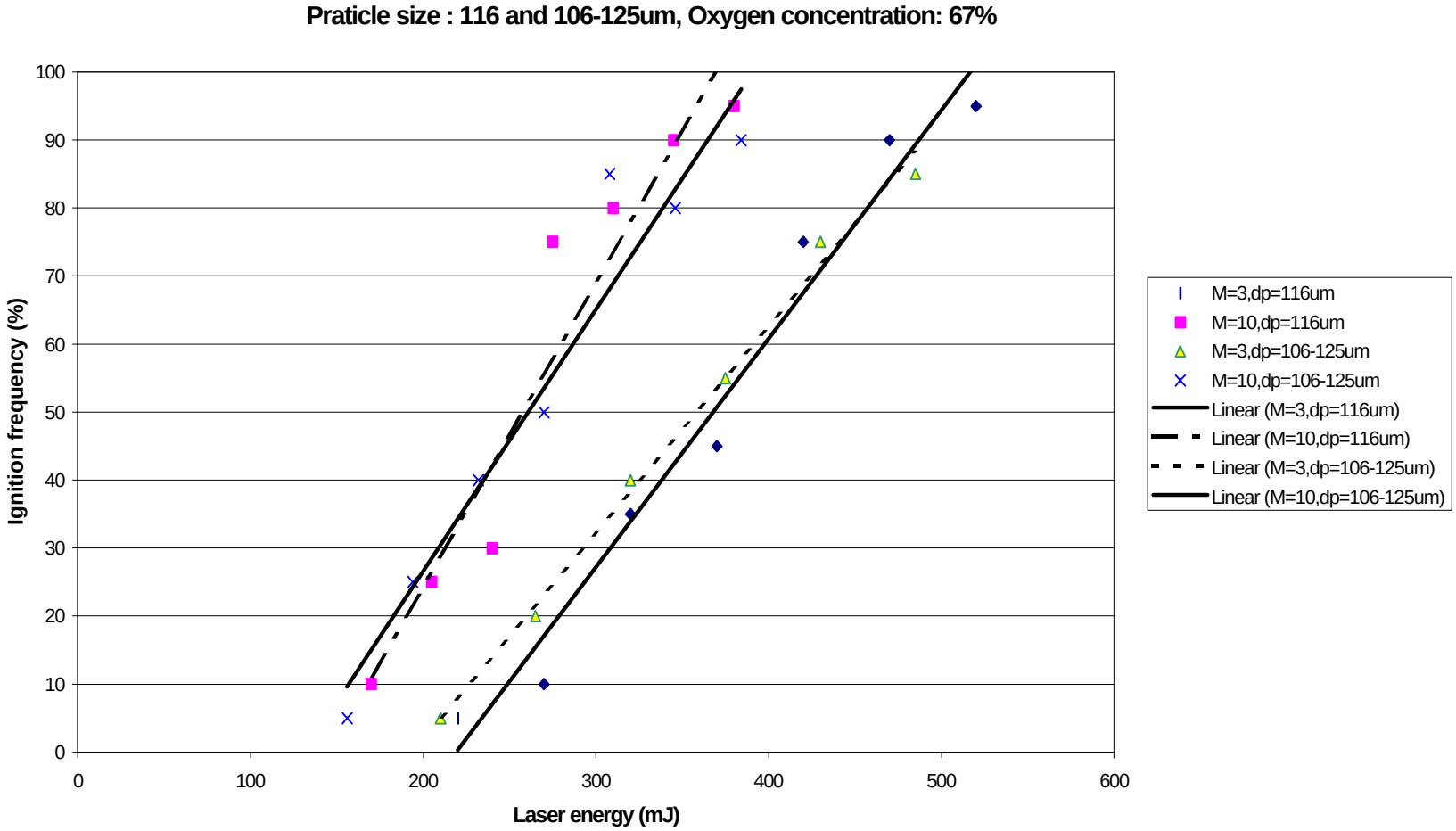

Figure 3.12 Modeling results showing the effect of the average particle size 116 μm and the range of particle size106-125 μm on ignition frequency. Oxygen concentration is 67%. All other parameters are as listed in Table 3.1. (a) Solid-line express particle size d_p=116μm; (b) Dash-line express distribution particle size d_p in 106-125μm.

3.3.2 Results of Simulation Laser Ignition Experiment

The simulations for the experiments were performed via a FORTRAN code (Appendix 3). The code was designed to produce frequency distribution data for a given particle size (diameter, dp) range, oxygen concentration and, temperature of particle and laser pulse energy. As discussed earlier, for each run two particles are selected randomly from 1300 particles. The particle size and activation energy are determined whether or not ignition occurred for the run. For each type coal, the parameters required as input are the average activation energy (E_0), standard deviation for the Gaussian distribution (σ), and pre-exponential factor (A_0).

Figure 3.13-3.15 show the experiment data for the Pittsburgh #8 coal with modeling results using anther method, that calculate average temperature and standard deviation to obtain the range of particle temperature at each condition. Figure 3.16-3.17 show the experiment data for the Pust coal with the modeling results using the range of particle temperature. Figure 3.18 shows the experiment data for the Wyodak coal with the modeling results using the range of particle temperature. The behavior of the model with respect to changes in each of the parameters was first observed. The parameters are then modified to obtain a final set of values to improve the model. The final parameters that fit our laser ignition experimental data of each type coal are given the following table.

Table 3.2 shows all Pittsburgh#8 coal's parameters of Figure 3.13-3.15. There are all Pust coal's parameters of Figure 3.16-3.17 in Table 3.3. There are all Wyodak coal's parameters of Figure 3.18 in Table 3.4.

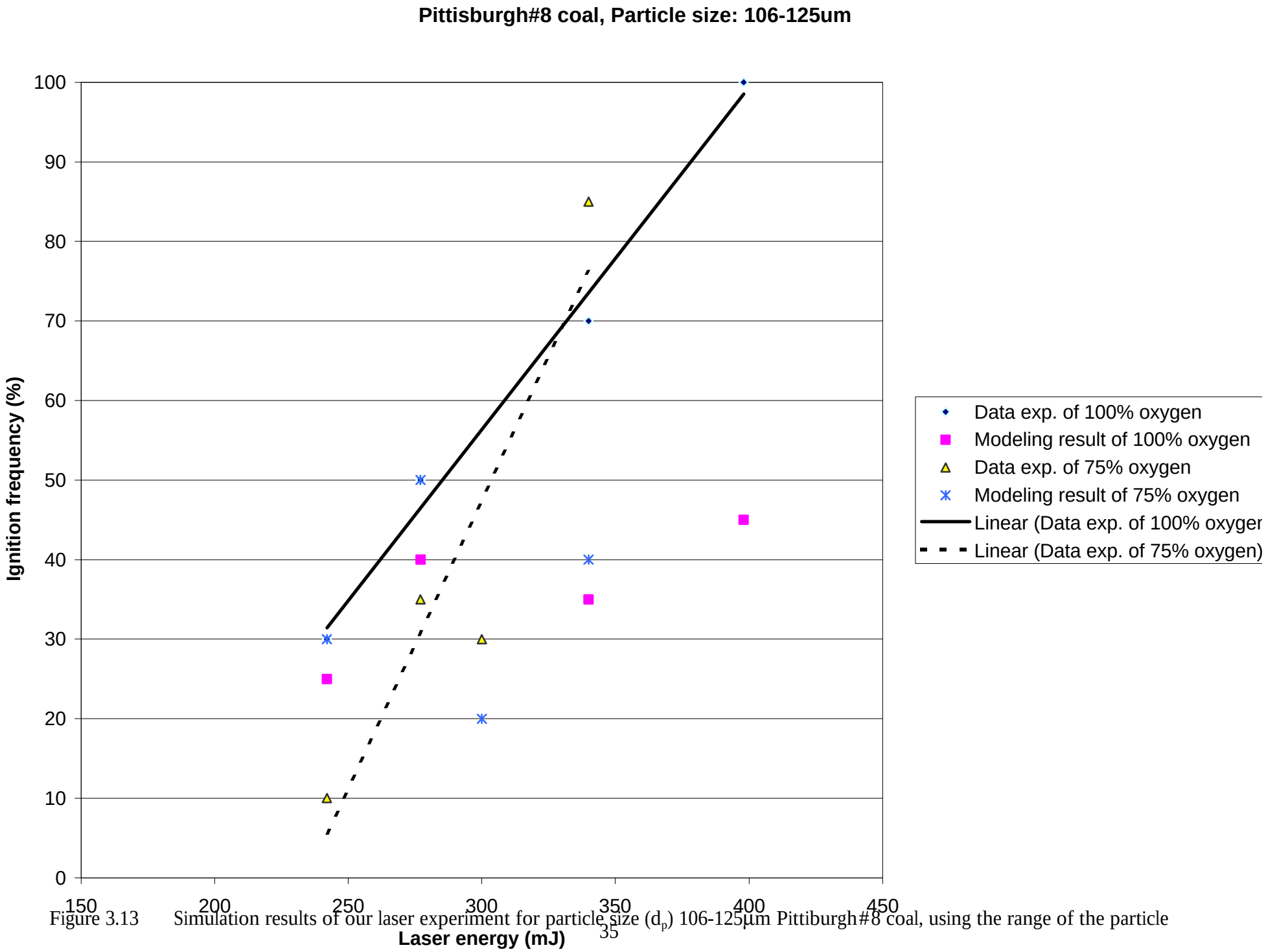

Figure 3.13 Simulation results of our laser experiment for particle size (d_p) 106-125μm Pittiburgh#8 coal, using the range of the particle

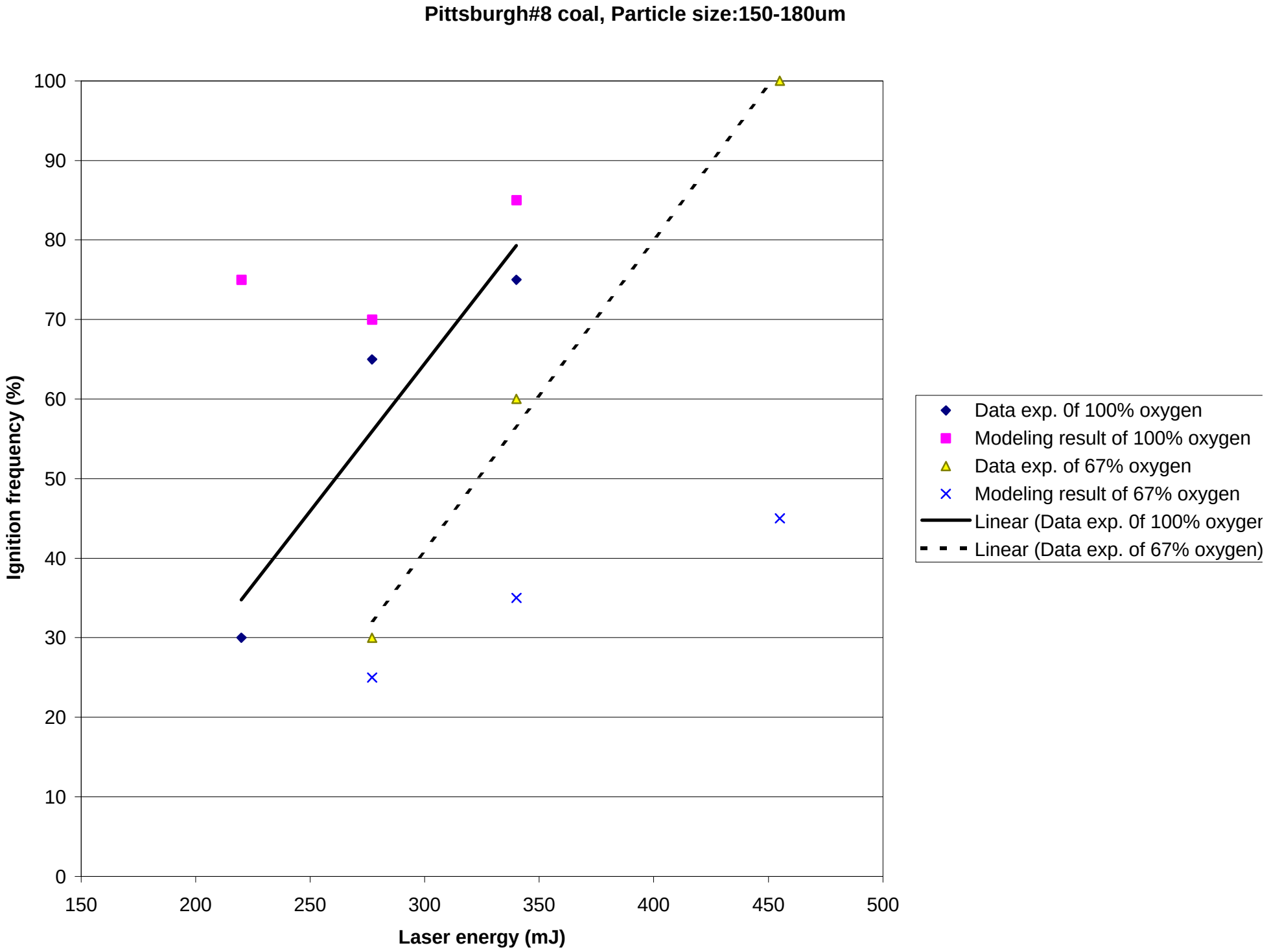
Pittsburgh#8 coal, Particle size:150-180um
Ignition frequency (%)
Laser energy (mJ)
0
10
20
30
40
50
60
70
80
90
100
150
200
250
300
350
400
450
500
Data exp. 0f 100% oxygen
Modeling result of 100% oxygen
Data exp. of 67% oxygen
Modeling result of 67% oxygen
Linear (Data exp. 0f 100% oxyger
Linear (Data exp. of 67% oxygen)

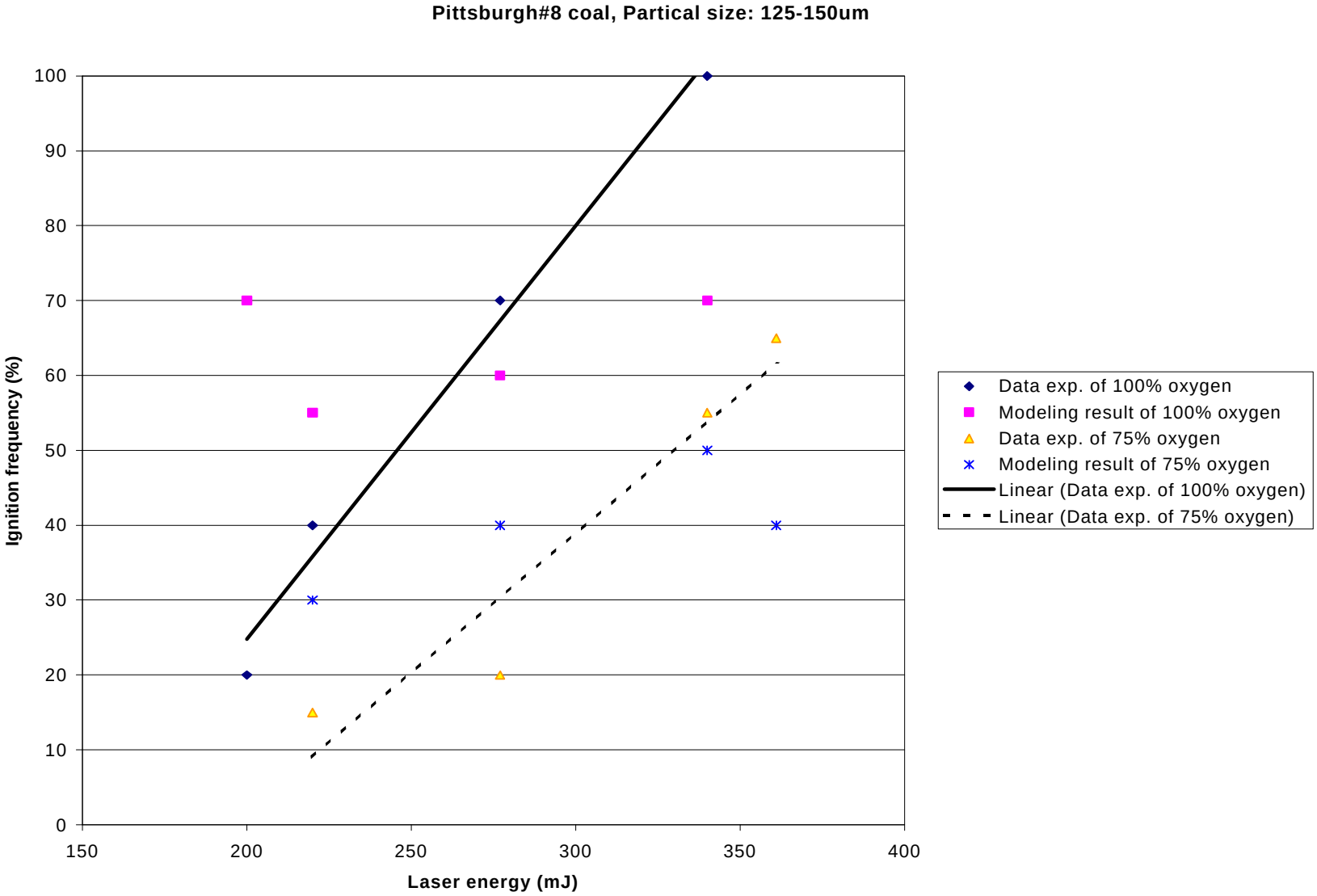

Figure 3.15 Simulation results of our laser experiment for particle size (d_p) 125-150μm Pittiburgh#8 coal, using the range of the particle temperatures. All other parameters are as listed in Table 3.2

Table 3.2 Parameters Simulate Pittsburgh#8 Coal in Laser Ignition Experiment using the range of measured particle temperature

Variable	Value
E_0	135 kJ/mol
A_0	250 kg/m^2s
σ	12 KJ/mol
n	1
ε	0.8

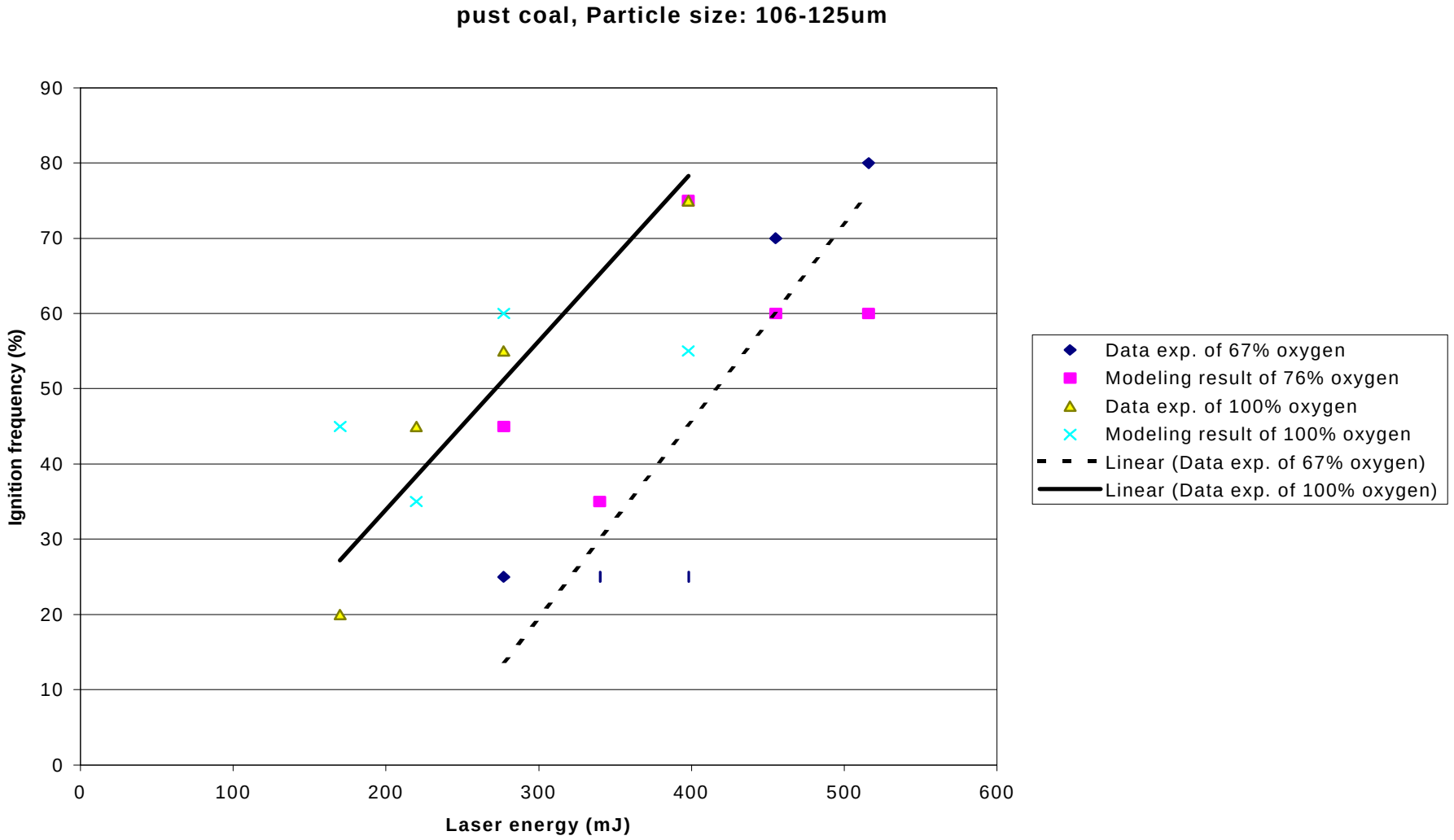

Figure 3.16 Simulation results of the laser Experiment for particle size (d_p) 106-125 μm Pust coal, using the range of the particle temperatures. All other parameters are as listed in table 3.3.

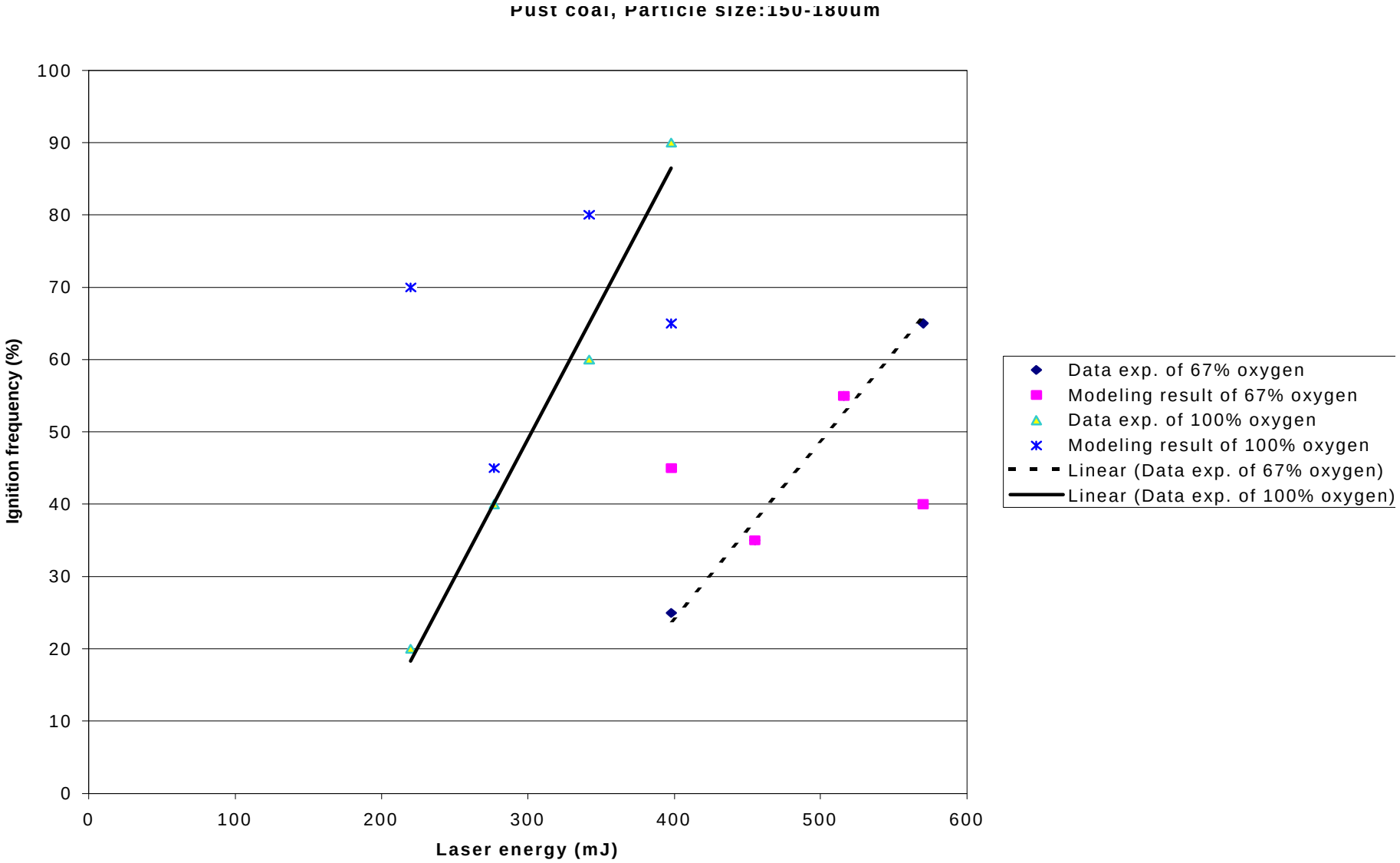

Figure 3.17 Simulation results of the laser Experiment for particle size (d_p) 150-180 μm Pust coal, using the range of particle temperatures. All other parameters are as listed in table 3.3.

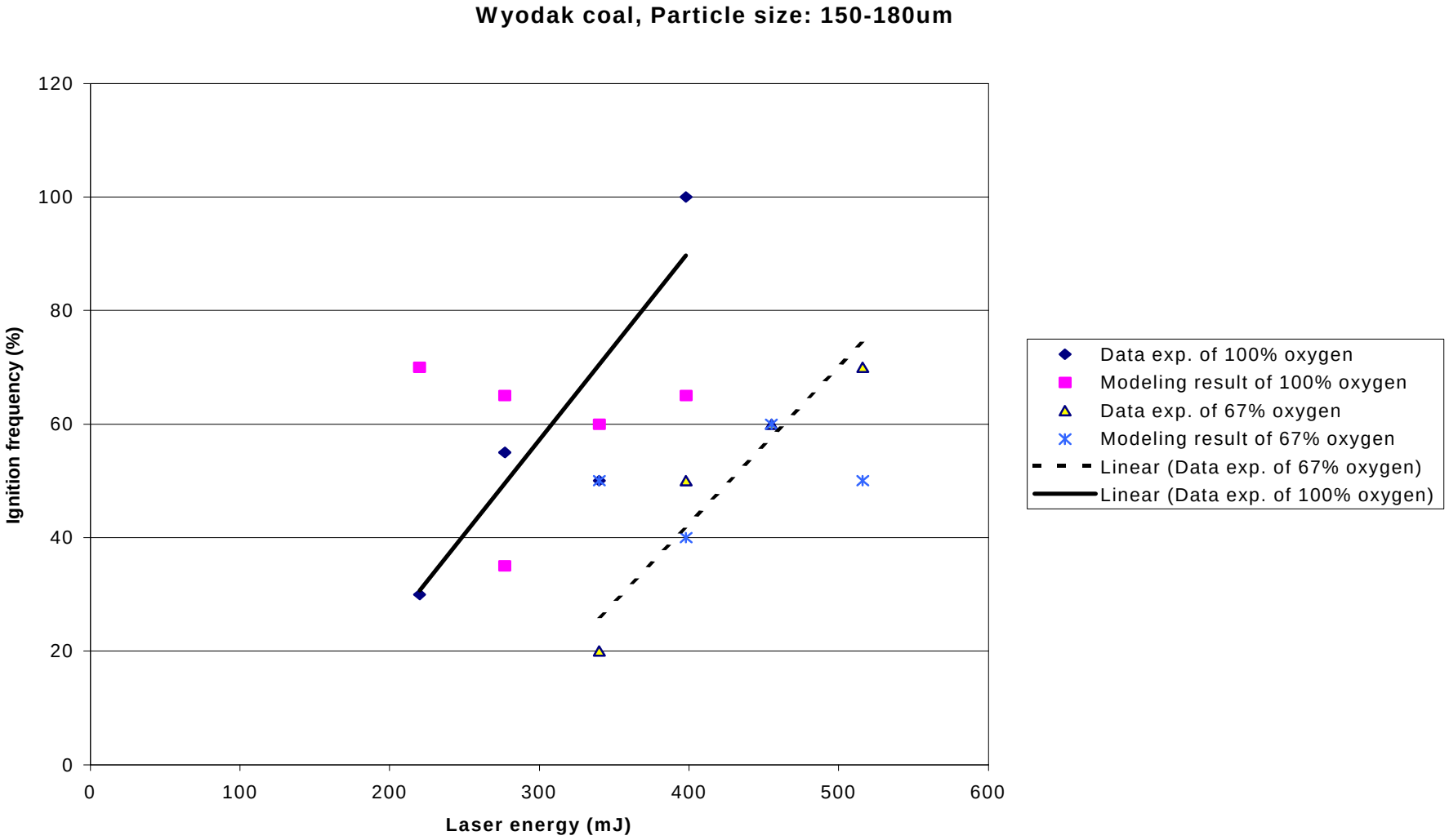

Figure3.18 Simulation results of the laser experiment for particle size 150-180μm Wyodak coal, using the range of particle temperatures. All other parameters are as listed in table 3.4.

Table 3.3 Parameters Simulate Pust Coal in Laser Ignition Experiment

Variable	Value
E_0	120 (kJ/mol)
A_0	200 (kg/m^2s)
σ	40 (KJ/mol)
n	1
ε	0.8

Table 3.4 Parameters Simulate Wyodak Coal in Laser Ignition Experiment

Variable	Value
E_0	115 (kJ/mol)
A_0	100 (kg/m^2s)
σ	40 (KJ/mol)
n	1
ε	0.8

3.3.3 Drop-Tube Experiment

The required simulations for drop-tube experiments have performed by a FORTRAN code (Appendix 2). The code was designed to produce frequency distribution data for a given average particle size (diameter dp) or the maximum diameter (dpmax) and minimum diameter (dpmin) of particle size range, oxygen concentration and, temperature of gas. The particle with the lowest activation energy determines whether or not ignition occurred for a run. The parameters required to be input were average activation energy (E_0), standard deviation for the Gaussian distribution (σ), preexponential factor (A_0) and reaction order (n).

Respectively, Figure 3.19-3.20 show the experiment data for coal#1 and coal#2 with the modeling results using distribution of particle size. There are all parameters of coal#1 and coal#2 for Figure 3.19-3.20 in Table 3.5 and Table 3.6. Figure 3.21-3.22 show the experiment data for coal#1 and coal#2 with the modeling results by average particle size. These parameters of coal#1 and coal#2 for Figure 3.21-3.22 are listed in Table 3.7 and Table 3.8.

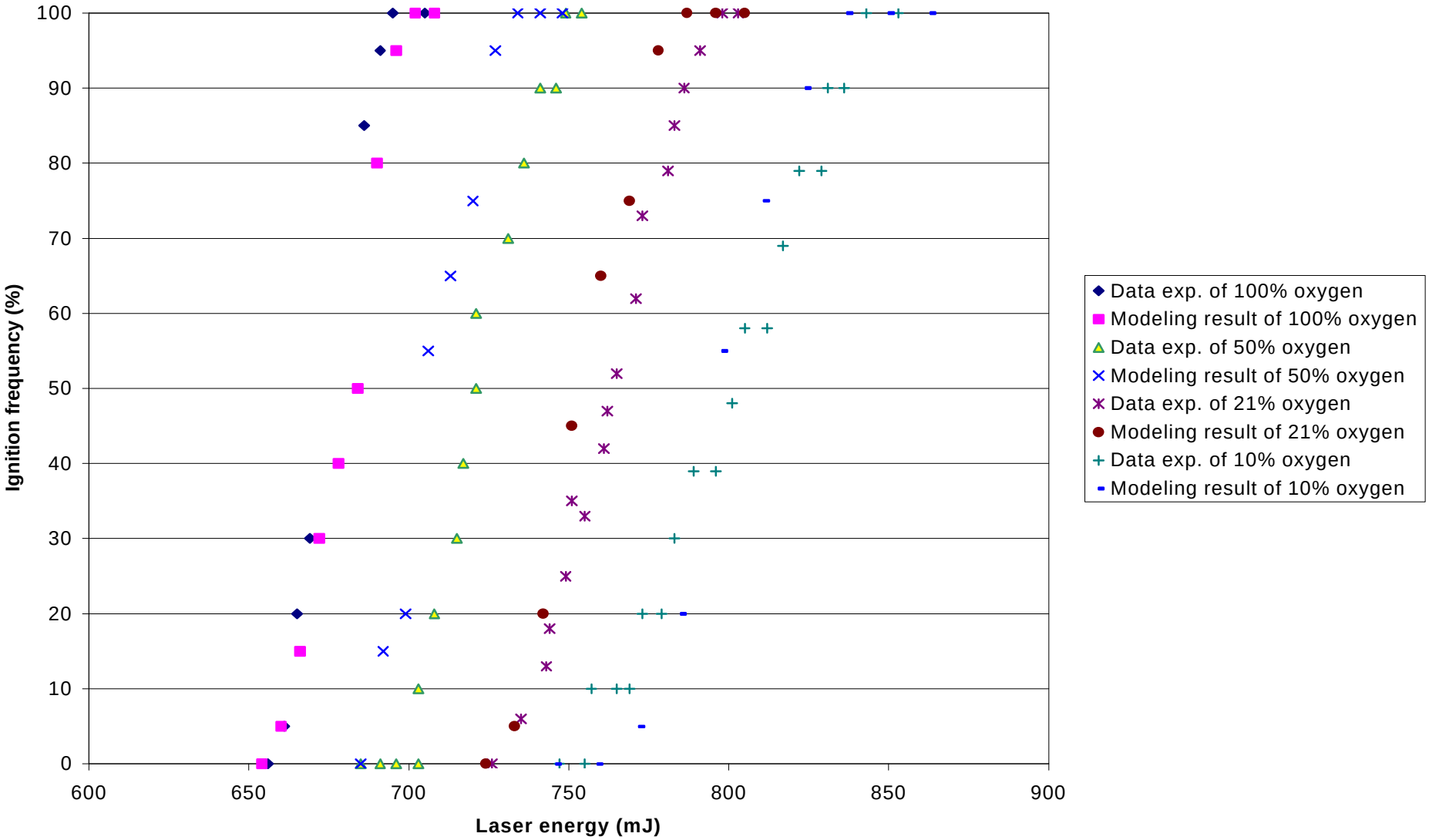

Figure3.19 Simulate result of drop-tube experiment [4] for particle size 75-90μm coal #1, using distribution particle size is incorporated into the DAEMI. All other parameters are as listed in Table 3.5.

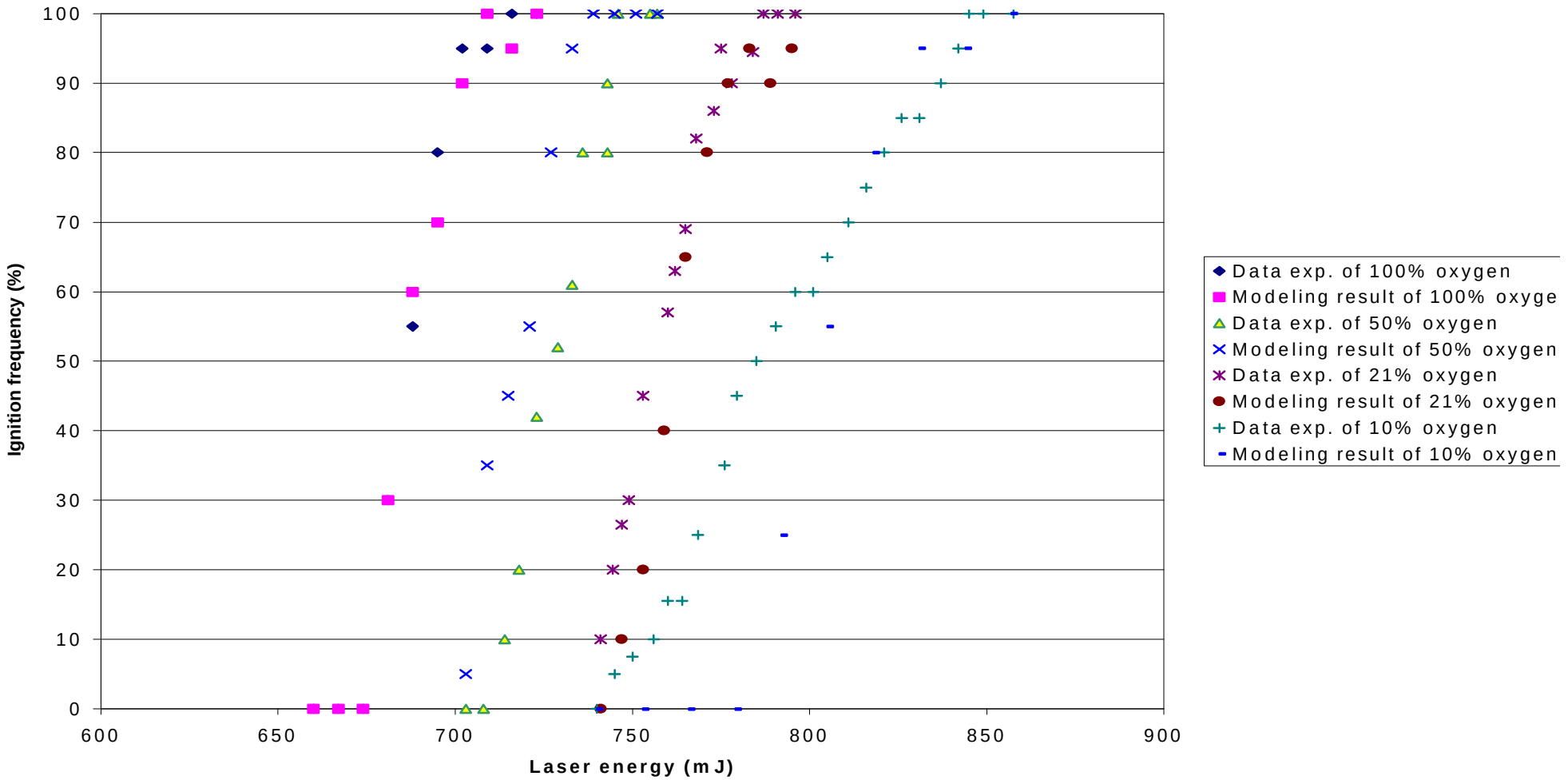

Figure 3.20 Simulation results of drop-tube experiment [1] for particle size 75-90 μm coal#2, using distribution particle size is incorporated into the DAEMI. All other parameters are as listed in Table 3.6.

Table 3.5 Parameters Simulate cola#1 in Drop-Tube Experiment [4] (Using distribution of particle size in DAEMI)

Variable	Value
E_0	70.0 (kJ/mol)
A_0	300.0 (kg/m^2s)
σ	1.0 (KJ/mol)
n	0.5
ε	0.8

Table 3.6 Parameters Simulate cola#2 in Drop-Tube Experiment [4] (Using distribution of particle size in DAEMI)

Variable	Value
E_0	71.0 (kJ/mol)
A_0	320.0 (kg/m^2s)
σ	1.0 (KJ/mol)
n	0.5
ε	0.8

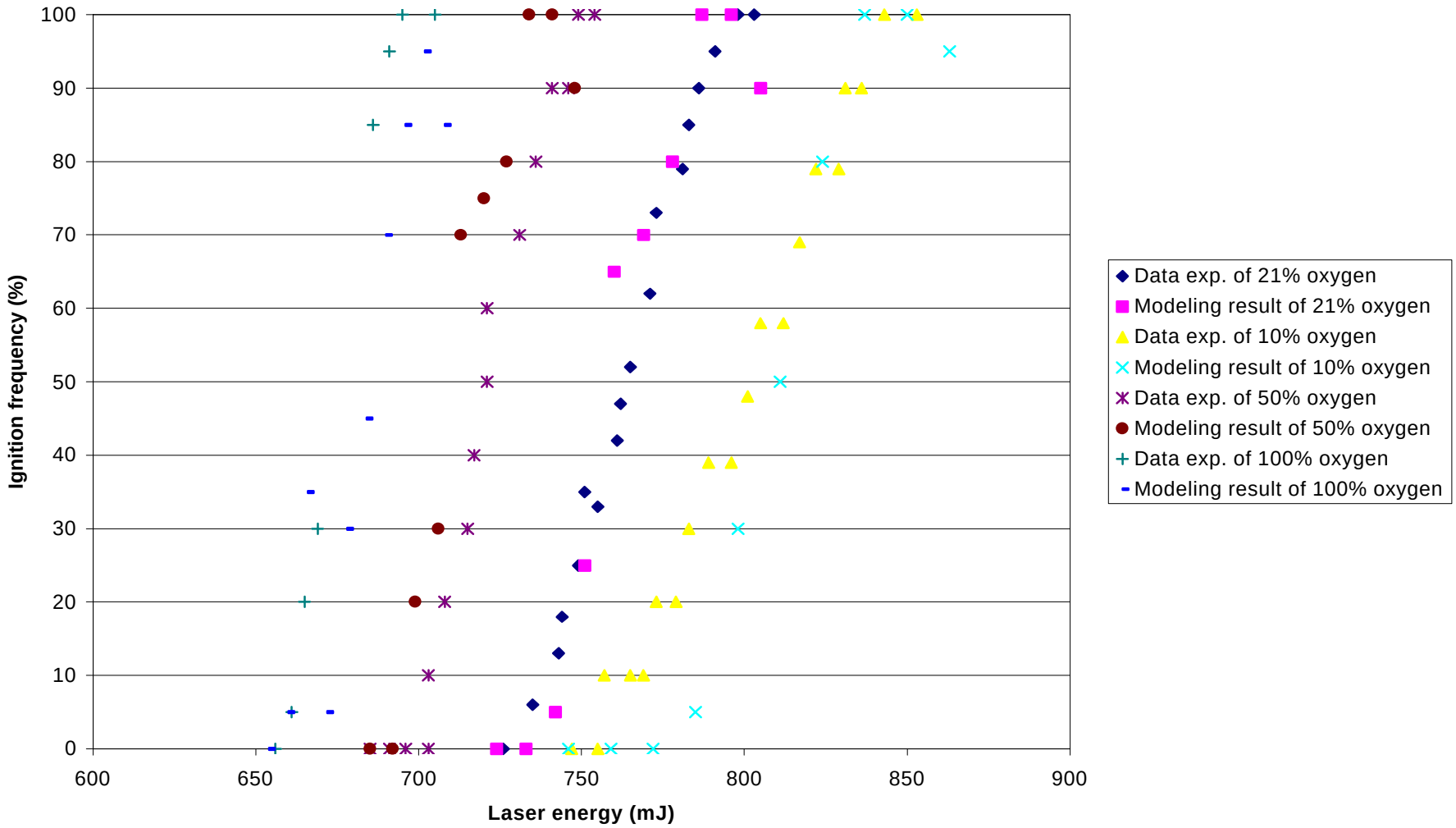

Figure 3.21 Simulation results of drop-tube experiment [4] for particle size 83 μm coal #1. All other parameters are as listed in Table 3.7.

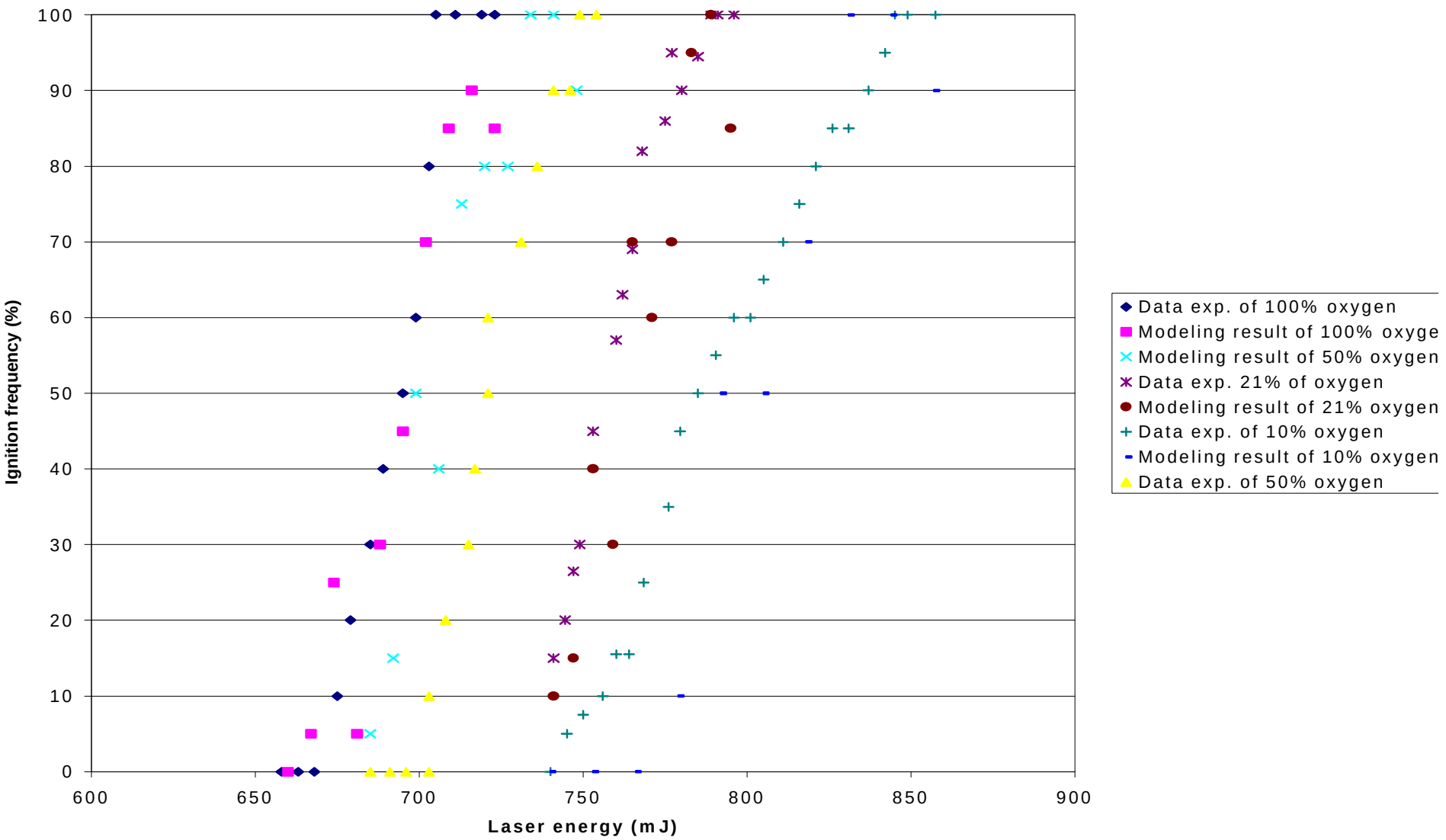

Figure 3.22 Simulation results of drop-tube experiment [4] for particle size 83 μm coal #2. All other parameters are as listed in Table 3.8

Table 3.7 Parameters Simulate cola#1 in Drop-Tube Experiment [4], using the average particle size.

Variable	Value
E_0	92 (kJ/mol)
A_0	110 (kg/m^2s)
σ	10 (KJ/mol)
n	0.44
ε	0.8

Table 3.8 Parameters Simulate cola#2 in Drop-Tube Experiment [4], using average particle size.

Variable	Value
E_0	98.6 (kJ/mol)
A_0	111 (kg/m^2s)
σ	12 (KJ/mol)
n	0.37
ε	0.8

DISCUSSION OF RESULTS

4.1 Comparison with Drop-Tube Experiment

Either the range of particle size (75-90μm) or the average particle size (83μm) can be used in the current version of DAEMI. The DAEMI can be fitted to the experimental data [4] shown in Figures 3.19-3.22. Figures 3.19-22 also shown the almost same effect of Distribution Particle Size in 75-90 μm and average particle size 83 μm on ignition frequency for oxygen concentration from 10% to 100%. The small standard deviation, σ (1.0 kJ/mol) is used to obtain the results from the current version of DAEMI using the distribution of particle size and the average particle size. The narrow distribution (small standard deviation) leads to a small energy range since most particles have similar activation energies. This behavior is due to the fact that a distribution of reactivity exists among the particles. The particle diameters are randomly selected from the range of particle size to calculate the critical activation energy. Different particle diameters correspond to the different critical activation energies. When the different critical activation energy is larger than the activation energy that a particle has, that particle is considered ignition.

The larger σ (10.0-12.0 kJ/mol) is used to obtain the modeling results from the old version of DAEMI using the average particle size. Since the subsidiary simulation condition is that the particle own the lowest activation energy in the batch could be ignited. According to the experiment phenomenon, it is not always true that only the particle own the lowest activation energy can be ignited. In Tables 3.7-3.8, these parameters that were obtain by consider the particle in the batch of 1170 particles could has the lowest activation

energy was ignited, are different with E_0=84.0 kJ/ml, σ=4.0 kJ/mol and n=0.4 that Dr. Chen got from the batch of 100 particles before. So the different simulation process and experiment value obtain the different simulation parameter.

Figures 3.19-3.22 show the effect of oxygen concentration for both the modeling results and experiment data: As oxygen level is decreased from 100% to 10%, the frequency distribution shifts to higher laser energies or, equivalently, higher particle temperatures. This is consistent with ignition theory since at decreased oxygen levels, higher temperatures are necessary for heat generations (due to chemical reactions) that exceed the heat loss from the particles and leads to ignition.

As shown in Tables3.5-3.6, whether we used the distribution of particle size or the average particle size, the modeling result that is obtained by one set of parameters only fits the experiment data of one type of coal. The results show clearly that ignition reactivity is strongly dependent on the coal type. Particle-to-particle variation in physical and/or chemical property of the fuel can be accounted for in order to model the ignition data correctly, and to accurately describe the ignition reactivity. In the future research, statistical test should be used to calculate the confidence intervals, according to a specified significance level to decide on the best set of ignition reactivity parameters.

According to the experimental data, for same coal type, oxygen concentration and particle size, ignition frequency increases with increasing gas temperature. This case is similar to the base case, namely, ignition frequency increases with particle or gas temperature. So the modeling results fit the Drop-Tube experiment data [4] of one particle size. The simulation gave the best results for the 75-90 μm coal#1 particle using E_0=70.0

kJ/mol, σ=1.0 kJ/mol, A_0=300 kg/m^2s, n=0.5. The model also was found to give the best fit to the 75-90 μm coal#2 particle for E_0=71.0 kJ/mol, σ=1.0 kJ/mol, A_0=320 kg/m^2s, n=0.5. It is also found that using n=1.0 difficult to fit to the experiment data [4].

4.2 Comparison with Laser Experiment

For the laser experiment, the DAEMI incorporated the distribution of particle size. The modeling results and the experimental data are shown in Figures 3.13-3.18. These figures all show the effect of oxygen concentration for both the modeling results and experimental data at the same particle size. As the oxygen level is decreased from 100% to 67%, the frequency distribution shifts to higher laser energies, this phenomenon is same as the Drop-Tube experiment. Using those different experimental techniques, we could improve the ignition theory.

Figures 3.13-18 and Tables 3.2-3.4 indicate that the model could account for particle-to-particle variations in reactivity by having a single pre-exponential factor and a Gaussian distribution of activation energies among the particles within a type coal (a sample). The simulation gives final result for the Pust coal all over the laser energies considered, the oxygen concentration and particle size using E_0=120.0 kJ/mol, σ=40.0 kJ/mol, A_0=200 kg/m^2s, n=1.0. The modeling results fit the Wyodak coal all over the laser energies, the oxygen concentration and the particle size using E_0=115.0 kJ/mol, σ=40.0 kJ/mol, A_0=100 kg/m^2s, n=1.0. The modeling results also fit the Pittsburgh#8 all over the laser energy, the oxygen concentration and the particle size using E_0=135.0 kJ/mol, σ=12.0 kJ/mol, A_0=250 kg/m^2s, n=1.0.

The measured particle temperatures of Pust and Wyodak coal are lower than the Pittsburgh#8. The simulation result of Pust and Wyodak are better than that of the Pittsburgh#8. The heat generated by a spherical carbon particle undergoing oxidation on its external surface, it is determined by the kinetic expression and the oxidant diffusion expression. At the lower range of particle temperature, the heat is mainly generated by the kinetic expression; at the higher range of particle temperature, the heat is mainly generated by the oxidant diffusion expression. In the current version of DAEMI, the generated heat is considered to be by the kinetic expression. So the simulation result of coal at the lower particle temperature is better than that at the higher particle temperature.

Figure 4.1 shows the measured particle temperature of the laser experiment. According to the DAEMI, the ignition frequency increases with increasing laser energy. The reason could be effect of the distribution of activation energies among the particles within a sample. When the higher laser energy is used, the ignition could happen between the higher and lower activation energy levels, so the ignition frequency at higher laser energy is higher than that at the lower laser energy. For each activation energy, we can calculate the particle temperature by the ignition theory, the higher range of particle temperature is obtained by the higher laser energy. But the measured particle temperatures of the laser experiment are not like this shown in Figure 4.1.

For the base case, Figures 3.9-3.12 also show the same effect of Distribution Particle Size in 106-125 μm, 150-180 μm and average particle size 116 μm, 165 μm on ignition frequency for oxygen concentration 67% and 100%.

For the heterogeneous coal ignition, it is well known that the product of carbon oxidation is both CO and CO_2, and the reaction order n is depended on the carbon

oxidation. The proportion of the product CO and CO_2 could assume is different using the different ignition experimental mechanism. Since the different particle temperature was obtained by the different ignition experimental mechanism [3]. So the reaction order n=0.5 obtained from simulating the Drop-Tube experiment, n=1.0 obtained from simulating the laser ignition experiment.

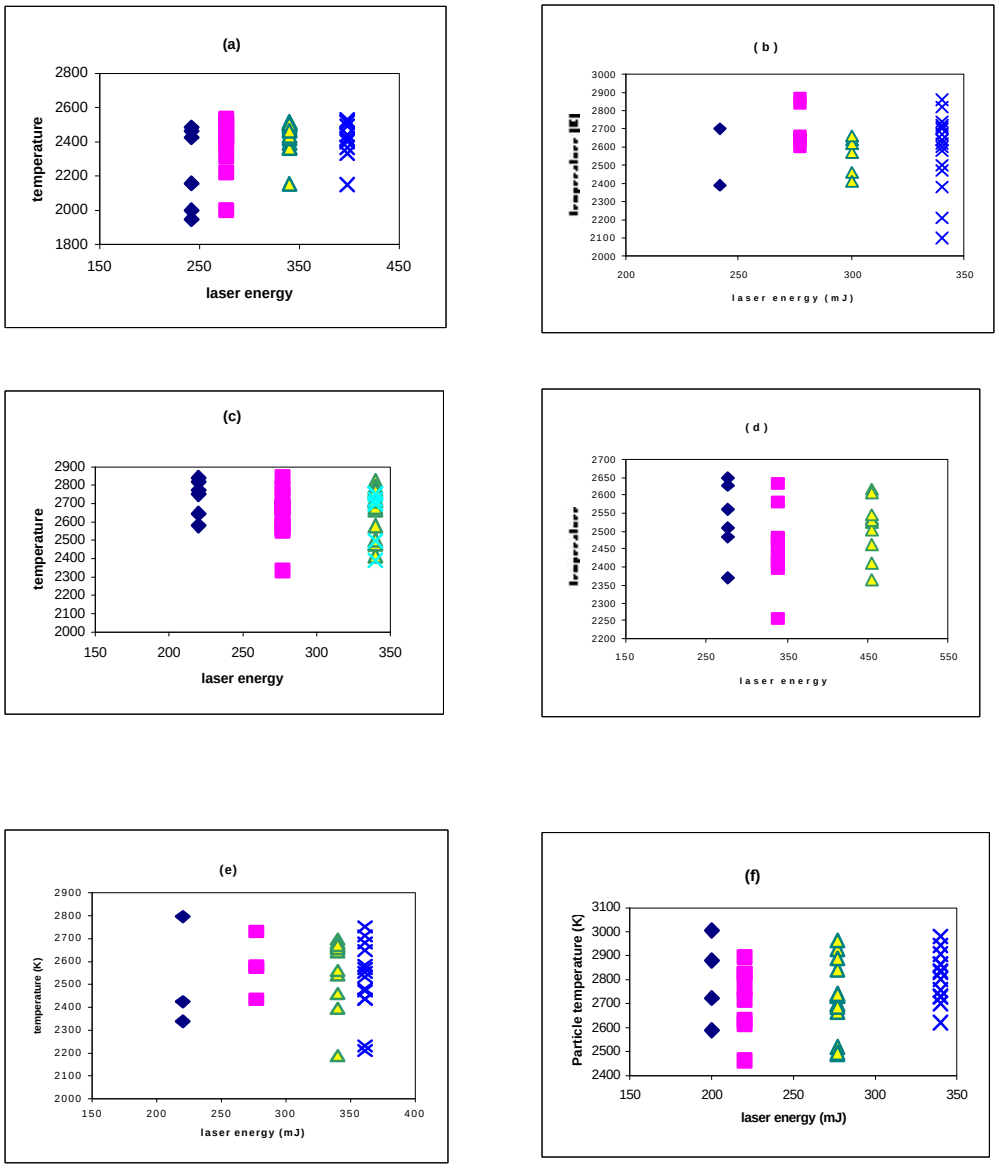

Figure 4.1 Temperature distribution versus laser energy for Pittsburgh#8 coal. (a) Particle size: 106-125μm, O_2: 100%; (b) Particle size: 106-125μm, O_2: 75%; (c) Particle size: 150-180μm, O_2: 100%; (d) Particle size: 150-180μm, O_2: 67%; (e) Particle size: 125-150μm, O_2: 75%; (f) Particle size: 125-150μm, O_2: 100%.